

# Attitude control for the Norwegian student satellite nCube

Master Thesis

Eli Jerpseth Øverby



Norwegian University of Science and Technology  
Department of Engineering Cybernetics  
TRONDHEIM  
May 31, 2004



## MASTEROPPGAVE

Kandidatens navn: Eli Jerpseth Øverby

Fag: Teknisk Kybernetikk

Oppgavens tittel (norsk): *Regulering av orientering for studentsatellitten nCube*

Oppgavens tittel (engelsk): *Attitude control for the Norwegian student satellite nCube*

Oppgavens tekst: Studentsatellitten nCube er et prosjekt som har som mål at studenter skal prosjektere, bygge og skyte opp en satellitt. Prosjektet har vært i gang siden høsten 2002, og studenter ved flere norske universiteter og høyskoler, deriblant NTNU, har definert nyttelast og struktur på satellitten. Arbeidet er nå inne i en byggefase og oppskyting er planlagt høsten 2004.

ADCS (Attitude determination and control system) for nCube er definert, men det er behov for å gå igjennom de løsningene som er foreslått, og vurdere disse opp mot hverandre og mot eventuelle nye forslag.

1. Sett deg inn i modellering og styring av orientering for satellitter og romskip
2. Presenter ADCS for nCube
3. Sammenlign regulatorene som er foreslått brukt på nCube med minst ett eget forslag. Konklusjoner skal trekkes på grunnlag av simuleringer utført i Simulink. Bruk samme modell som tidligere prosjekter/hovedoppgaver på Ncube.
4. Styring av orientering ved hjelp av magnetpoler baserer seg på måling av jordas magnetfelt. I stabilitetsanalyse (Krasovskii-LaSalle teoremet) av slik regulering baserer man seg på at jordfeltet er periodisk, se for eksempel publikasjoner av R. Wisnievski. Presenter dette arbeidet.
5. Er antagelsen om periodisk magnetfelt (sett fra satellitten) realistisk? Presenter modeller for internt og eksternt magnetfelt og diskuter dette.
6. En mulighet for å bevise stabilitet uten antagelsen om periodisitet ligger i bruk av Matrosov's teorem. Bruk dette og bevis at reguleringen kan bevises å være UGAS selv uten antagelsen om periodisk felt.

Oppgaven gitt: 5. januar 2004

Besvarelsen leveres: 31. mai 2004

Besvarelsen levert:

Utført ved Institutt for teknisk kybernetikk

Trondheim, den 12. januar 2004

Jan Tommy Gravdahl  
Faglærer

# PREFACE

This work is the concluding thesis of the Master of Science/ Siv. ing. education at the Norwegian University of Technology and Science (NTNU). It has been carried out at the Department of Engineering Cybernetics. First I would like to thank my supervisor Professor Jan Tommy Gravdahl for his support during this work. I would also like to thank Marianne Vinje Tantillo, Project Manager nCube, Egil Eide, Project Coordinator nCube, and the other members of the nCube project for interesting and inspiring meetings.

Trondheim 31. May 2004

---

Eli Jerpseth Øverby

## Abstract

The Norwegian student satellite project nCube was started autumn 2002 and the project is in its concluding phase. The launch of the satellite is planned for late 2004. The project is a cooperative venture between several universities in Norway and it will be the first Norwegian satellite. nCube is a nano-satellite based on the Cubesat concept. This means that its mass is restricted to 1 kg, and its size is restricted to a cube measuring 10 cm on all sides. It also contains a gravitation boom, which will be used for passive attitude stabilization. The main tasks for nCube will be to monitor ship and reindeer movement in Norway.

This thesis gives a presentation of the Attitude Determination and Control System (ADCS) for nCube. The review of the ADCS design is divided into different control modes and does also focus on evaluation of environmental forces that influence the orientation of the satellite. In the thesis, a comparison between different attitude control laws that have been suggested used for nCube and their robustness in the different control modes is presented. Energy based attitude controllers are found in earlier work, while this thesis proposes a linear quadratic (LQ) controller. The attitude control of the satellite is based on feedback from a magnetometer measuring the Earth's magnetic field.

The stability analysis of the nonlinear controllers are performed using energy considerations and Lyapunov methods. Under the assumption that the geomagnetic field is periodic, uniform global asymptotic stability is proved based on Krasovskii-LaSalle's Theorem. It is discussed if the assumption of a periodic geomagnetic field is realistic, from the satellites point of view. Different models for the internal and external geomagnetic field are presented. The controllers are also shown to be uniform global asymptotic stable without the assumption of a periodic geomagnetic field. Matrosov's Theorem ensures stability for non-periodic systems and is used in the thesis; therefore it is feasible to conclude that the nCube-controllers will be asymptotically stable irrespective of the periodicity of the geomagnetic field. The theoretical results are supported with simulations of the satellite and ADCS.

# CONTENTS

<b>I</b>	<b>Theoretical modeling</b>	<b>4</b>
<b>1</b>	<b>Introduction</b>	<b>5</b>
1.1	The nCube student satellite project . . . . .	5
1.2	Previous work . . . . .	6
1.3	Outline of the report . . . . .	6
1.4	Tools . . . . .	7
<b>2</b>	<b>Definitions and notations</b>	<b>8</b>
2.1	Reference frames . . . . .	8
2.2	Vector transformations . . . . .	8
2.2.1	Rotation matrix . . . . .	9
2.2.2	Attitude (Euler angles) . . . . .	10
2.2.3	Unit quaternions . . . . .	10
2.2.4	The inertia matrix . . . . .	10
2.2.5	Summary . . . . .	11
2.3	Lyapunov stability . . . . .	12
2.3.1	Positive definite function . . . . .	12
2.3.2	Stability of autonomous systems . . . . .	12
2.3.3	Uniform global stability . . . . .	13
2.3.4	Uniform global attractivity . . . . .	13
2.3.5	Uniform global asymptotic stability . . . . .	13
2.4	Periodic and non periodic systems . . . . .	13
<b>3</b>	<b>Mathematical modelling</b>	<b>14</b>
3.1	Satellite model . . . . .	14
3.1.1	Dynamics . . . . .	14
3.1.2	Kinematics . . . . .	14
3.2	Magnetic torque . . . . .	15
3.3	Gravitational torque . . . . .	16

3.4	Disturbance torques . . . . .	16
3.4.1	Solar radiation . . . . .	17
3.4.2	Aerodynamic torque . . . . .	19
3.4.3	Internal noise . . . . .	19
3.5	Linearization . . . . .	19
3.5.1	Linearization of the satellite model . . . . .	21
<b>4</b>	<b>Energy Considerations and Lyapunov Stability</b>	<b>23</b>
4.1	Energy Considerations . . . . .	23
4.2	Lyapunov function . . . . .	24
4.2.1	Finding the derivative of the lyapunov function . . . . .	24
<b>5</b>	<b>The Earth's magnetic field</b>	<b>26</b>
5.1	Internal magnetic field . . . . .	28
5.2	External magnetic field . . . . .	29
5.3	Magnetic anomalies . . . . .	30
5.4	International Geomagnetic Reference Field (IGRF) . . . . .	30
5.5	Periodicity in the geomagnetic field . . . . .	32
<b>6</b>	<b>Stabilization</b>	<b>33</b>
6.1	Periodic systems . . . . .	33
6.1.1	Krasovskii-LaSalle theorem . . . . .	33
6.1.2	Used on nCube . . . . .	34
6.2	Non periodic systems . . . . .	35
6.2.1	Matrosov's theorem . . . . .	35
6.2.2	Used on nCube . . . . .	36
<b>II</b>	<b>Control</b>	<b>38</b>
<b>7</b>	<b>ADCS design</b>	<b>39</b>
7.1	Mission requirements . . . . .	40
7.2	Determination . . . . .	40
7.3	Control modes . . . . .	40
7.3.1	Passive and active control . . . . .	40
7.3.2	Detumbling . . . . .	41
7.3.3	Stabilization . . . . .	41
7.3.4	Spin and Inverted boom recovery . . . . .	41

7.4	Evaluation of disturbances . . . . .	42
7.4.1	Solar radiation . . . . .	42
7.4.2	Gravity gradient torque . . . . .	42
7.4.3	Aerodynamic torque . . . . .	43
7.4.4	Resulting disturbing torques . . . . .	43
<b>8</b>	<b>Controller design</b>	<b>45</b>
8.1	Previous work in stabilization . . . . .	45
8.1.1	Energy based angular velocity feedback . . . . .	45
8.1.2	Energy based attitude feedback . . . . .	45
8.2	Linear control . . . . .	46
<b>9</b>	<b>Simulations</b>	<b>49</b>
9.1	Energy based controllers . . . . .	49
9.1.1	Angular velocity feedback . . . . .	49
9.1.2	Attitude feedback . . . . .	53
9.2	Linear control . . . . .	56
9.3	Comparison . . . . .	59
<b>III</b>	<b>Conclusion</b>	<b>60</b>
<b>10</b>	<b>Concluding remarks</b>	<b>61</b>
<b>IV</b>	<b>Appendix</b>	<b>64</b>
<b>A</b>	<b>Appendix; Detailed Derivations</b>	<b>65</b>
A.1	Devation of the total energy . . . . .	65
A.2	Obtaining the linearized satellite model . . . . .	65
<b>B</b>	<b>Appendix; Vectors and Skew-Symmetric Matrices</b>	<b>68</b>
<b>C</b>	<b>Appendix; STEC 2004</b>	<b>69</b>
<b>D</b>	<b>Appendix; nCube Poster</b>	<b>72</b>
<b>E</b>	<b>Appendix; Matlab and simulink</b>	<b>74</b>

**Part I**  
**Theoretical modeling**

# 1. INTRODUCTION

## 1.1. The nCube student satellite project

The nCube student satellite project was initiated and funded by the Norwegian Space Center with support from Andøya Rocket Range in 2001. The project is an experimental spacecraft that is developed and built by students from four Norwegian universities and is now in the integration and test phase. The four partners are Narvik University College, Norwegian University of Science and Technology (NTNU), Agricultural University of Norway and University of Oslo. The launch of the satellite will be in late 2004 from Kazakhstan.

nCube is based on the CubeSat concept. A CubeSat is a cube-shaped spacecraft with side length of  $10\text{cm}$  and a mass of  $1\text{kg}$ . The CubeSats are education spacecrafts that are of low cost and launched into low Earth Orbit. The concept was developed at Stanford University by Bob Twiggs.

The main mission of the satellite is to demonstrate ship movement surveillance from a satellite using the maritime Automatic Identification System (AIS) recently introduced by the International Maritime Organization (IMO). Another objective of the satellite project is to demonstrate reindeer herd monitoring from space by equipping a reindeer with a AIS transponder during a limited period.

The project was divided into five subtasks; Mechanical Structure, Power System, Attitude Determination and Control System (ADCS), Payload, Space Communication System (COM) and Ground Segment (GSEG). This thesis concerns the ADCS.

For more information on the nCube see <http://www.rocketrange.no/ncube> and for information on the CubeSat visit <http://www.cubesat.com>.

## 1.2. Previous work

This thesis is based on earlier work done on the ADCS which is accomplished by [2], [5], [6], [7], [21], [22] and [23]. By integrating measurements from a three-axis magnetometer with current measurements from the solar panels, the determination part of the ADCS is solved in a Kalman filter. The Control part is divided into active and passive control by using magnetic coils and a gravity boom respectively.

The boom is going to be 1,5m and has a tip made of lead. When the satellite is safely launched and in right orbit, the boom will be deployed. The gravitation boom was supposed to be of measuring tape. Measuring tape is quite flexible and if exposed for pressure at the tip it may result in wave motions in the measuring tape, which could lead to inverting the boom. Due to this it was decided that the boom should be made of copper-beryllium(CuBe). This material has greater stiffness and will not induce the same problem as for the measuring tape.

This thesis is concerns mainly the Control system for nCube and a summary of some of the previous work is presented in the control part of this report.

## 1.3. Outline of the report

Chapter 2 and 3 cover the definitions and equations necessary to model and understand the attitude dynamics of the satellite. Chapter 4 shows the energy considerations for nCube. Chapter 5 discusses some aspects of the geomagnetic field, while chapter 6 discusses stability of the satellite based on periodicity and nonperiodicity of the geomagnetic field. Chapter 7 discusses some control issues. Controllers are introduced in chapter 8 and simulation of the controller are done in chapter 9. Chapter 10 concludes the report.

Appendix A and B list some mathematical properties. Appendix C contains a short summary from the Space Technology Education Conference in Lausanne. Appendix D is a poster on the nCube project. Appendix E shows Simulink models and Matlab files.

## **1.4. Tools**

The report is written in Scientific Workplace. The controllers are designed and simulated in Simulink and Matlab.

## 2. DEFINITIONS AND NOTATIONS

### 2.1. Reference frames

This section introduces different reference frames for representing nCube's position and attitude.

**Inertial frame** The Earth-centered inertial frame (ECI) is an inertial frame for terrestrial navigation, which means that it is a nonacceleration reference frame in which Newton's laws of motion apply. The origin of the frame is orientated at the center of the Earth.

**Orbit frame** The orbit frame has its origin in the satellite's center of mass. The  $x_o$ -axis points in the normal direction of the orbital plane, while the  $z_o$ -axis points to the Earth center and the  $y_o$ -axis completes the right-hand orthogonal system.

**Body frame** The body-fixed reference frame is a moving coordinate frame which is fixed on the vessel. The axes are locked in the satellite,  $x_b$ -axis is forward,  $z_b$ -axis is downwards and the  $y_b$ -axis completes the right-hand orthogonal system. The origin is situated at the center of mass. The position and orientation of the vessel are described relative to the ECI frame see (2.20). The linear and angular velocity is expressed in the body-fixed reference frame.

### 2.2. Vector transformations

This section contains the main principles when transforming between different reference frames, and introduces unit quaternions and the inertia matrix.

### 2.2.1. Rotation matrix

The rotation matrix  $\mathbf{R} \in SO(3)$  between two frames  $a$  and  $b$  is denoted as  $\mathbf{R}_b^a$ .  $SO(3)$  is the *special group of order 3* is defined as:

$$SO(3) = \{\mathbf{R} | \mathbf{R} \in \mathbb{R}^{3 \times 3}, \mathbf{R} \text{ is orthogonal and } \det \mathbf{R} = 1\} \quad (2.1)$$

The rotation matrix is used to rotate between two frames, but can also be used to rotate within a reference frame. Through this paper the following notation will be used when transforming a vector from one coordinate frame to another:

$$r^{to} = \mathbf{R}_{from}^{to} r^{from} \quad (2.2)$$

**Definition 1.** (*Cross product operator*) The vector cross product  $\times$  is defined by:

$$\boldsymbol{\lambda} \times \mathbf{a} = \mathbf{S}(\boldsymbol{\lambda})\mathbf{a} \quad (2.3)$$

where  $\mathbf{S} \in SS(3)$  is defined as:

$$\mathbf{S}(\boldsymbol{\lambda}) = -\mathbf{S}^T(\boldsymbol{\lambda}) = \begin{bmatrix} 0 & -\lambda_3 & \lambda_2 \\ \lambda_3 & 0 & -\lambda_1 \\ -\lambda_2 & \lambda_1 & 0 \end{bmatrix}, \boldsymbol{\lambda} = \begin{bmatrix} \lambda_1 \\ \lambda_2 \\ \lambda_3 \end{bmatrix} \quad (2.4)$$

The angle-axis parameterization of the rotation matrix,  $\mathbf{R}_{\boldsymbol{\lambda}, \theta}$ , corresponding to a rotation  $\theta$  about the  $\boldsymbol{\lambda}$ -axis:

$$\mathbf{R}_{\boldsymbol{\lambda}, \theta} = \mathbf{I}_{3 \times 3} + \sin \theta \mathbf{S}(\boldsymbol{\lambda}) + (1 - \cos \theta) \mathbf{S}^2(\boldsymbol{\lambda}) \quad (2.5)$$

(where  $\mathbf{I}_{3 \times 3}$  is the identity matrix) is a useful parameterization.

**Definition 2.** (*Rotation matrix differential equation*) The time derivative of the rotation matrix between a frame  $a$  and a frame  $b$  is:

$$\dot{\mathbf{R}}_a^b = \mathbf{R}_a^b \mathbf{S}(\boldsymbol{\omega}_{ba}^a) \quad (2.6)$$

$\boldsymbol{\omega}_{ba}^a$  is the angular velocity of  $a$  with respect to  $b$  expressed in  $a$ .

### 2.2.2. Attitude (Euler angles)

The attitude ( $\Theta$ ) of a satellite can be represented by the roll( $\phi$ ), pitch( $\theta$ ) and yaw( $\psi$ ) angles,

$$\Theta = \begin{bmatrix} \phi \\ \theta \\ \psi \end{bmatrix} \quad (2.7)$$

where roll is the rotation about the  $x_0$ -axis, pitch about the  $y_0$ -axis and yaw about the  $z_0$ -axis. For the nCube satellite model the roll, pitch and yaw angles are only used as input and output to the simulation, internally quaternions are used.

### 2.2.3. Unit quaternions

The main reason for using unit quaternions or Euler parameters is to avoid singularity which can occur when using Euler angles. Euler parameters is a four-parameter method, where  $\mathbf{q}$  is a complex number with one real part  $\eta$  and three imaginary parts given by the  $\boldsymbol{\varepsilon}$  vector, where  $\theta$  is a rotation about the unit vector  $\boldsymbol{\lambda}$ :

$$\eta = \cos \frac{\theta}{2}, \quad \boldsymbol{\varepsilon} = \begin{bmatrix} \varepsilon_1 \\ \varepsilon_2 \\ \varepsilon_3 \end{bmatrix} = \boldsymbol{\lambda} \sin \frac{\theta}{2}, \quad \mathbf{q} = \begin{bmatrix} \eta \\ \varepsilon_1 \\ \varepsilon_2 \\ \varepsilon_3 \end{bmatrix} \quad (2.8)$$

Since the unit quaternion satisfies  $\mathbf{q}^T \mathbf{q} = \mathbf{1}$ , the set  $Q$  of unit quaternions are:

$$Q = \{\mathbf{q} | \mathbf{q}^T \mathbf{q} = \mathbf{1}, \mathbf{q} = [\eta, \boldsymbol{\varepsilon}]^T, \boldsymbol{\varepsilon} \in \Re^3 \text{ and } \eta \in \Re\} \quad (2.9)$$

which also means that:

$$\eta^2 + \varepsilon_1^2 + \varepsilon_2^2 + \varepsilon_3^2 = \mathbf{1} \quad (2.10)$$

From (2.8) and (2.9) the rotation matrix  $\mathbf{R}_{\boldsymbol{\varepsilon}, \eta}$  can be derived:

$$\mathbf{R}_{\boldsymbol{\varepsilon}, \eta} = \mathbf{I}_{3 \times 3} + 2\eta \mathbf{S}(\boldsymbol{\varepsilon}) + 2\mathbf{S}^2(\boldsymbol{\varepsilon}) \quad (2.11)$$

### 2.2.4. The inertia matrix

The inertia matrix  $\mathbf{I}_o \in \Re^{3 \times 3}$  about  $O$  (arbitrary origin) is defined according to [19]:

$$\mathbf{I}_o := \begin{bmatrix} I_x & -I_{xy} & -I_{xz} \\ -I_{yx} & I_y & -I_{yz} \\ -I_{zx} & -I_{zy} & I_z \end{bmatrix}, \quad \mathbf{I}_o = \mathbf{I}_o^T > 0 \quad (2.12)$$

where  $I_x, I_y$  and  $I_z$  are the moments of inertia about the  $x_b, y_b$  and  $z_b$ -axes, and  $I_{xy} = I_{yx}, I_{xz} = I_{zx}$  and  $I_{yz} = I_{zy}$  are the products of inertia defined as:

$$I_x = \int_V (y^2 + z^2) \rho_m dV; \quad I_{xy} = I_{yx} = \int_V xy \rho_m dV \quad (2.13)$$

$$I_y = \int_V (x^2 + z^2) \rho_m dV; \quad I_{xz} = I_{zx} = \int_V xz \rho_m dV \quad (2.14)$$

$$I_z = \int_V (x^2 + y^2) \rho_m dV; \quad I_{yz} = I_{zy} = \int_V yz \rho_m dV \quad (2.15)$$

If the axes of the body frame coincides with the principal axes of inertia, the inertia matrix reduces to:

$$\mathbf{I} = \begin{bmatrix} I_x & 0 & 0 \\ 0 & I_y & 0 \\ 0 & 0 & I_z \end{bmatrix} \quad (2.16)$$

Through out this paper the inertia matrix will be defined as  $\mathbf{I}$  while the identity matrix will be referred to as  $\mathbf{I}_{n \times n}$  or  $\mathbf{1}$ .

### 2.2.5. Summary

The rotation matrix between the orbit and body system is given as

$$\mathbf{R}_b^o(\mathbf{q}) = \mathbf{I}_{3 \times 3} + 2\eta \mathbf{S}(\boldsymbol{\varepsilon}) + 2\mathbf{S}^2(\boldsymbol{\varepsilon}) \quad (2.17)$$

More frequently the rotation matrix in the opposite direction is used

$$\mathbf{R}_o^b = (\mathbf{R}_b^o)^T \quad (2.18)$$

The matrix  $\mathbf{R}_o^b$  can be written as

$$\mathbf{R}_o^b = [\mathbf{c}_1^b \quad \mathbf{c}_2^b \quad \mathbf{c}_3^b], \quad (2.19)$$

where  $\mathbf{c}_i^b = [c_{ix}^b \quad c_{iy}^b \quad c_{iz}^b]^T$  are column vectors.  $\mathbf{c}_1^b, \mathbf{c}_2^b$  and  $\mathbf{c}_3^b$  are the projection of the  $x_o, y_o$  and  $z_o$  axes in the body frame. The deviation between the  $z_b$ -axis and the  $z_o$ -axis is  $c_{iz}^b$ , if  $c_{iz}^b$  equals to  $\pm 1$  the axes are aligned. The angular velocity of the body frame with respect to the orbit frame can be found by using:

$$\boldsymbol{\omega}_{ob}^b = \boldsymbol{\omega}_{ib}^b - \boldsymbol{\omega}_o \mathbf{c}_1^b = \boldsymbol{\omega}_{ib}^b - \mathbf{R}_o^b \boldsymbol{\omega}_{io}^o \quad (2.20)$$

## 2.3. Lyapunov stability

Lyapunov stability concern the stability of a systems equilibrium points. For more details see [3].

An autonomous system is defined;

$$\dot{x} = f(x) \tag{2.21}$$

A nonautonomous system is defined in (2.22), where  $f(\cdot, x)$  is continuous and  $f(t, \cdot)$  is locally Lipschitz uniformly in  $t$ .

$$\dot{x} = f(t, x) \tag{2.22}$$

### 2.3.1. Positive definite function

A function  $V(x)$  is positive definite if  $V(0) = 0$  and  $V(x) > 0$  for  $x \neq 0$ , and it is positive semidefinite if  $V(x) \geq 0$  for  $x \neq 0$ . A function is negative definite and negative semidefinite if  $-V(x)$  is positive definite or positive semidefinite, respectively.

A function  $V(t, x)$  is positive semidefinite if  $V(t, x) \geq 0$ . It is positive definite if  $V(t, x) \geq W_1(x)$  for some positive definite function  $W_1(x)$  and it is radially unbounded if  $W_1(x)$  is so, and decrescent if  $V(t, x) \leq W_2(x)$ .

### 2.3.2. Stability of autonomous systems

**Definition 3.** *The equilibrium point  $x = 0$  of (2.21) is stable in  $D \subset \mathbb{R}^n$  (the domain containing  $x$ ), if the continuously differentiable function  $V : D \rightarrow \mathbb{R}^n$*

$$\begin{aligned} V(0) &= 0 \text{ and } V(x) > 0 \text{ in } D - \{0\} \\ \dot{V}(x) &\leq 0 \text{ in } D - \{0\} \end{aligned} \tag{2.23}$$

*And asymptotically stable if*

$$\dot{V}(x) < 0 \text{ in } D - \{0\}$$

### 2.3.3. Uniform global stability

**Definition 4.** A continuous function  $\alpha : [0, a) \rightarrow [0, \infty)$  is said to belong to class  $\kappa$  if it is strictly increasing and  $\alpha(0) = 0$ . It is said to belong to class  $\kappa_\infty$  if  $a = \infty$  and  $\alpha(r) \rightarrow \infty$  as  $r \rightarrow \infty$ .

**Definition 5.** The origin of a nonautonomous system as (2.22) is said to be uniformly globally stable (UGS) if there exists  $\alpha \in \kappa_\infty$  such that, for each  $(t_o, x_o) \in \mathbb{R} \times \mathbb{R}^n$  each solution  $x(\cdot, t_o, x_o)$  satisfies (2.24).

$$|x(t, t_o, x_o)| \leq \alpha(|x_o|) \quad \forall t \geq t_o \quad (2.24)$$

### 2.3.4. Uniform global attractivity

**Definition 6.** The origin of a nonautonomous system as (2.22) is said to be uniformly globally attractive if for each  $r, \sigma > 0$  there exists  $T > 0$  such that (2.25) is satisfied for each solution.

$$|x_o| \leq r \implies \|x(t, t_o, x_o)\| \leq \sigma \quad \forall t \geq t_o + T \quad (2.25)$$

### 2.3.5. Uniform global asymptotic stability

A sufficient condition for uniform global asymptotic stability (UGAS) of the origin of the system (2.22) is if it is UGS and uniformly globally attractive.

## 2.4. Periodic and non periodic systems

A periodic function is a function whose values recur at fixed intervals as the variable uniformly increases. While a non periodic function is the opposite, and may not be predicted.

## 3. MATHEMATICAL MODELLING

### 3.1. Satellite model

#### 3.1.1. Dynamics

A satellite can be regarded as an ideal rigid body. The dynamic model of the satellite is derived using a Newton-Euler formulation, where the angular momentum change related to applied torque. The satellite model is:

$$\mathbf{I}\dot{\boldsymbol{\omega}}_{ib}^b + \boldsymbol{\omega}_{ib}^b \times (\mathbf{I}\boldsymbol{\omega}_{ib}^b) = \boldsymbol{\tau}^b, \boldsymbol{\tau}^b = \boldsymbol{\tau}_{grav}^b + \boldsymbol{\tau}_m^b \quad (3.1)$$

where  $\mathbf{I}$  is the moment of inertia see (2.12),  $\boldsymbol{\omega}_{ib}^b$  is the angular velocity of the body frame with respect to the inertial frame and  $\boldsymbol{\tau}^b$  are the torques acting on the satellite also decomposed in body frame.  $\boldsymbol{\tau}_{grav}^b$  is the gravitational torque working on the satellite body. This is an environmental torque which is exploited by rigging the satellite with a gravity boom, for passive stabilization.  $\boldsymbol{\tau}_m^b$  is the torque applied by the magnetic coils. Another way of representing (3.1) is:

$$\mathbf{I}\dot{\boldsymbol{\omega}}_{ib}^b + \mathbf{S}(\boldsymbol{\omega}_{ib}^b)\mathbf{I}\boldsymbol{\omega}_{ib}^b = \boldsymbol{\tau}^b \quad (3.2)$$

The angular velocity of the satellite relative to the inertial frame is expressed in the body frame according to (3.3).

$$\boldsymbol{\omega}_{ib}^b = \boldsymbol{\omega}_{io}^b + \boldsymbol{\omega}_{ob}^b = \mathbf{R}_o^b \boldsymbol{\omega}_{io}^o + \boldsymbol{\omega}_{ob}^b \quad (3.3)$$

Where  $\boldsymbol{\omega}_{io}^o$  is the angular velocity of the body frame with respect to the inertial frame.

#### 3.1.2. Kinematics

The kinematics describes the satellite's orientation in space and is derived by integration of the angular velocity. The angular velocity of the satellite model can

be described by unit quaternions and is formulated in (3.4).

$$\dot{\mathbf{q}} = \begin{bmatrix} \dot{\eta} \\ \dot{\boldsymbol{\varepsilon}} \end{bmatrix} = \frac{1}{2} \begin{bmatrix} -\boldsymbol{\varepsilon}^T \\ \eta \mathbf{I}_{3 \times 3} + \mathbf{S}(\boldsymbol{\varepsilon}) \end{bmatrix} \boldsymbol{\omega}_{ob}^b \quad (3.4)$$

To find the rotation velocity for the body frame relative to the orbit frame, see equation(3.5).

$$\boldsymbol{\omega}_{ob}^b = \boldsymbol{\omega}_{ib}^b - \boldsymbol{\omega}_o \mathbf{c}_1^b = \boldsymbol{\omega}_{ib}^b - \mathbf{R}_o^b \boldsymbol{\omega}_{io}^o \quad (3.5)$$

For more details about kinematics, see [1].

## 3.2. Magnetic torque

The actuator used on nCube is three magnetic coils, the background for this choice is presented in [5]. The basic idea behind the magnetic coils is based on reacting together with the Earth's magnetic field. The magnetic coil produces a magnetic dipole when currents flow through it's windings, which is proportional to the ampere-turns and the area enclosed by the coil. The actuator effect of the magnetic torquers will then have as purpose to react with the Earth's magnetic field to place the satellite in it's right attitude. The measurements of the geomagnetic field is done by magnetometers. The torque generated by the magnetic coils can be modelled as:

$$\boldsymbol{\tau}_m^b = \mathbf{m}^b \times \mathbf{B}^b \quad (3.6)$$

the magnetic dipolemoment generated by the coils  $\mathbf{m}^b$  is shown in (3.7) and  $\mathbf{B}^b = [B_x^b \ B_y^b \ B_z^b]^T$  is the local geomagnetic field vector, see Figure (5.5), relative to the satellite,

$$\mathbf{m}^b = \mathbf{m}_x^b + \mathbf{m}_y^b + \mathbf{m}_z^b = \begin{bmatrix} N_x i_x A_x \\ N_y i_y A_y \\ N_z i_z A_z \end{bmatrix} = \begin{bmatrix} m_x \\ m_y \\ m_z \end{bmatrix} \quad (3.7)$$

where  $N_k$  is number of windings in the magnetic coil,  $i_k$  is the coil current and  $A_k$  is the span area of the coil. An easy way of representing the magnetic torque is then:

$$\boldsymbol{\tau}_m^b = \mathbf{S}(\mathbf{m}^b) \mathbf{B}^b = \begin{bmatrix} B_z^b m_y - B_y^b m_z \\ B_x^b m_z - B_z^b m_x \\ B_y^b m_x - B_x^b m_y \end{bmatrix} \quad (3.8)$$

One off the effects of using magnetic torques is that they will contribute to the measurements of the Earth's magnetic field. According to [7] the maximal quantity of this contribution is  $3.42 \cdot 10^{-4} T$  *elsa* which is considerable larger than the

magnitude of the geomagnetic field, and must be compensated for in the controllers.

### 3.3. Gravitational torque

A satellite orbiting Earth is affected by the gravitational field (actually it is affected by every object in the universe but only the Earth's gravitational field is taken into consideration). The torque is derived in [6] and is used for passive stabilization with a gravity boom that will utilize this effect. When assuming homogenous mass distribution of the Earth, the gravity gradient is derived as:

$$\boldsymbol{\tau}_{grav} = \frac{3\mu}{R_0^3} \mathbf{u}_e \times (\mathbf{I} \mathbf{u}_e) \quad (3.9)$$

where:

$\mu = 3.986 \times 10^{14} m^3/s^2$	Earth's gravitational coefficient
$R_0$	Distance from Earth's center (m)
$\mathbf{I}$	Inertia matrix
$\mathbf{u}_e$	Unit vector toward nadir

Equation (3.9) in body frame yields:

$$\boldsymbol{\tau}_{grav} = 3\omega_o^2 \mathbf{c}_3^b \times (\mathbf{I} \mathbf{c}_3^b), \quad \omega_o^2 = \frac{\mu}{R_0^3} \quad (3.10)$$

The expression of the worst-case gravity torque is

$$\tau_{grav-worst} = \frac{3\mu}{2R_0^3} |I_z - I_x| \sin 2\theta \quad (3.11)$$

where  $I_z$  is the moment of inertia about  $z_b$ ,  $I_x$  is the moment of inertia about  $x_b$  and  $\theta$  is the deviation from nadir.

### 3.4. Disturbance torques

This section gives a description on some disturbance torques effecting nCube. The section is based on [8] and [9].

### 3.4.1. Solar radiation

Solar radiation are particles that are drawn of the Sun under solar activity. The solar radiation is a rather fluctuating perturbation and it has more effect at high altitudes. The solar radiation causes periodic variations in all of the orbital elements. It has most effect on light objects with a large surface. The surface area of the satellite which faces the Sun is essential when in determination of the resulting acceleration caused by solar radiation.

The intensity of the solar radiation varies over time, this makes the determination of its energy and frequencies difficult. Most analysis uses the solar radiation constant  $SF$ :

$$SF = 1353 \text{ W/m}^2 \quad (3.12)$$

the force of solar pressure,  $p_{SR}$ , per unit area is then given by (3.13) where  $c$  is the speed of light.

$$p_{SR} = \frac{SF}{c} = \frac{1353}{3 \times 10^8} \frac{\text{W/m}^2}{\text{m/s}} = 4.51 \times 10^{-6} \text{ N/m}^2 \quad (3.13)$$

**Remark 1.** *More exact calculation of solar radiation constant will change the value of the solar pressure.*

The expression of the force due to solar radiation on the satellite then becomes:

$$F_{SR} = -p_{SR} * c_R * A_{\odot} * r_{\oplus\odot} \quad (3.14)$$

Where  $A_{\odot}$  is the exposed area to the Sun. ( $\odot$  is the symbol for the Sun.) The reflectivity,  $c_R$ , indicates how the satellite reflects incoming radiation, and its value is between 0.0 and 2.0. If  $c_R$  equals the value 0.0 the object is transparent to solar radiation forces, but there may arise some refraction. If the value is 1.0 all the radiation is absorbed (black body), and the value 2.0 then indicates that all the radiation is reflected and twice the force is transmitted to the satellite. For a satellite of various materials  $c_R$  is virtually impossible to predict. Because  $c_R$  is time variant and the constant change in orientation of the object. The reflectivity should thus be determined by differential correction to a parameter, in most cases.

The reflection process is shown in Figure (3.1). The incident beam, or *solar radiation pressure* ( $p_{SR}$ ), reaches the surface area facing the sun at an incident

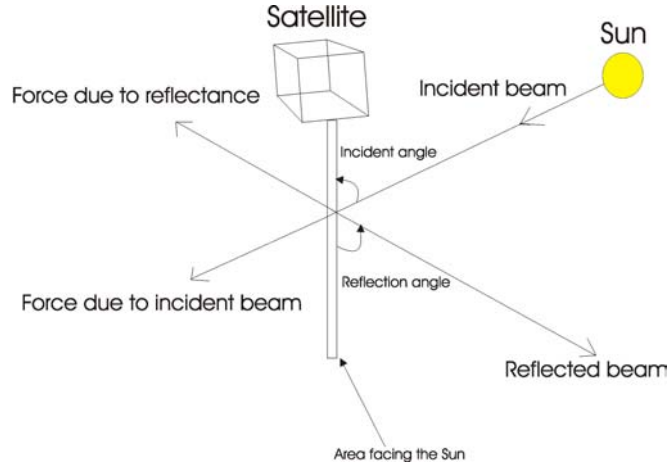


Figure 3.1: The incident and corresponding reflection beam, and forces.

angle  $\phi_{inc}$  and results in a force  $F_{inc}$  on the satellite. The solar radiation pressure is then reflected with an angle  $\phi_{ref}$  and results in a force  $F_{ref}$  on the satellite. Assuming that the surface  $A_{\odot}$  maintains a constant attitude perpendicular to the Sun, implies setting  $\phi_{inc} = 0$ .

**Remark 2.** *Setting  $\phi_{inc} = 0$  is not very realistic but it gives a rough estimate of the solar radiation problem.*

Using Newtons second law makes it possible to determine the acceleration with the given force:

$$a_{radiation} = \frac{F_{SR}}{m} = \frac{p_{SR} * c_R * A_{\odot}}{m} \quad (3.15)$$

The direction of the acceleration will always be away from the Sun see, (3.1), therefore a unit vector to the satellite to the Sun gives the correct direction. The acceleration vector then becomes:

$$\vec{a}_{radiation} = \frac{p_{SR} * c_R * A_{\odot}}{m} \frac{\vec{r}_{\odot sat}}{|\vec{r}_{\odot sat}|} \quad (3.16)$$

Equation (3.16) is commonly used for numerical simulations, where it is favorable that  $A_{\odot}$  is some average effective cross-section that implicitly incorporates  $c_R$ . The worst case expression of the resulting torque can be expressed as:

$$\tau_{solarradiation} = F_{SR}(c_{pSR} - cg) \quad (3.17)$$

where  $c_{pSR}$  is the center of pressure and  $cg$  is the center of mass of the satellite.

### 3.4.2. Aerodynamic torque

Satellites orbiting the Earth at low altitude will be influenced by the air density. This may reduce the velocity of the satellite, and the result will be lower altitude for the satellite. The torque is written:

$$\tau_{aero} = \frac{1}{2}\rho V^2 C_d A_{inc} (\mathbf{u}_v \times (\mathbf{c}_{pa} - \mathbf{c}g)), \quad F_{aero} = \frac{1}{2}\rho V^2 C_d A_{inc} \quad (3.18)$$

where:

$\rho$	Atmospheric density ( $kg/m^3$ )
$A_{inc}$	Area perpendicular to $\mathbf{u}_v$ ( $m^2$ )
$\mathbf{u}_v$	Unit vector in velocity direction
$C_d$	Drag coefficient
$V$	Velocity ( $m/s$ )
$\mathbf{c}_{pa}$	Center of pressure
$\mathbf{c}g$	Center of gravity

The worst-case expression of the torque is:

$$\tau_{aero} = F_{aero}(\mathbf{c}_{pa} - \mathbf{c}g) \quad (3.19)$$

The effect of the aerodynamic torque will probably be negligible due to nCube's small size.

### 3.4.3. Internal noise

This disturbance torque is caused by sources inside the satellite. The magnetic field generated by the electric circuits will interact with the geomagnetic field. According to the Ørsted satellite project this is 10% of the commanded torque. To reduce the influence of these disturbances it is important that the satellites electric circuits are constructed to induce a minimal magnetic field. In the magnetometers on nCube there will also be included a lowpass filter to avoid high peaks of magnetic disturbances.

## 3.5. Linearization

This section contains the linearized satellite model, which makes the satellite easier to analyze. This is done since we are to derive linear controllers.

**Kinematics** The kinematics of the satellite is described in (3.4) as:

$$\dot{\mathbf{q}} = \begin{bmatrix} \dot{\eta} \\ \dot{\boldsymbol{\varepsilon}} \end{bmatrix} = \frac{1}{2} \begin{bmatrix} -\boldsymbol{\varepsilon}^T \\ \eta \mathbf{I}_{3 \times 3} + \mathbf{S}(\boldsymbol{\varepsilon}) \end{bmatrix} \boldsymbol{\omega}_{ob}^b \quad (3.20)$$

We linearize the system around the points  $\eta = 1$  and  $\boldsymbol{\varepsilon} = 0$  which results in the system:

$$\dot{\mathbf{q}} = \begin{bmatrix} \dot{\eta} \\ \dot{\boldsymbol{\varepsilon}} \end{bmatrix} = \begin{bmatrix} 0 \\ \frac{1}{2} \boldsymbol{\omega}_{ob}^b \end{bmatrix}, \quad \boldsymbol{\omega}_{ob}^b = 2\dot{\boldsymbol{\varepsilon}} \quad (3.21)$$

**Rotation matrix** The linearization of the rotation matrix between body and orbit frame (2.17), around the points  $\eta = 1$  and  $\boldsymbol{\varepsilon} = 0$  results in the linearized rotation matrix:

$$\mathbf{R}_b^o = \mathbf{I}_{3 \times 3} + 2\mathbf{S}(\boldsymbol{\varepsilon}) \quad (3.22)$$

**Angular velocity** From equation (2.18) we have that:

$$\mathbf{R}_o^b = (\mathbf{R}_b^o)^T \quad (3.23)$$

Using this together with (3.22) the linearized expression for  $\mathbf{R}_o^b$  becomes:

$$\mathbf{R}_o^b = \mathbf{I}_{3 \times 3} - 2\mathbf{S}(\boldsymbol{\varepsilon}) \quad (3.24)$$

which means that:

$$\mathbf{R}_o^b = 2 \begin{bmatrix} \frac{1}{2} & \varepsilon_3 & -\varepsilon_2 \\ -\varepsilon_3 & \frac{1}{2} & \varepsilon_1 \\ \varepsilon_2 & -\varepsilon_1 & \frac{1}{2} \end{bmatrix} \quad (3.25)$$

The angular velocity in body frame relative to inertial frame was derived in (3.3) as:

$$\boldsymbol{\omega}_{ib}^b = \mathbf{R}_o^b \boldsymbol{\omega}_{io}^o + \boldsymbol{\omega}_{ob}^b \quad (3.26)$$

Insertion of (3.25) and (3.21) in (3.26) results in the linearized model for  $\boldsymbol{\omega}_{ib}^b$  (3.27).

$$\boldsymbol{\omega}_{ib}^b = \begin{bmatrix} \omega_x \\ \omega_y \\ \omega_z \end{bmatrix} = \begin{bmatrix} 2\dot{\varepsilon}_1 - 2\omega_o \varepsilon_3 \\ 2\dot{\varepsilon}_2 + \omega_o \\ 2\dot{\varepsilon}_3 + 2\omega_o \varepsilon_1 \end{bmatrix} \quad (3.27)$$

the time derivative of  $\boldsymbol{\omega}_{ib}^b$  is then:

$$\dot{\boldsymbol{\omega}}_{ib}^b = \begin{bmatrix} \dot{\omega}_x \\ \dot{\omega}_y \\ \dot{\omega}_z \end{bmatrix} = \begin{bmatrix} 2\ddot{\varepsilon}_1 - 2\omega_o \dot{\varepsilon}_3 \\ 2\ddot{\varepsilon}_2 \\ 2\ddot{\varepsilon}_3 - 2\omega_o \dot{\varepsilon}_1 \end{bmatrix} \quad (3.28)$$

**Gravitational torque** According to [7] the gravitational torque can be expressed by quaternions according to (3.29) in body frame,

$$\tau_{grav}^b = 3\omega_o^2 \begin{bmatrix} 2(I_z - I_y)(\varepsilon_2\varepsilon_3 + \eta\varepsilon_1)(1 - 2(\varepsilon_1^2 + \varepsilon_2^2)) \\ 2(I_x - I_z)(\varepsilon_1\varepsilon_3 + \eta\varepsilon_2)(1 - 2(\varepsilon_1^2 + \varepsilon_2^2)) \\ 4(I_y - I_x)(\varepsilon_1\varepsilon_1 + \eta\varepsilon_2)(\varepsilon_2\varepsilon_3 + \eta\varepsilon_1) \end{bmatrix} \quad (3.29)$$

Linearized around  $\eta = 1$  and  $\varepsilon = 0$ :

$$\tau_{grav}^b = 3\omega_o^2 \begin{bmatrix} (I_z - I_y)\varepsilon_1 \\ (I_z - I_x)\varepsilon_2 \\ 0 \end{bmatrix} \quad (3.30)$$

**Magnetometer torques** The magnetometer torque is expressed in (3.6) may be represented in orbit frame by using (2.17):

$$\tau_m^b = \mathbf{S}(\mathbf{m}^b)\mathbf{B}^b = \mathbf{S}(\mathbf{m}^b)\mathbf{R}_o^o\mathbf{B}^o = \mathbf{S}(\mathbf{m}^b) [\mathbf{I}_{3 \times 3} - 2\eta\mathbf{S}(\varepsilon) + 2\mathbf{S}^2(\varepsilon)] \mathbf{B}^o \quad (3.31)$$

linearization around  $\eta = 1$  and  $\varepsilon = 0$  gives:

$$\tau_m^b = \mathbf{S}(\mathbf{m}^b)\mathbf{B}^o = \begin{bmatrix} B_z^o m_y - B_y^o m_z \\ B_x^o m_z - B_z^o m_x \\ B_y^o m_x - B_x^o m_y \end{bmatrix} \quad (3.32)$$

### 3.5.1. Linearization of the satellite model

Equation (3.1), (3.29) and (3.31) results in the satellite model:

$$\mathbf{I}\dot{\boldsymbol{\omega}}_{ib}^b = -\boldsymbol{\omega}_{ib}^b \times (\mathbf{I}\boldsymbol{\omega}_{ib}^b) + \tau_{grav}^b + \mathbf{S}(\mathbf{m}^b)\mathbf{B}^o \quad (3.33)$$

produce as components results in (this is deduced in Appendix A.2):

$$\begin{aligned} \ddot{\varepsilon}_1 &= (1 - k_x)\omega_o\dot{\varepsilon}_3 - 4k_x\omega_o^2\varepsilon_1 + \frac{1}{2I_x}(B_z^o m_y - B_y^o m_z) \\ \ddot{\varepsilon}_2 &= -3k_y\omega_o^2\varepsilon_2 + \frac{1}{2I_y}(B_x^o m_z - B_z^o m_x) \\ \ddot{\varepsilon}_3 &= -(1 - k_z)\omega_o\dot{\varepsilon}_1 - k_z\omega_o^2\varepsilon_3 + \frac{1}{2I_x}(B_y^o m_x - B_x^o m_y) \end{aligned} \quad (3.34)$$

where:

$$\begin{aligned}
k_x &= \frac{I_y - I_z}{I_x} \\
k_y &= \frac{I_x - I_z}{I_y} \\
k_z &= \frac{I_y - I_x}{I_z}
\end{aligned} \tag{3.35}$$

Introducing the state vector  $\mathbf{x}$  and torque vector  $\mathbf{u}$ :

$$\mathbf{x} = \left[ \varepsilon_1 \quad \dot{\varepsilon}_1 \quad \varepsilon_2 \quad \dot{\varepsilon}_2 \quad \varepsilon_3 \quad \dot{\varepsilon}_3 \right]^T \tag{3.36}$$

$$\mathbf{u} = \left[ m_x \quad m_y \quad m_z \right]^T \tag{3.37}$$

the model can be written as:

$$\dot{\mathbf{x}}(t) = \mathbf{A}\mathbf{x}(t) + \mathbf{B}(t)\mathbf{u}(t) \tag{3.38}$$

where  $\mathbf{A}$  and  $\mathbf{B}(t)$  are matrices:

$$\mathbf{A} = \begin{bmatrix} 0 & 1 & 0 & 0 & 0 & 0 \\ -4k_x\omega_o^2 & 0 & 0 & 0 & 0 & (1 - k_x)\omega_o \\ 0 & 0 & 0 & 1 & 0 & 0 \\ 0 & 0 & -3k_y\omega_o^2 & 0 & 0 & 0 \\ 0 & 0 & 0 & 0 & 0 & 1 \\ 0 & -(1 - k_z)\omega_o & 0 & 0 & -k_z\omega_o^2 & 0 \end{bmatrix} \tag{3.39}$$

and

$$\mathbf{B}(t) = \begin{bmatrix} 0 & 0 & 0 \\ 0 & \frac{1}{2I_x}B_z^o & -\frac{1}{2I_x}B_y^o \\ 0 & 0 & 0 \\ -\frac{1}{2I_y}B_z^o & 0 & \frac{1}{2I_y}B_x^o \\ 0 & 0 & 0 \\ \frac{1}{2I_z}B_y^o & -\frac{1}{2I_z}B_x^o & 0 \end{bmatrix} \tag{3.40}$$

## 4. ENERGY CONSIDERATIONS AND LYAPUNOV STABILITY

### 4.1. Energy Considerations

The total energy of the satellite is divided into kinetic and potential energy. The kinetic energy is principally a result of the rotation in the inertial and orbit frame. The sources for the potential energy is the gravity gradient and gyro effects due to revolution about the Earth. The expressions is based on [2] and [10].

**Kinetic energy** The expression for the kinetic energy is revolved in body frame with respect to the orbit frame, and assuming a near circular orbit makes the orbit rate  $\omega_o$  constant.

$$E_{kin} = \frac{1}{2}(\omega_{ob}^b)^T \mathbf{I} \omega_{ob}^b \quad (4.1)$$

**Potential energy** The potential energy due to the gravity gradient is represented in (4.2) and the potential energy due to revolution of the satellite about the Earth is given in (4.3).

$$E_{gg} = \frac{3}{2}\omega_o^2((\mathbf{c}_3^b)^T \mathbf{I} \mathbf{c}_3^b - I_z) \quad (4.2)$$

$$E_{gyro} = \frac{1}{2}\omega_o^2(I_x - (\mathbf{c}_1^b)^T \mathbf{I} \mathbf{c}_1^b) \quad (4.3)$$

**Total energy**

$$E_{tot} = E_{kin} + E_{gg} + E_{gyro} \quad (4.4)$$

Complete form of the total energy

$$E_{tot} = \frac{1}{2}(\omega_{ob}^b)^T \mathbf{I} \omega_{ob}^b + \frac{3}{2}\omega_o^2((\mathbf{c}_3^b)^T \mathbf{I} \mathbf{c}_3^b - I_z) + \frac{1}{2}\omega_o^2(I_x - (\mathbf{c}_1^b)^T \mathbf{I} \mathbf{c}_1^b) \quad (4.5)$$

The terms of the total energy may also be represented as in (4.6) which is derived in Appendix A.

$$E_{tot} = \frac{1}{2}(\omega_{ob}^b)^T \mathbf{I} \omega_{ob}^b + \frac{3}{2}\omega_o^2((I_x - I_z)c_{13}^2 + (I_y - I_z)c_{23}^2) + \frac{1}{2}\omega_o^2((I_x - I_y)c_{21}^2 + (I_x - I_z)c_{31}^2) \quad (4.6)$$

## 4.2. Lyapunov function

**Proposition 1.** *The lyapunov candidate*

$$\mathbf{V}(\mathbf{x}) = E_{tot} \quad (4.7)$$

where  $E_{tot}$  is defined in (4.5) satisfies

$$\mathbf{V}(\mathbf{0}) = 0 \quad (4.8)$$

$$\mathbf{V}(\mathbf{x}) > 0 \quad \forall \mathbf{x} \neq \mathbf{0} \quad (4.9)$$

when the four equilibria of  $\mathbf{V}(\mathbf{0})$  is

$$\{(\omega_{ob}^b, \mathbf{c}_1^b, \mathbf{c}_3^b) : (0, \pm \mathbf{c}_1^o, \pm \mathbf{c}_3^o)\} \quad (4.10)$$

**Proof.** From (4.6) it is clear that

$$\mathbf{x} = [\omega_{ob}^b, \mathbf{c}_{21}, \mathbf{c}_{31}, \mathbf{c}_{13}, \mathbf{c}_{23}]^T \quad (4.11)$$

so if  $\mathbf{x} = \mathbf{0}$  then  $\mathbf{V}(\mathbf{0}) = 0$ . To ensure that  $\mathbf{V}(\mathbf{x}) > 0 \quad \forall \mathbf{x} \neq \mathbf{0}$  the requirement for the inertial constrains is then

$$I_x > I_y > I_z \quad (4.12)$$

and the energy function is positive definite. ■

### 4.2.1. Finding the derivative of the lyapunov function

**Proposition 2.** *The time derivative of  $\mathbf{V}$  is*

$$\dot{\mathbf{V}} = (\omega_{ob}^b)^T \tau_m^b \quad (4.13)$$

where  $\tau_m^b$  is the moment generated by the magnetic coils.

**Proof.** The time derivative of  $\mathbf{V}$  (4.5) is

$$\dot{\mathbf{V}} = \frac{1}{2}(\omega_{ob}^b)^T \mathbf{I} \dot{\omega}_{ob}^b + 3\omega_o^2 (\mathbf{c}_3^b)^T \mathbf{I} \dot{\mathbf{c}}_3^b - \omega_o^2 (\mathbf{c}_1^b)^T \mathbf{I} \dot{\mathbf{c}}_1^b \quad (4.14)$$

The satellites dynamics (3.1):

$$\mathbf{I} \dot{\omega}_{ib}^b + \omega_{ib}^b \times (\mathbf{I} \omega_{ib}^b) = \boldsymbol{\tau}_m^b + 3\omega_o^2 \mathbf{c}_3^b \times (\mathbf{I} \mathbf{c}_3^b) \quad (4.15)$$

Based on the following relations inserted in (4.15): ((4.17) is the same as (2.6).)

$$(\omega_{ob}^b)^T \mathbf{S}(\omega_{ob}^b) = 0 \quad (4.16)$$

$$\dot{\mathbf{c}}_i^b = \mathbf{S}(\mathbf{c}_i^b) \omega_{ob}^b \quad (4.17)$$

$$\omega_{ib}^b = \omega_{ob}^b + \omega_o \mathbf{c}_1^b \implies \quad (4.18)$$

$$\dot{\omega}_{ib}^b = \dot{\omega}_{ob}^b + \omega_o \dot{\mathbf{c}}_1^b \iff \dot{\omega}_{ib}^b = \dot{\omega}_{ob}^b + \omega_o \mathbf{S}(\mathbf{c}_1^b) \omega_{ob}^b \quad (4.19)$$

the expression for  $\mathbf{I} \dot{\omega}_{ob}^b$  becomes:

$$\mathbf{I} \dot{\omega}_{ob}^b = -\mathbf{I} \omega_o \mathbf{S}(\mathbf{c}_1^b) \omega_{ob}^b - \omega_{ob}^b - \omega_o \mathbf{c}_1^b \mathbf{S}(\mathbf{I} \omega_{ob}^b + \omega_o \mathbf{c}_1^b) + \boldsymbol{\tau}_m^b + 3\omega_o^2 \mathbf{c}_3^b \mathbf{S}(\mathbf{I} \mathbf{c}_3^b) \quad (4.20)$$

inserted in (4.14) gives:

$$\dot{\mathbf{V}} = \frac{1}{2}(\omega_{ob}^b)^T (-\mathbf{I} \omega_o \mathbf{S}(\mathbf{c}_1^b) \omega_{ob}^b - \omega_{ob}^b - \omega_o \mathbf{c}_1^b \mathbf{S}(\mathbf{I} \omega_{ob}^b + \omega_o \mathbf{c}_1^b) + \boldsymbol{\tau}_m^b + 3\omega_o^2 \mathbf{c}_3^b \mathbf{S}(\mathbf{I} \mathbf{c}_3^b)) + 3\omega_o^2 (\mathbf{c}_3^b)^T \mathbf{I} \mathbf{S}(\mathbf{c}_3^b) \omega_{ob}^b - \omega_o^2 (\mathbf{c}_1^b)^T \mathbf{I} \mathbf{S}(\mathbf{c}_1^b) \omega_{ob}^b \quad (4.21)$$

$$\quad (4.22)$$

using (B.7) shows that:

$$\dot{\mathbf{V}} = (\omega_{ob}^b)^T \boldsymbol{\tau}_m^b \quad (4.23)$$

as stated. ■

## 5. THE EARTH'S MAGNETIC FIELD

Attitude control with magnetic coils is based on measurement of the geomagnetic field. nCube use magnetometers to measure the geomagnetic field. The ability to measure the geomagnetic field will influence the performance of the attitude control system. This thesis investigates how the geomagnetic field will affect the stability of the satellite.

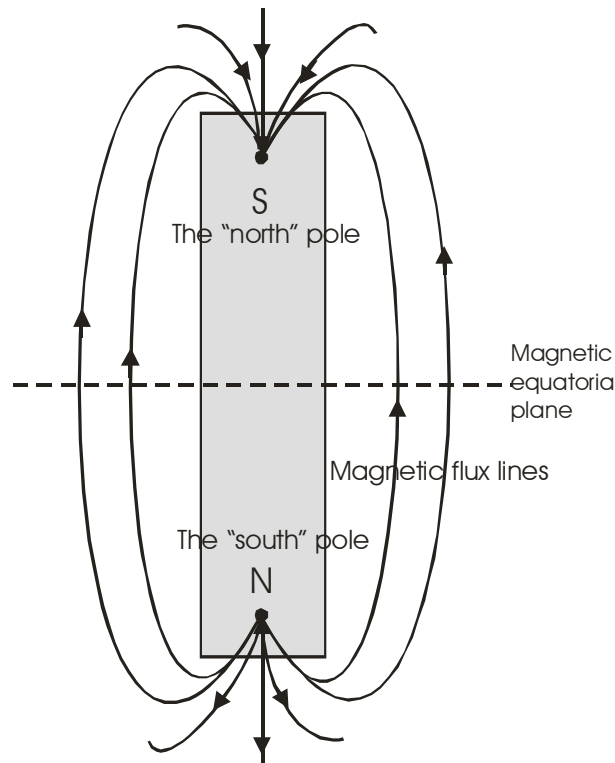


Figure 5.1: Basic dipolar magnet.

The basic concept of geomagnetism is shown in Figure 5.1. Magnetic flux is

developed in proximity of a bar magnet and it flows from one end of the bar to the other. The points within the magnet where the flux converges are known as the poles of the magnet. For more details, see [11]. The total measured magnetic field is divided into four different sources, described in (5.1). The geomagnetic field varies in strength from about  $25000nT$  (nanoTesla) in equatorial regions to about  $70000nT$  at the poles.

$$\mathbf{B}_{observed} = \mathbf{B}_{internal} + \mathbf{B}_{external} + \mathbf{B}_{local} + \mathbf{B}_{disturbance} \quad (5.1)$$

$\mathbf{B}_{internal}$	Sources inside the earth, weak time-dependence.
$\mathbf{B}_{external}$	Sources outside the earth, strong time-dependence.
$\mathbf{B}_{reference}$	$\mathbf{B}_{internal} + \mathbf{B}_{external}$ are far from localized anomalies.
$\mathbf{B}_{local}$	Local variations, caused by local inhomogenities.
$\mathbf{B}_{disturbance}$	Magnetic disturbances from electronics in the satellite.

This chapter gives a view of some aspects of these geomagnetic sources, first a short introduction to the quantified  $\mathbf{B}_{reference}$  and then the local variations  $\mathbf{B}_{local}$ . The IGRF model is introduced. The  $\mathbf{B}_{disturbance}$  is discussed in Chapter 7.4.4.

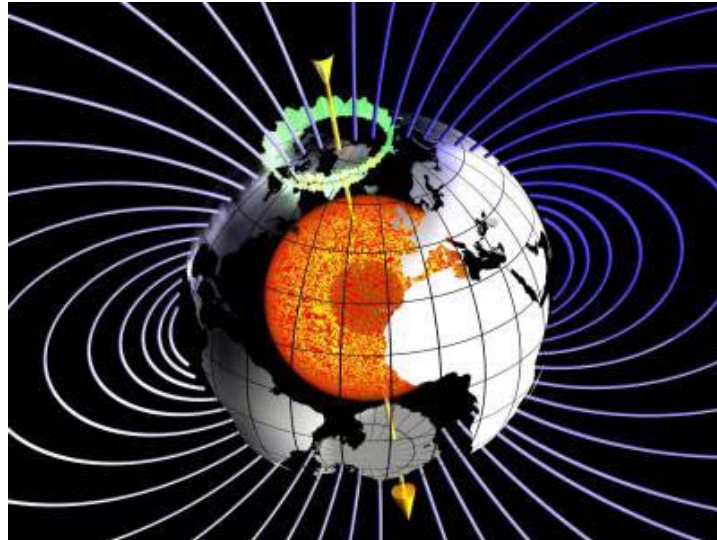


Figure 5.2: The Earth's self-sustaining dynamo operating in the fluid outer-core. The figure is from [14].

## 5.1. Internal magnetic field

The internal magnetic field is the main component of the geomagnetic field. Some of the sources are shown in Figure 5.3. It is also called the dipolar field, as it behaves like a dipolar electromagnet, see Figure 5.1, where the center is in the middle of the earth and it is inclined at  $11,5^\circ$  of the rotation axis. According to [11], 90% of the total geomagnetic field can be represented through the theoretical dipolar magnetic field.

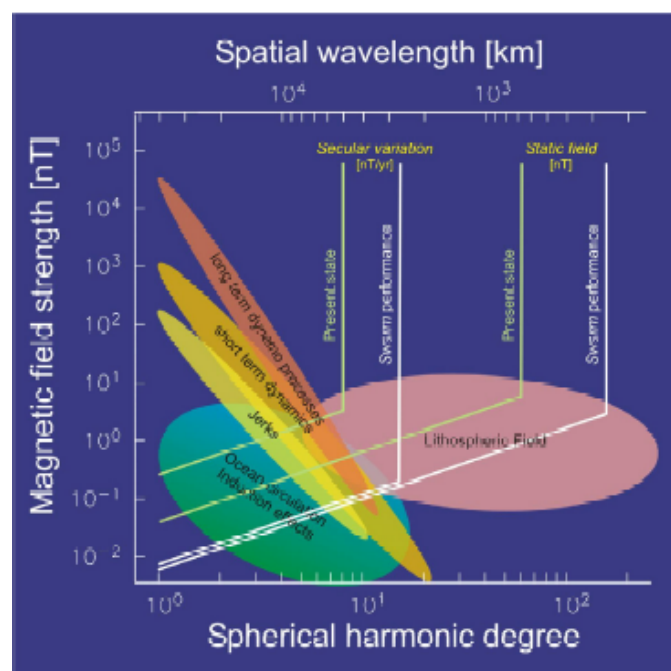


Figure 5.3: Signal amplitude at orbit altitude of the contributions from processes contributing to the magnetic field as a function of spatial scale. Source terms from within the solid Earth and the oceans. The figure is from [13].

The cause of the internal geomagnetic field is attributed to a dynamo action produced by circulation of charged particles in coupled convective cells within the outer, fluid part of the Earth's core. See Figure 5.2. The periodic polarity changes of the geomagnetic field is caused by the cells exchange of dominance.

The circulation patterns in the core are not fixed and change slowly with time. They are called *secular variations* and are predictable.

## 5.2. External magnetic field

The magnetic effects caused by external origins makes the geomagnetic field vary on a daily and local basis. External magnetic effects is also called *diurnal variations*. The diurnal variations are divided into two types of days: quiet days (Q) and disturbed days (D).

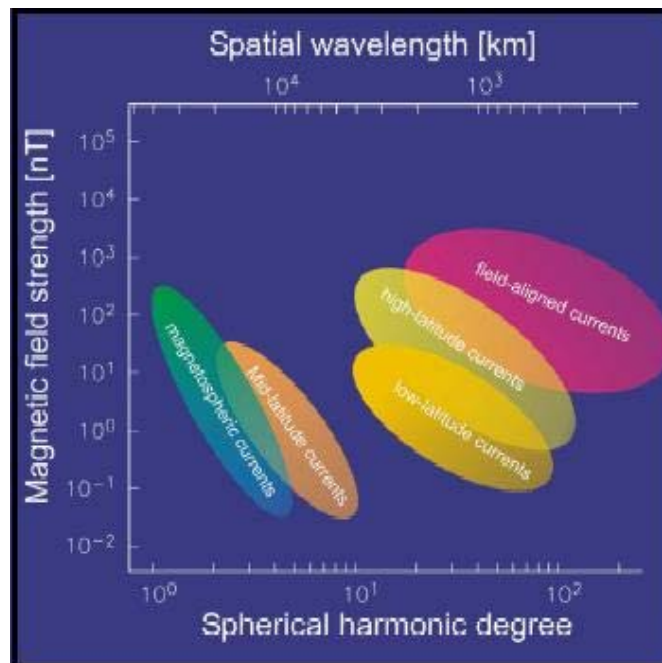


Figure 5.4: Signal amplitude at orbit altitude of the contributions from processes contributing to the magnetic field as a function of spatial scale, from external geomagnetic sources. The figure is from [13].

**Q-days** Quiet days may also be referred to as normal conditions. The diurnal variations are smooth and regular and has an amplitude of approximately  $20 - 80nT$ , with a maximum in polar regions. The source for the variations is the magnetic field induced by the flow of charged particles within the ionosphere towards the magnetic poles.

**D-days** In contrast to the regular diurnal variations of a quiet day, disturbed days involves large short-term disturbances in the geomagnetic field. The amplitudes of a D-day variation may be up to  $1000nT$ , often called magnetic storms. The source for the magnetic storm is usually a result of intense solar activity which lead to charged solar particles in the ionosphere. Under these storms magnetic surveying should be discontinued because of the impossibility of correcting such rapid changes in the amplitude of the geomagnetic field.

According to [13] the external current system is ordered primarily by local time, unlike the Earth-fixed internal sources. To cover the various geomagnetic field it is needed a dedicated space-time strategy. Sources for the external magnetic field are shown in Figure 5.4.

### 5.3. Magnetic anomalies

Common causes of magnetic anomalies include dykes, faulted, folded or truncated sills and lava flows, massive basic intrusions, metamorphic basement rocks and magnetite ore bodies. The magnetic anomalies are superimposed on the geomagnetic field in both amplitude and direction. The anomalies range in amplitude from a few tens of  $nT$  over deep metamorphic basement to several hundred  $nT$  over basic intrusions and may reach an amplitude of several thousand  $nT$  over magnetite ores.

### 5.4. International Geomagnetic Reference Field (IGRF)

If the internal geomagnetic field is subtracted from the observed magnetic field, the residual field can then be approximated by the effects of a second, smaller, dipole. To simulate the observed geomagnetic field, this approximation can be done to a required degree of accuracy. This method is known as a spherical harmonic analysis, and is used to compute the International Geomagnetic Reference Field (IGRF), which defines the theoretical undisturbed geomagnetic field at any point

on the Earth's surface. The geomagnetic field used in the satellite model is the IGRF model created by the IAGA (International Association of Geomagnetism and Aeronomy). The IGRF model is revised every fifty year, and in the simulations of nCube the IGRF2000 is used, computed from (5.2) according to [12].

$$V(r, \theta, \phi) = a \sum_{n=1}^{\infty} \sum_{m=0}^n \left(\frac{a}{r}\right)^{n+1} (g_n^m \cos(m\phi) + h_n^m \sin(m\phi) P_n^m(\cos(\theta))) \quad (5.2)$$

Here  $V$  is the potential function of the field about the Earth (given in spherical coordinates in ECEF frame),  $a$  is the mean radius of the Earth. The  $P_n^m(\cos(\theta))$  are Schmidt quasynormalized associated Legendre functions of degree  $n$  and order  $m$ . And  $g_n^m$  and  $h_n^m$  are the constant Gaussian.

Figure 5.5 shows the geomagnetic field  $\mathbf{B}^o = [B_x^o \ B_y^o \ B_z^o]^T$  computed in the orbit frame using a 10th order spherical harmonic model, using IGRF2000 coefficients.

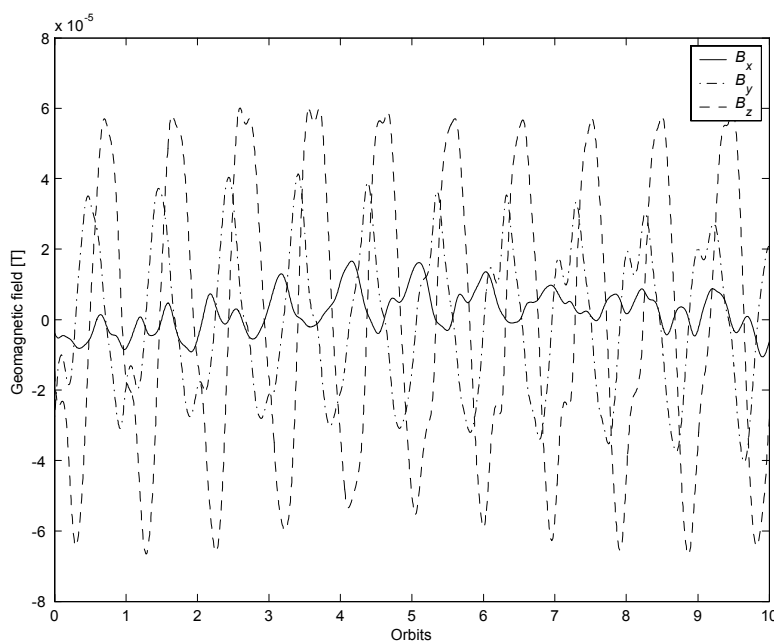


Figure 5.5: Local geomagnetic field  $\mathbf{B}^o$ , the IGRF2000 coefficients.

## 5.5. Periodicity in the geomagnetic field

The geomagnetic field seen from a satellite in a Earth near polar orbit is illustrated in Figure 5.5. Thus from nCube's point of view the geomagnetic field will approximately be periodic. This is a sufficient approximation due to the fact that the nonperiodic diurnal variations is of a much lower magnitude than the internal geomagnetic field. Stability of the satellite should also be proven for a non periodic geomagnetic field model. On days with intense solar activity it will affect the satellite though these days are rater seldom according to [15]. Figure 5.3 and Figure 5.4 are summarized in the following table, based on data from [13]. The first 5 rows are internal sources while row 6 is external sources.

<b>Source</b>	<b>Time range</b>	<b>Size</b>	<b>Wavelength (wl)</b>
Core dynamics and	static	$\pm 65000nT$	3000 – <i>global</i> km wl
geodynamo processes	3 months/decades	$\pm 200nT$	2800 – <i>global</i> km wl
Lithosphere	decades/static	$\pm 25nT$	300 – 3000 km wl
3-D conductivity	hours/years	$\pm 200nT$	300 – <i>global</i> km wl
Ocean circulations	hours/years	$\pm 5nT$	600 – 10000 km wl
External currents	sec/years	$\pm 1000nT$	1 – <i>global</i> km wl

## 6. STABILIZATION

This chapter shows that the satellite model is *uniformly global asymptotically stable* regardless of the periodicity of the geomagnetic field for the Wisniewski controller from [10]. The Wisniewski controller

$$\mathbf{m}^b = \mathbf{H}\omega_{ob}^b \times \mathbf{B}^b \quad (6.1)$$

inserted in (4.13)

$$\dot{\mathbf{V}} = (\omega_{ob}^b)^T \boldsymbol{\tau}_m^b = (\omega_{ob}^b)^T (\mathbf{H}\omega_{ob}^b \times \mathbf{B}^b) \times \mathbf{B}^b \quad (6.2)$$

$$\begin{aligned} \dot{\mathbf{V}} &= (\omega_{ob}^b)^T \mathbf{S}(\mathbf{B}^b) \mathbf{S}(\mathbf{B}^b) \mathbf{H}\omega_{ob}^b \\ \dot{\mathbf{V}} &= -(\omega_{ob}^b)^T \mathbf{S}^T(\mathbf{B}^b) \mathbf{S}(\mathbf{B}^b) \mathbf{H}\omega_{ob}^b \end{aligned} \quad (6.3)$$

(6.3) is derived using equations listed in appendix A.

### 6.1. Periodic systems

#### 6.1.1. Krasovskii-LaSalle theorem

**Theorem 1. (Krasovskii-LaSalle)** Suppose the system  $\dot{x} = f(t, x)$  is periodic. Suppose there exists a  $\kappa$  function  $V : \mathbb{R}_+ \times \mathbb{R}^n \rightarrow \mathbb{R}$  having the same period as the system such that:

1.  $V$  is a positive definite function and radially unbounded
2.  $\dot{V}(t, x) \leq 0, \forall t \geq 0, \forall x \in \mathbb{R}^n$

then if

$$R = \left\{ x \in \mathbb{R}^n : \exists t \geq 0 \text{ such that } \dot{V}(t, x) = 0 \right\} \quad (6.4)$$

does not contain any trajectories of the system other than the trivial trajectory. Then the equilibrium  $\mathbf{0}$  is UGAS.

**Proof.** See [4]. ■

### 6.1.2. Used on nCube

The discussion in this section is based on [10] and [16].

**Proposition 3.** *The Wisniewski controller*

$$\mathbf{m}^b = \mathbf{H}\omega_{ob}^b \times \mathbf{B}^b \quad (6.5)$$

makes the equilibrium  $\mathbf{x} = \mathbf{0}$  of the system (3.1) UGAS, if  $\mathbf{B}^b$  is periodic.

**Proof.** This proof is given by using Krasovskii-LaSalle's theorem. The satellite model is according to (3.1)

$$\mathbf{I}\dot{\boldsymbol{\omega}}_{ib}^b + \boldsymbol{\omega}_{ib}^b \times (\mathbf{I}\boldsymbol{\omega}_{ib}^b) = \tau_{grav}^b + \tau_m^b \quad (6.6)$$

and it is periodic under the assumption of a periodic geomagnetic field. The Lyapunov function (4.5) has the same period as the satellite model. From section 4.2 claim no.1 in Krasovskii-LaSalle's theorem is satisfied

$$\mathbf{V}(\mathbf{0}) = 0, \quad \mathbf{V}(\mathbf{x}) > 0 \quad \forall \mathbf{x} \neq \mathbf{0} \quad (6.7)$$

and the Lyapunov function is radially unbounded:

$$\mathbf{V}(\mathbf{x}) \rightarrow \infty \quad \text{as} \quad \|\mathbf{x}\| \rightarrow \infty \quad (6.8)$$

The derivative of the Lyapunov function with the Wisniewski controller is derived in (6.3)

$$\dot{\mathbf{V}} = -(\boldsymbol{\omega}_{ob}^b)^T \mathbf{S}^T(\mathbf{B}^b) \mathbf{S}(\mathbf{B}^b) \mathbf{H}\boldsymbol{\omega}_{ob}^b \quad (6.9)$$

due to the fact that:

$$\mathbf{S}^T(\mathbf{B}^b) \mathbf{S}(\mathbf{B}^b) \geq 0 \quad \text{and that} \quad \mathbf{H} > \mathbf{0} \quad (6.10)$$

the time derivative of the Lyapunov function

$$\dot{\mathbf{V}}(\mathbf{t}, \mathbf{x}) \leq \mathbf{0} \quad (6.11)$$

The set  $R$  (6.12) must then not contain any trajectories other than the trivial trajectory ( $\boldsymbol{\omega}_{ob}^b \equiv \mathbf{0}$ ).

$$R = \left\{ x \in \mathbb{R}^n : \exists t \geq 0 \text{ such that } \dot{V}(t, x) = 0 \right\} \quad (6.12)$$

It is therefore essential to make sure that either  $\omega_{ob}^b$  or  $\mathbf{H}\omega_{ob}^b$  is parallel to  $\mathbf{B}^b$ .

$$\mathbf{B}^b \times \omega_{ob}^b \neq 0 \text{ and } \mathbf{B}^b \times \mathbf{H}\omega_{ob}^b \neq 0 \quad (6.13)$$

If  $\mathbf{B}^b \times \omega_{ob}^b = 0$  or  $\mathbf{B}^b \times \mathbf{H}\omega_{ob}^b = 0$  for each  $t > t_0$  the control torque equals zero, as seen from equation (6.1) and (3.6). The geomagnetic field determines the  $\mathbf{B}^b$  vector and is shown in Figure (5.5) as illustrated by the figure  $\omega_{ob}^b$  (or  $\mathbf{H}\omega_{ob}^b$ ) is only parallel to  $\mathbf{B}^b$  instantaneously. Since nCube has a nonzero inclination (89 deg) the largest set contained in  $R$  is the trivial trajectory  $\omega_{ob}^b \equiv 0$ . The angular velocity is thus zero for all  $t \geq 0$  and the trajectory of the torquefree motion coincides with a stable equilibrium. There are four stable equilibria for the torque free motion [16] as shown in chapter 4.1:

$$\{(\omega_{ob}^b, \mathbf{c}_1^b, \mathbf{c}_3^b) : (0, \pm \mathbf{c}_1^o, \pm \mathbf{c}_3^o)\} \quad (6.14)$$

According to Krasovskii-LaSalles theorem the Wisniewski controller is uniformly globally asymptotically stable. ■

## 6.2. Non periodic systems

### 6.2.1. Matrosov's theorem

This section presents an extension of Matrosov's theorem and is based on [17] and [18].

**Theorem 2. (Extension of Matrosov's)** A nonautonomous system is defined in (2.22), where  $f(\cdot, x)$  is continuous and  $f(t, \cdot)$  is locally Lipschitz uniformly in  $t$ . Under the following 4 assumptions the origin of the system (6.15) is UGAS:

$$\dot{x} = f(t, x) \quad (6.15)$$

**Assumption 1.** The origin of the system (6.15) is UGS.

**Assumption 2.** There exist integers  $j, m > 0$  and for each  $\Delta > 0$  there exist

1. a number  $\mu > 0$
2. locally Lipschitz continuous functions  $V_i : \mathbb{R} \times \mathbb{R}^n \rightarrow \mathbb{R}, i \in \{1, \dots, j\}$
3. a (continuous) function  $\phi : \mathbb{R} \times \mathbb{R}^n \rightarrow \mathbb{R}^m, i \in \{1, \dots, m\}$
4. continuous functions  $Y_i : \mathbb{R}^n \times \mathbb{R}^m \rightarrow \mathbb{R}, i \in \{1, \dots, j\}$

such that, for almost all  $(t, x) \in \mathbb{R} \times \beta(\Delta)$ ,

$$\max \{|V_i(t, x)|, |\phi(t, x)|\} \leq \mu \quad (6.16)$$

$$\dot{V}_i(t, x) \leq Y_i(x, \phi(t, x)) \quad (6.17)$$

**Assumption 3.** For each integer  $k \in \{1, \dots, j\}$  we have that

1.  $\{(z, \psi) \in \beta(\Delta) \times \beta(\mu), Y_i(z, \psi) = 0 \forall i \in \{1, \dots, k-1\}\}$  implies
2.  $\{Y_k(z, \psi) \leq 0\}$

**Assumption 4.** We have that

1.  $\{(z, \psi) \in \beta(\Delta) \times \beta(\mu), Y_i(z, \psi) = 0 \forall i \in \{1, \dots, j\}\}$  implies
2.  $\{z = 0\}$

**Proof.** The proof may be found in [18]. ■

### 6.2.2. Used on nCube

**Proposition 4.** The Wisniewski controller

$$\mathbf{m}^b = \mathbf{H}\omega_{ob}^b \times \mathbf{B}^b \quad (6.18)$$

makes the equilibrium  $\mathbf{0}$  of nCube UGAS, if  $\mathbf{B}^b$  is nonperiodic.

**Proof.** Matrosov's theorem proves that proposition 4 is valid, for a nonperiodic geomagnetic field. The Lyapunov function candidate in equation (4.5) has been used.

$$\mathbf{V}_1 = \frac{1}{2}(\omega_{ob}^b)^T \mathbf{I}\omega_{ob}^b + \frac{3}{2}\omega_o^2((\mathbf{c}_3^b)^T \mathbf{I}\mathbf{c}_3^b - I_z) + \frac{1}{2}\omega_o^2(I_x - (\mathbf{c}_1^b)^T \mathbf{I}\mathbf{c}_1^b) \quad (6.19)$$

The time derivative of  $\mathbf{V}$  along the solution trajectories of (3.1) is:

$$\dot{\mathbf{V}}_1 = -(\omega_{ob}^b)^T \mathbf{S}^T(\mathbf{B}^b)\mathbf{S}(\mathbf{B}^b)\mathbf{H}\omega_{ob}^b = Y_1 \leq 0 \quad (6.20)$$

this proven in section 6.1.2. Since  $\mathbf{V}_1$  is positive definite and  $\dot{\mathbf{V}}_1$  is negative semidefinite the origin of (6.19) is UGS, and Assumption 1 in theorem 2 is satisfied. Assumption 2 is satisfied for  $i = 1$ . The auxiliary function  $\mathbf{V}_2$  is defined:

$$\mathbf{V}_2 = -(\mathbf{c}_3^b)^T \mathbf{I}^T \mathbf{S}^T(\mathbf{c}_3^b) \mathbf{I}\omega_{ob}^b \quad (6.21)$$

and is derivated

$$\dot{\mathbf{V}}_2 = -(\dot{\mathbf{c}}_3^b)^T \mathbf{I}^T \mathbf{S}^T(\mathbf{c}_3^b) \mathbf{I}\omega_{ob}^b - (\mathbf{c}_3^b)^T \mathbf{I}^T \mathbf{S}^T(\dot{\mathbf{c}}_3^b) \mathbf{I}\omega_{ob}^b - (\mathbf{c}_3^b)^T \mathbf{I}^T \mathbf{S}^T(\mathbf{c}_3^b) \mathbf{I}\dot{\omega}_{ob}^b \quad (6.22)$$

As the satellite model and the time derivative of  $\mathbf{V}_1$  is stable the sates are bounded.  $\dot{\mathbf{V}}_2$  is then upper bounded:

$$\dot{\mathbf{V}}_2 \leq -(\mathbf{c}_3^b)^T \mathbf{I}^T \mathbf{S}^T(\mathbf{c}_3^b) \mathbf{I}\dot{\omega}_{ob}^b + v_1 |\omega_{ob}^b| \quad (6.23)$$

where the number  $v$  denote a generic bound on continuous functions. Inserting (3.1)  $\dot{\mathbf{V}}_2$  can further be bounded:

$$\begin{aligned}
\dot{\mathbf{V}}_2 &\leq -(\mathbf{c}_3^b)^T \mathbf{I}^T \mathbf{S}^T(\mathbf{c}_3^b) (3\omega_o^2 \mathbf{S}(\mathbf{c}_3^b) \mathbf{I} \mathbf{c}_3^b - \omega_o^2 \mathbf{S}(\mathbf{c}_1^b) \mathbf{I} \mathbf{c}_1^b) + v_2 |\omega_{ob}^b| & (6.24) \\
&= -3\omega_o^2 (\mathbf{c}_3^b)^T \mathbf{I}^T \mathbf{S}^T(\mathbf{c}_3^b) \mathbf{S}(\mathbf{c}_3^b) \mathbf{I} \mathbf{c}_3^b + \omega_o^2 (\mathbf{c}_3^b)^T \mathbf{I}^T \mathbf{S}^T(\mathbf{c}_3^b) \mathbf{S}(\mathbf{c}_1^b) \mathbf{I} \mathbf{c}_1^b + v_2 |\omega_{ob}^b| \\
&= -3\omega_o^2 (\mathbf{c}_3^b)^T \mathbf{I}^T \mathbf{S}^T(\mathbf{c}_3^b) \mathbf{S}(\mathbf{c}_3^b) \mathbf{I} \mathbf{c}_3^b - \omega_o^2 (\mathbf{c}_3^b)^T \mathbf{I}^T \mathbf{S}(\mathbf{c}_3^b) \mathbf{S}(\mathbf{c}_1^b) \mathbf{I} \mathbf{c}_1^b + v_2 |\omega_{ob}^b| \\
&= -3\omega_o^2 (\mathbf{c}_3^b)^T \mathbf{I}^T \mathbf{S}^T(\mathbf{c}_3^b) \mathbf{S}(\mathbf{c}_3^b) \mathbf{I} \mathbf{c}_3^b \\
&\quad - \omega_o^2 (\mathbf{c}_3^b)^T \mathbf{I}^T (\mathbf{c}_1^b (\mathbf{c}_3^b)^T - (\mathbf{c}_3^b)^T \mathbf{c}_1^b \mathbf{I}_{3 \times 3}) \mathbf{I} \mathbf{c}_1^b + v_2 |\omega_{ob}^b| \\
&= -3\omega_o^2 (\mathbf{c}_3^b)^T \mathbf{I}^T \mathbf{S}^T(\mathbf{c}_3^b) \mathbf{S}(\mathbf{c}_3^b) \mathbf{I} \mathbf{c}_3^b - \omega_o^2 (\mathbf{c}_3^b)^T \mathbf{I}^T \mathbf{c}_1^b (\mathbf{c}_3^b)^T \mathbf{I} \mathbf{c}_1^b + v_2 |\omega_{ob}^b| \\
&\leq -3\omega_o^2 (\mathbf{c}_3^b)^T \mathbf{I}^T \mathbf{S}^T(\mathbf{c}_3^b) \mathbf{S}(\mathbf{c}_3^b) \mathbf{I} \mathbf{c}_3^b + v_2 |\omega_{ob}^b| & (6.25)
\end{aligned}$$

where it has been used that  $\mathbf{c}_1^b$  and  $\mathbf{c}_3^b$  are unit vectors. Therefore  $(\mathbf{c}_3^b)^T \mathbf{c}_1^b = 0$  and (B.12) is used and the fact that  $\mathbf{S}^T(\mathbf{c}_3^b) \mathbf{S}(\mathbf{c}_3^b) > 0$ . Then:

$$Y_1 \equiv 0 \Rightarrow \dot{\mathbf{V}}_2 \leq -3\omega_o^2 (\mathbf{c}_3^b)^T \mathbf{I}^T \mathbf{S}^T(\mathbf{c}_3^b) \mathbf{S}(\mathbf{c}_3^b) \mathbf{I} \mathbf{c}_3^b = Y_2 \leq 0 \quad (6.26)$$

and assumption 2 and 3 are satisfied for  $i = 2$ . The auxiliary function  $\mathbf{V}_3$  is defined:

$$\mathbf{V}_3 = (\mathbf{c}_1^b)^T \mathbf{I}^T \mathbf{S}^T(\mathbf{c}_1^b) \mathbf{I} \omega_{ob}^b \quad (6.27)$$

the time derivative of  $\mathbf{V}_3$  is derived in the same manner as for  $\dot{\mathbf{V}}_2$  and the same conditions are used:

$$\begin{aligned}
\dot{\mathbf{V}}_3 &= (\dot{\mathbf{c}}_1^b)^T \mathbf{I}^T \mathbf{S}^T(\mathbf{c}_1^b) \mathbf{I} \omega_{ob}^b + (\mathbf{c}_1^b)^T \mathbf{I}^T \mathbf{S}^T(\dot{\mathbf{c}}_1^b) \mathbf{I} \omega_{ob}^b + (\mathbf{c}_1^b)^T \mathbf{I}^T \mathbf{S}^T(\mathbf{c}_1^b) \mathbf{I} \dot{\omega}_{ob}^b & (6.28) \\
&\leq (\mathbf{c}_1^b)^T \mathbf{I}^T \mathbf{S}^T(\mathbf{c}_1^b) \mathbf{I} \dot{\omega}_{ob}^b + v_3 |\omega_{ob}^b| \\
&\leq (\mathbf{c}_1^b)^T \mathbf{I}^T \mathbf{S}^T(\mathbf{c}_1^b) (3\omega_o^2 \mathbf{S}(\mathbf{c}_3^b) \mathbf{I} \mathbf{c}_3^b - \omega_o^2 \mathbf{S}(\mathbf{c}_1^b) \mathbf{I} \mathbf{c}_1^b) + v_3 |\omega_{ob}^b| \\
&= 3\omega_o^2 (\mathbf{c}_1^b)^T \mathbf{I}^T \mathbf{S}^T(\mathbf{c}_1^b) \mathbf{S}(\mathbf{c}_3^b) \mathbf{I} \mathbf{c}_3^b - \omega_o^2 (\mathbf{c}_1^b)^T \mathbf{I}^T \mathbf{S}^T(\mathbf{c}_1^b) \mathbf{S}(\mathbf{c}_1^b) \mathbf{I} \mathbf{c}_1^b + v_3 |\omega_{ob}^b| \\
&\leq -\omega_o^2 (\mathbf{c}_1^b)^T \mathbf{I}^T \mathbf{S}^T(\mathbf{c}_1^b) \mathbf{S}(\mathbf{c}_1^b) \mathbf{I} \mathbf{c}_1^b + v_4 |\omega_{ob}^b| + v_5 |\mathbf{c}_3^b| & (6.29)
\end{aligned}$$

here the fact that  $\omega_{ob}^b$  and  $\mathbf{c}_3^b$  are bounded has been used and  $\mathbf{S}^T(\mathbf{c}_1^b) \mathbf{S}(\mathbf{c}_1^b) > 0$ . Then:

$$Y_1 \equiv Y_2 \equiv 0 \Rightarrow \dot{\mathbf{V}}_3 \leq -\omega_o^2 (\mathbf{c}_1^b)^T \mathbf{I}^T \mathbf{S}^T(\mathbf{c}_1^b) \mathbf{S}(\mathbf{c}_1^b) \mathbf{I} \mathbf{c}_1^b = Y_3 \leq 0 \quad (6.30)$$

and assumption 2 and 3 are satisfied for  $i = 3$ . Finally

$$Y_i \equiv 0, i = \{1, 2, 3\} \Rightarrow \mathbf{x} = \mathbf{0} \quad (6.31)$$

assumption 4 of Matrosov's theorem is satisfied and the nCube satellite model is UGAS with the Wisniewski controller. ■

# Part II

## Control

## 7. ADCS DESIGN

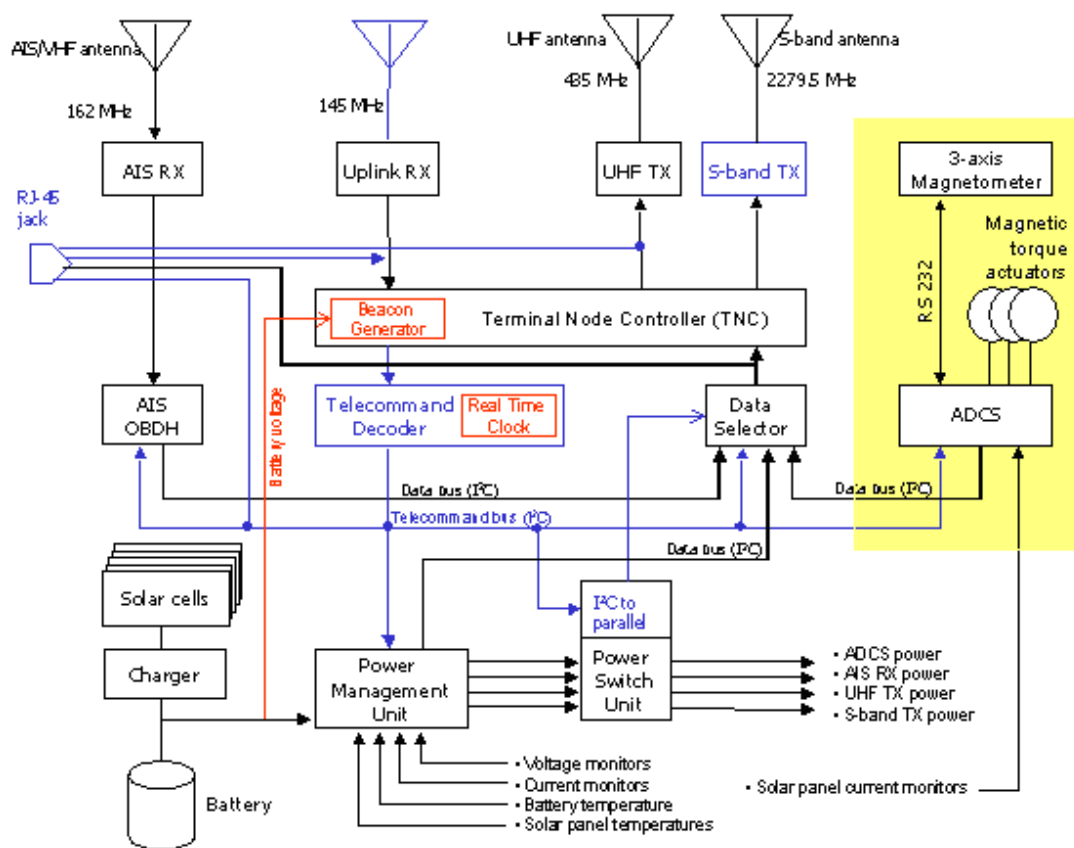


Figure 7.1: Satellite system architecture ref.[24].

The satellite system architecture is shown in Figure 7.1 where the marked area is the ADCS part of the system. For more reading on the total system architecture

for nCube see [24]. This chapter gives an overview of the ADCS of nCube.

## **7.1. Mission requirements**

The objective of the payload of nCube is to demonstrate ship traffic surveillance from a LEO satellite using the maritime Automatic Identification System (AIS). The success criteria is based on receiving, storing and retransmitting at least one AIS-message from a ship. Another objective is to demonstrate reindeer herd monitoring from space by equipping a reindeer with an AIS transponder during a limited experimental period. The third mission of nCube is the topic for this thesis; efficient attitude control.

## **7.2. Determination**

The Determination part is solved by integrating measured data from the digital magnetometer and from solar panels currents in a Kalman filter. The three-axis magnetometer used is "smart digital magnetometer from Honeywell HMR2300". The determination system is not inside the scope of this thesis, for more reading see [23] and [22].

## **7.3. Control modes**

The control system operates in one of two modes detumbling and stabilization.

### **7.3.1. Passive and active control**

The attitude control of nCube is divided into passive and active control. Passive control; gravity-gradient control uses the inertial properties of a vehicle to keep it pointed toward the Earth. This relies on the fact that an elongated object in a gravity field tends to align its longitudinal axis through the attractive body's center. This is a tendency used on simple spacecraft in LEO, nCube realizes this through a gravity boom which also works as an antenna for the satellite. The boom is to be made of a material called copper-beryllium(CuBe) and is 1,5m long. The active control is already mentioned in chapter 3.2, and is three magnetic coils that uses the measurements of the geomagnetic field for active control.

### 7.3.2. Detumbling

After the satellite has been released from the launcher it will have an initial angular velocity in the inertial frame. The satellite's angular velocity must then be reduced before the boom can be deployed, and the body frame must be aligned with the orbit frame. This phase can be divided into rate detumbling and angle detumbling.

**Rate detumbling** High angular velocity makes it difficult to estimate the satellite's orientation. The angular velocity must be reduced and the kinetic energy must be dumped. Requirements is that the angular velocities must be reduced to:

$$\omega_{ib}^b < [ 5 \times 10^{-3} \quad 5 \times 10^{-3} \quad 5 \times 10^{-3} ]^T \frac{rad}{s} \quad (7.1)$$

And the only available sensor will be the magnetometer.

**Angle detumbling** The attitude of the satellite after the rate detumbling mode finishes, will be random. Before boom deployment the  $z_b$ -axis has to be aligned with the  $z_o$ -axis to ensure that the boom not is deployed in a wrong direction, which can make it difficult to restore to the proper attitude. The requirements for boom deployment is that the  $z_b$  must be less than  $|30^\circ|$  from the  $z_o$ -axis.

### 7.3.3. Stabilization

In this mode the knowledge of the satellite's attitude is a necessity. After the boom is deployed the satellite is passively stabilized, but the orientation will oscillate. Disturbance torques will also inflict on orientation of the satellite. The controller for this mode has to ensure a pointing accuracy of  $20^\circ$  about nadir, and counteract oscillations and disturbance.

### 7.3.4. Spin and Inverted boom recovery

For nCube it is not necessary to have accurate control about the yaw-axis but it is convenient to have an upper bound on the spin rate. If the boom as a consequence of a fatal error or unexpected disturbances should change the satellite's orientation severely, the actuators should be sized large enough to turn the satellite to the right direction.

## 7.4. Evaluation of disturbances

### 7.4.1. Solar radiation

Implementing the solar radiation torque in to the ADCS, as already mentioned in section 3.4.1, is rather difficult due to uncertain parameter information. Since nCube consist of different surface materials the reflectance factor is very hard to find. At the moment finding information about reflectance factor for the boom made of copper-beryllium is not available. The reflectance factor for measuring the worst-case solar radiation is then assumed to be 0.6 according to [21]. The surfacearea facing the Sun is also quite difficult to determine, here the assumption of worst case area facing the Sun is used. The worst case torque from solar radiation is evaluated here:

$p_{SR} = 4.51 \times 10^{-6} N/m^2$	Solar pressure
$c_R = 1.6$	Reflectivity
$A_{\odot} = 0.0295$	Maximum area facing the Sun
$c_{ps} = 0.06$	Estimated center of pressure
$cg = 0$	Center of gravity

According to (3.17)the worst case torque is derived from:

$$\tau_{solarradiation} = p_{SR} * c_R * A_{\odot} * (c_{p_{SR}} - cg) \quad (7.2)$$

which results in the torque:

$$\tau_{solarradiation} = 7.6951 \times 10^{-8} Nm \quad (7.3)$$

Since nCube is a low Earth Orbit (LEO) satellite the solar radiation has very little influence on the satellite, and the torque is not implemented in the ADCS design. For further work may be investigated the possibility that nCube can approach a situation where it will act as a solar sail. A solar sail is that the solar radiation pressure becomes the "wind" to move the satellite in a "low-thrust-like" maneuver, but this effect occurs rarely and likely not at LEO.

### 7.4.2. Gravity gradient torque

The expression of the worst-case gravity torque is given in (3.11) according to:

$$\tau_{grav-worst} = \frac{3\mu}{2R_0^3} |I_z - I_x| \sin 2\theta \quad (7.4)$$

The most critical situation is if we want to invert the boom then we have to overcome a gravitygradient for the case of  $\theta = \frac{\pi}{4}$ . While in normal operations  $\theta \approx 0$ .

$$\begin{array}{ll}
\mu = 3.986 \times 10^{14} m^3/s^2 & \text{Earth's gravitational coefficient} \\
R_0 = 6.986 \times 10^6 m & \text{Distance from Earth's center (m)} \\
I_x = 0.1043 kgm^2 & \text{Moments of inertia about } x_b[6] \\
I_z = 0.0031 kgm^2 & \text{Moments of inertia about } z_b[6] \\
\theta = \frac{\pi}{4} & \text{Deviation from nadir}
\end{array}$$

$$\tau_{grav-worst} = 1.7747 \times 10^{-7} Nm \quad (7.5)$$

### 7.4.3. Aerodynamic torque

From equation (3.19) we have that the worst case aerodynamic torque is:

$$\begin{aligned}
\tau_a &= F(c_{pa} - cg) \quad \text{where} \\
F &= 0.5(\rho C_d AV^2)
\end{aligned} \quad (7.6)$$

Inserting the following variables yields:

$$\begin{array}{llll}
C_d = 2.2 & \rho = 2.89 \times 10^{-13} kg/m^3 & V = 7.5 \times 10^3 m/s & \\
c_{pa} = 0.05m & A = 0.01m^2 & = & \\
\tau_a = 1.5371 \times 10^{-8} Nm & & & (7.7)
\end{array}$$

### 7.4.4. Resulting disturbing torques

In addition to the mentioned torques there is also internal disturbance due to the magnetic field generated by electrical circuits in the satellite. According to [7] it will be of a magnitude of 10% of the generated torque, and is of size:

$$\tau_{mag} = 1 \times 10^{-6} Nm \quad (7.8)$$

Then the total resulting disturbing torques will be:

<b>Disturbance</b>	<b>Value</b>
Solar radiation	$7.6951 \times 10^{-8} Nm$
Aerodynamic drag	$1.5371 \times 10^{-8} Nm$
Gravity gradient	$1.7747 \times 10^{-7} Nm$
Internal	$1.0000 \times 10^{-6} Nm$
<b>Total</b>	$1.2698 \times 10^{-6} Nm$

The magnitude of the control torque requirement then becomes:

$$|\mathbf{m}^b| = \frac{|\boldsymbol{\tau}_m^b|}{|\mathbf{B}^b|} = \frac{1.3 \times 10^{-6}}{5 \times 10^{-5}} Am^2 = 0.0254 Am^2 \quad (7.9)$$

The maximal torque delivered by nCube is  $0.1 Am^2$  thus this gives a good margin to counteract the disturbing torques.

## 8. CONTROLLER DESIGN

In [21] controllers for the different control modes have been suggested. The detumbling controllers, spin controllers and inverted boom recovery controllers works satisfactory and therefore this thesis will only concern the stabilization mode controllers. This chapter gives a short introduction of two energy controllers introduced by earlier work. Then a linear quadratic controller is derived. The reason for introducing an alternative linear optimal controller is because this has not been investigated for nCube, and according to [26] an LQ-controller will give satisfying accuracy and low power consumption.

### 8.1. Previous work in stabilization

When going through the earlier thesis on the attitude control for nCube, [21] and [7], the two controllers proposed for stabilization are the energy based controllers. The controllers are the angular velocity feedback and the attitude feedback.

#### 8.1.1. Energy based angular velocity feedback

**Proposition 5.** *The angular velocity feedback controller is introduced in chapter 6 as the Wisniewski controller,*

$$\mathbf{m}^b = \mathbf{H}\omega_{ob}^b \times \mathbf{B}^b \quad (8.1)$$

and it is UGAS according to Krasovskii-LaSalle theorem this controller is stable about the equilibria:

$$\{(\omega_{ob}^b, \mathbf{c}_1^b, \mathbf{c}_3^b) : (0, \pm \mathbf{c}_1^o, \pm \mathbf{c}_3^o)\} \quad (8.2)$$

#### 8.1.2. Energy based attitude feedback

**Proposition 6.** *The attitude feedback controller may be defined as:*

$$\mathbf{m}^b = \mathbf{H}\omega_{ob}^b \times \mathbf{B}^b - \alpha\epsilon \times \mathbf{B}^b \quad (8.3)$$

where  $\epsilon$  is the vector part of the attitude quaternion. The controller makes the satellite locally stable about the equilibria:

$$\{(\omega_{ob}^b, \mathbf{c}_1^b, \mathbf{c}_3^b) : (0, \mathbf{c}_1^o, \mathbf{c}_3^o)\} \quad (8.4)$$

**Proof.** [7] ■

## 8.2. Linear control

Traditionally LQ (Linear Quadratic) controllers has been used on magnetic actuated satellites because of their reliability and robustness. The LQ-strategy is based on linearizing the systems dynamics, defining an object function which shall be minimized and generate a gainmatrix which is used for feedback. For more details on LQ-control problems see [19] and [25].

The linearization of the satellites attitude was derived in section 3.5.

$$\dot{\mathbf{x}}(t) = \mathbf{A}\mathbf{x}(t) + \mathbf{B}(t)\mathbf{u}(t) \quad (8.5)$$

with:

$$\mathbf{A} = \begin{bmatrix} 0 & 1 & 0 & 0 & 0 & 0 \\ -4k_x\omega_o^2 & 0 & 0 & 0 & 0 & (1 - k_x)\omega_o \\ 0 & 0 & 0 & 1 & 0 & 0 \\ 0 & 0 & -3k_y\omega_o^2 & 0 & 0 & 0 \\ 0 & 0 & 0 & 0 & 0 & 1 \\ 0 & -(1 - k_z)\omega_o & 0 & 0 & -k_z\omega_o^2 & 0 \end{bmatrix} \quad (8.6)$$

and

$$\mathbf{B}(t) = \begin{bmatrix} 0 & 0 & 0 \\ 0 & \frac{1}{2I_x}B_z^o & -\frac{1}{2I_x}B_y^o \\ 0 & 0 & 0 \\ -\frac{1}{2I_y}B_z^o & 0 & \frac{1}{2I_y}B_x^o \\ 0 & 0 & 0 \\ \frac{1}{2I_z}B_y^o & -\frac{1}{2I_z}B_x^o & 0 \end{bmatrix} \quad (8.7)$$

And the output then yields:

$$\mathbf{y}(t) = \mathbf{C}\mathbf{x}(t) \quad (8.8)$$

The cost function which should be to minimized is:

$$J(u) = \frac{1}{2} \int_{t_0}^T [\tilde{\mathbf{x}}^T \mathbf{Q} \tilde{\mathbf{x}} + \mathbf{u}^T \mathbf{P} \mathbf{u}] dt \quad (8.9)$$

where:

$$\tilde{\mathbf{x}}(\mathbf{t}) = \mathbf{x}(\mathbf{t}) - \mathbf{x}_d(\mathbf{t}) \quad (8.10)$$

Where  $\mathbf{x}_d(\mathbf{t})$  is the reference trajectory.  $\tilde{\mathbf{x}}(\mathbf{t})$  is the difference which we want to be zero for the system.  $\mathbf{Q}$  and  $\mathbf{P}$  are positive semidefinite matrices used to weigh respectively state deviation and actuator usage. To control the state and actuator usage the system must fulfill the controllability condition according to [19]:

**Definition 7.** (*Controllability*)

*The state and input matrix (A,B) must satisfy the controllability condition to ensure that there exists a control  $\mathbf{u}(t_0)$  which can drive any arbitrary state  $\mathbf{x}(t_1)$  for  $t_1 > t_0$ . The controllability condition requires that the matrix:*

$$\mathbf{C} = [\mathbf{B} \mid \mathbf{A}\mathbf{B} \mid \dots \mid (\mathbf{A})^{n-1}\mathbf{B}] \quad (8.11)$$

*must be of full row rank such that a least a right inverse exist.*

The solution to the LQ-problem is given by the Ricatti equation

$$\dot{\mathbf{R}}(\mathbf{t}) = -\mathbf{R}(\mathbf{t})\mathbf{A} - \mathbf{A}^T \mathbf{R}(\mathbf{t}) + \mathbf{R}(\mathbf{t})\mathbf{B}(\mathbf{t})\mathbf{P}^{-1}\mathbf{B}(\mathbf{t})^T \mathbf{R}(\mathbf{t}) - \tilde{\mathbf{Q}}(\mathbf{t}) \quad (8.12)$$

where  $\tilde{\mathbf{Q}} = \mathbf{C}^T \mathbf{Q} \mathbf{C} = \mathbf{Q}$  if all the states are known. The solution of the LQ-problem yields the time varying controller:

$$\mathbf{u}(\mathbf{t}) = -\mathbf{P}^{-1}\mathbf{B}(\mathbf{t})^T \mathbf{R}(\mathbf{t})\mathbf{x}(\mathbf{t}) \quad (8.13)$$

The controller 8.13 is very computational demanding, due to the fact that for each step the  $\mathbf{R}(\mathbf{t})$  must be computed. One solution to this problem is to compute  $\mathbf{R}(\mathbf{t})$  off line for a predefined orbit and store it in a look-up table. Another problem is that all the states has to be known or estimated.

Introducing the LQG-controler (linear quadratic optimal gain) is an attractive option. Based on the fact that the geomagnetic field in section 5.5 is nearly

periodic it is possible to take the mean value of  $\mathbf{B}^o$ , assuming it gives a time invariant model

$$\dot{\mathbf{x}} = \mathbf{A}\mathbf{x} + \mathbf{B}\mathbf{u} \quad (8.14)$$

Solving the Algebraic Ricatti Equation

$$\mathbf{0} = -\mathbf{R}\mathbf{A} + \mathbf{A}^T\mathbf{R} - \mathbf{R}\mathbf{B}\mathbf{P}^{-1}\mathbf{B}^T\mathbf{R} + \mathbf{Q} \quad (8.15)$$

results in the controller:

$$\mathbf{u}(\mathbf{t}) = -\mathbf{P}^{-1}\mathbf{B}^T\mathbf{R}\mathbf{x}(\mathbf{t}) \quad (8.16)$$

This gain controller gives satisfactory results.

Choosing the weight matrices  $\mathbf{Q}$  and  $\mathbf{P}$  are done by backward integration. They are defined by:

$$\begin{aligned} \mathbf{P} &= \text{diag}([p_1, p_2, \dots, p_{n_a}]) \\ \mathbf{Q} &= \text{diag}([q_1, q_2, \dots, q_{n_s}]) \end{aligned} \quad (8.17)$$

where  $n_a$  is the number of actuators on the control system and  $n_s$  is the number of interesting states. For nCube  $n_a = 3$  and  $n_s = 6$ . The performance of the system is adjusted by choosing different weights. As in [5] the weights are chosen:

$$p_i = \frac{1}{(\Delta x_i)^2} \quad \text{and} \quad q_i = \frac{1}{(\Delta u_i)^2} \quad (8.18)$$

The maximum dipolemoment for the actuators is  $0.1Am^2$ ;

$$\Delta x_i = 8 * \frac{\pi}{180} \quad \text{and} \quad \Delta u_i = 0.1 \quad (8.19)$$

this values is used in the simulations of nCube.

## 9. SIMULATIONS

Based on the previous chapter the three suggested controllers are simulated for the stabilization mode for nCube. The data parameters used in the simulations are listed under:

Parameter	Value
Weight	1 kg
Size	$10 \times 10 \times 10$ cm
Boom length	1.5 m
Moments of inertia	$I_x = 0.1043, I_y = 0.1020, I_z = 0.0031$ kgm <sup>2</sup>
Maximum magnetic moment	0.1 Am <sup>2</sup>
Desired Euler values $[\phi \ \theta \ \psi]$	$[0 \ 0 \ 0]$

### 9.1. Energy based controllers

The two energy controllers suggested by [21] and [7] is simulated in the stabilization mode.

#### 9.1.1. Angular velocity feedback

The Angular velocity feedback controller is introduced in the previous chapter (8.1).

$$\mathbf{m}^b = \mathbf{H}\omega_{ob}^b \times \mathbf{B}^b \quad (9.1)$$

The stability properties are investigated with the following:

Initial values:  $\omega_{ob}^b = [0.00050 \ 0.0003 - 0.003]^T$

$$[\phi \ \theta \ \psi] = [20^\circ \ 40^\circ \ 60^\circ]$$

Controller parameters:  $h = 2.25 \times 10^5$

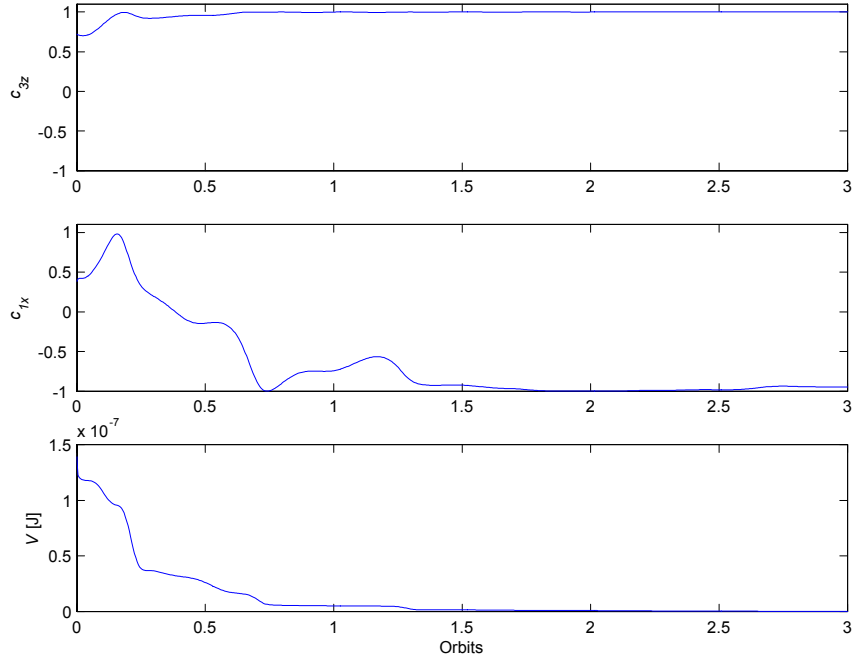


Figure 9.1: Simulation of the angular velocity feedback controller in (9.1), with  $h = 2.25 \times 10^5$ . Initial angular velocity is  $\omega_{ob}^b = [0.00050.0003 - 0.003]^T$  and the initial orientation is  $[\phi \theta \psi] = [20^\circ 40^\circ 60^\circ]$  which is roll, pitch and yaw.  $c_{3z}$  is the projection of the  $z_o$ -axis on the  $z_b$ -axis.  $V$  is the total energy of the system.  $c_{1x}$  is the projection of the  $x_o$ -axis on the  $x_b$ -axis.

**Simulation verification 1.** *Figure 9.1 shows the simulation of the angular velocity feedback controller stability properties without any disturbances. The satellite attitude converges to the equilibrium  $(\omega_{ob}^b, \mathbf{c}_1^b, \mathbf{c}_3^b) : (0, -\mathbf{c}_1^o, \mathbf{c}_3^o)$ . The lower plot shows that the total energy,  $V$ , is indeed dissipated from the system.*

The following are used when simulating (8.1):

$$\begin{aligned} \text{Initial values:} \quad & \omega_{ob}^b = [0.00050.0003 - 0.003]^T \\ & [\phi \theta \psi] = [30^\circ 80^\circ 60^\circ] \\ \text{Controller parameters:} \quad & h = 2.25 \times 10^5 \end{aligned}$$

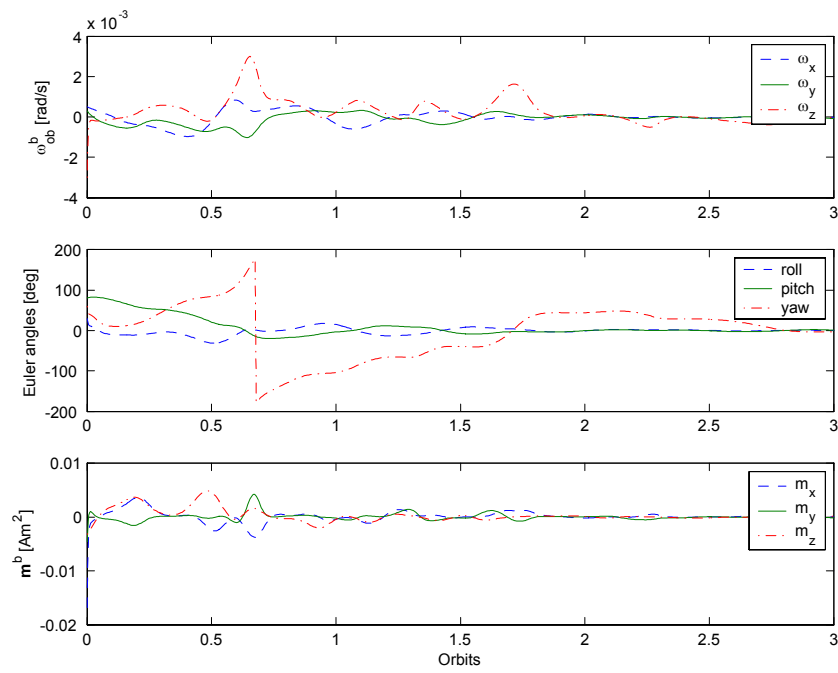


Figure 9.2: The angular velocity feedback controller. Topmost plot shows the angular velocities, middle plot shows the euler angles and the lower plot shows the applied torque.

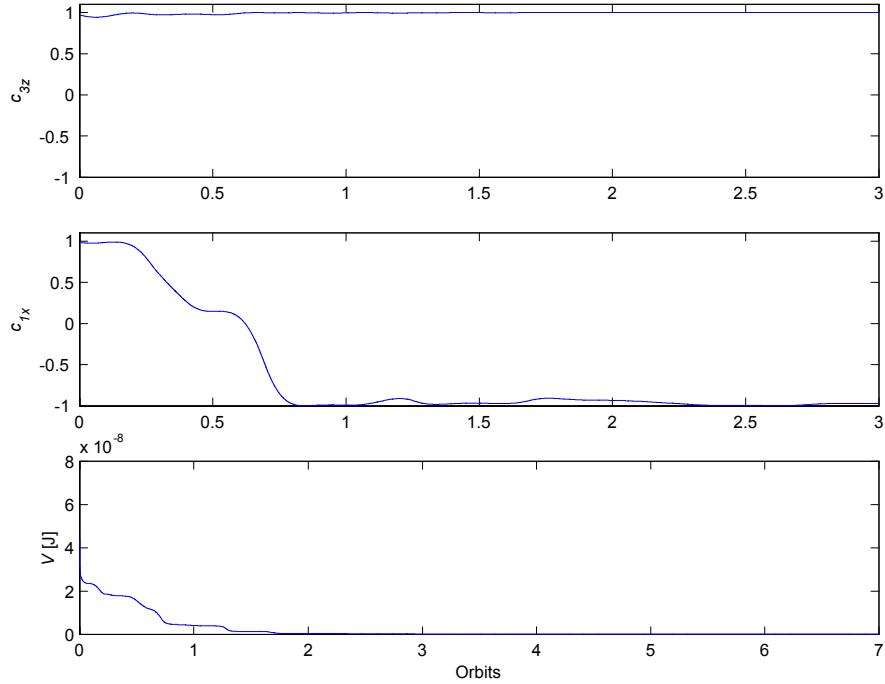


Figure 9.3: Simulation of the angular velocity feedback controller in (9.1), included external noise 10% on the igrf2000 model.  $c_{3z}$  is the projection of the  $z_o$ -axis on the  $z_b$ -axis.  $V$  is the total energy of the system.

**Simulation verification 2.** Figure 9.2 shows the simulation of the angular velocity feedback controller. The angular velocities are aligned with the geomagnetic field after 2.5 orbits. The Euler angles also reaches the desired value after 2.5 orbits. And the applied torque is of a low magnitude.

**Simulation verification 3.** Figure 9.3 shows the simulation of the angular velocity feedback controller, with Gaussian with noise on 10% of the igrf2000 model. Responding to the non periodic part of the geomagnetic field, this is based on the results in Chapter 5. The energy is indeed dissipating and the satellite converges to the equilibrium  $(\omega_{ob}^b, \mathbf{c}_1^b, \mathbf{c}_3^b) : (0, -\mathbf{c}_1^o, \mathbf{c}_3^o)$ . This verifies that the satellite with the angular velocity feedback controller (Wisniewski controller) is UGAS regardless of the periodicity of the geomagnetic field.

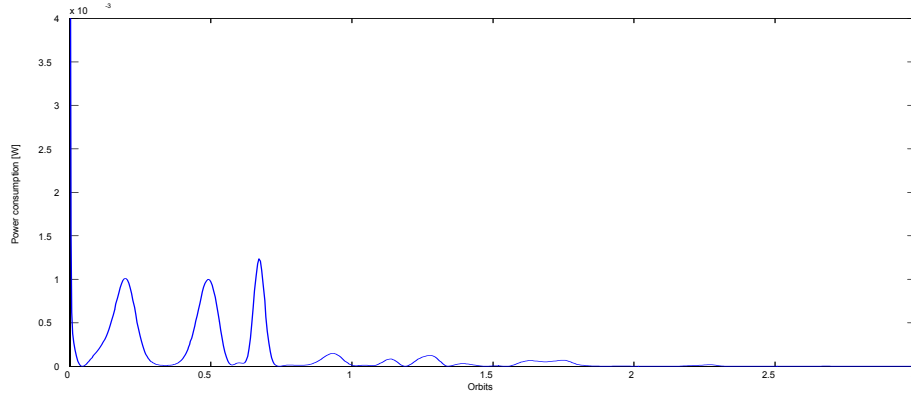


Figure 9.4: The power consumption by the angular velocity feedback controller.

**Simulation verification 4.** *Figure 9.4 shows the power consumption of the angular velocity feedback controller, and the power consumption is very low. The performance of the controller is very good.*

### 9.1.2. Attitude feedback

The following are used when simulating the attitude feedback controller:

$$\mathbf{m}^b = \mathbf{H}\omega_{ob}^b \times \mathbf{B}^b - \alpha\epsilon \times \mathbf{B}^b \quad (9.2)$$

Initial values:  $\omega_{ob}^b = [0.00050.0003 - 0.003]^T$   
 $[\phi \ \theta \ \psi] = [20^\circ \ 40^\circ \ 60^\circ]$

Controller parameters:  $h = 2.25 \times 10^5$   
 $\alpha = 900$

**Simulation verification 5.** *Figure 9.5 shows the attitude feedback controller stability properties without any disturbances. The satellite converges to the equilibrium  $(\omega_{ob}^b, \mathbf{c}_1^b, \mathbf{c}_3^b) : (0, -\mathbf{c}_1^o, \mathbf{c}_3^o)$ . The lower plot shows that the total energy,  $V$ , is not decreasing.*

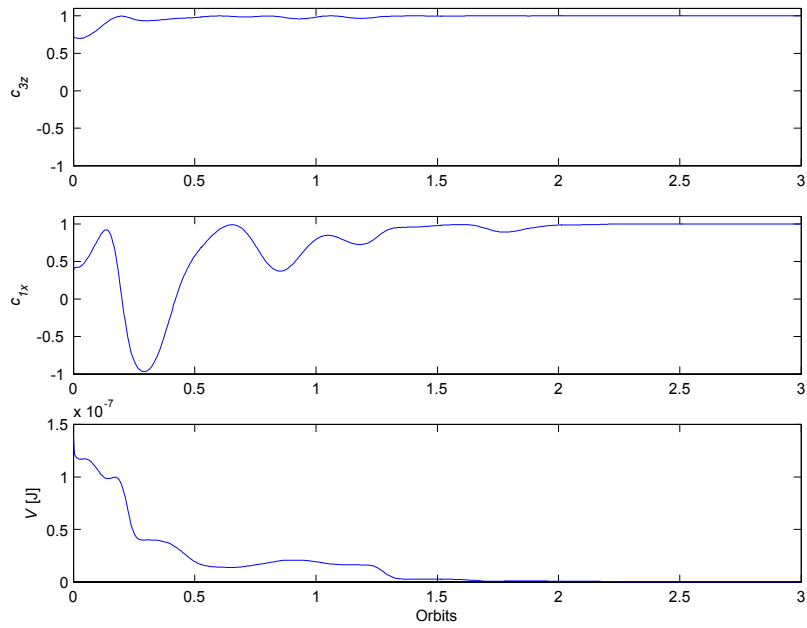


Figure 9.5: Simulation of the attitude feedback controller in (9.2), with  $h = 2.25 \times 10^5$  and  $\alpha = 900$ . Initial angular velocity is  $\omega_{ob}^b = [0.00050.0003 - 0.003]^T$  and the initial orientation is  $[\phi \theta \psi] = [20^\circ 40^\circ 60^\circ]$  which is roll, pitch and yaw.  $c_{3z}$  is the projection of the  $z_o$ -axis on the  $z_b$ -axis.  $V$  is the total energy of the system.  $c_{1x}$  is the projection of the  $x_o$ -axis on the  $x_b$ -axis.

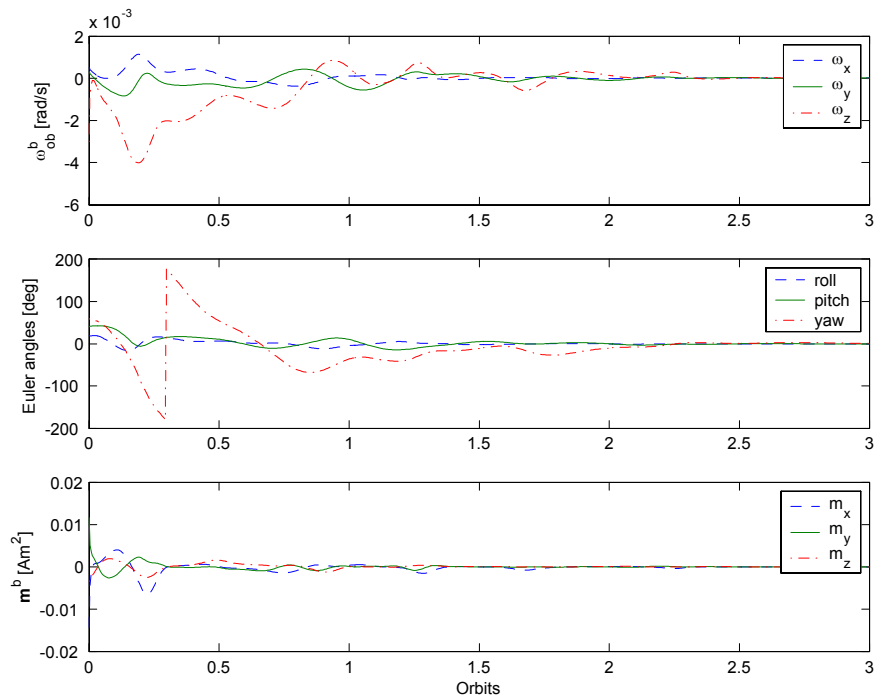


Figure 9.6: The attitude feedback controller. Topmost shows the angular velocities, middle shows the euler angles and the lowest plot shows the applied torque.

**Simulation verification 6.** *Figure 9.6 shows the simulation of the attitude feedback controller. The angular velocities are aligned with the geomagnetic field after 2 orbits. The Euler angles also reaches the desired value after 2 orbits. And the applied torque is of a low magnitude.*

**Simulation verification 7.** *Figure 9.7 shows the power consumption of the angular velocity feedback controller, and the power consumption is very low.*

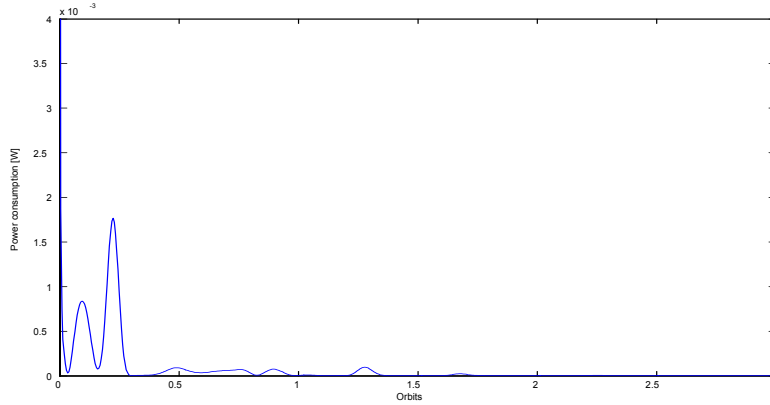


Figure 9.7: The power consumption by the attitude feedback controller.

## 9.2. Linear control

The linear quadratic controller is introduced in the previous chapter (8.13).

$$\mathbf{u}(\mathbf{t}) = -\mathbf{P}^{-1}\mathbf{B}(\mathbf{t})^T\mathbf{R}(\mathbf{t})\mathbf{x}(\mathbf{t}) \quad (9.3)$$

The stability properties are investigated with the following:

Initial values:  $\omega_{ob}^b = 0$   
 $[\phi \ \theta \ \psi] = [10^\circ \ -3^\circ \ 10^\circ]$

Weight parameters:  $Q = \frac{1}{\left(\frac{10\pi}{180}\right)^2} \text{diag}([101010])$   
 $P = \frac{1}{(0.001)^2} \text{diag}([111])$

**Simulation verification 8.** Figure 9.8 shows the simulation of the linear controller stability properties without any disturbances. The satellite converges to the equilibrium  $(\omega_{ob}^b, \mathbf{c}_1^b, \mathbf{c}_3^b) : (0, \mathbf{c}_1^o, \mathbf{c}_3^o)$ . The lower plot shows that the total energy,  $V$ , is indeed dissipated from the system.

**Simulation verification 9.** Figure 9.9 shows the simulation of the LQ-controller. The angular velocities are aligned with the geomagnetic field after 1.5 orbits. The Euler angles also reaches the desired value after 1.5 orbits. And the applied torque is of a low magnitude.

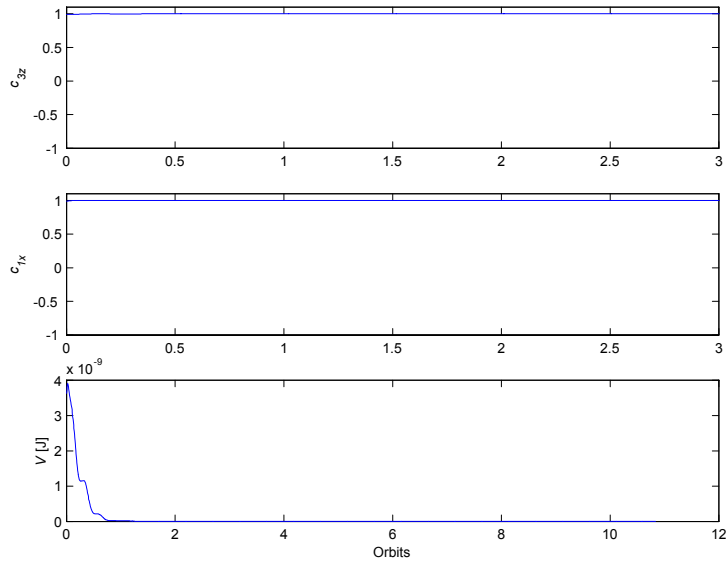


Figure 9.8: The LQ-controller is in (9.3), with  $Q = \frac{1}{\left(\frac{10\pi}{180}\right)^2} \text{diag}([101010])$  and  $P = \frac{1}{(0.001)^2} \text{diag}([111])$ . Initial angular velocity is  $\omega_{ob}^b = 0$  and the initial orientation is  $[\phi \ \theta \ \psi] = [10^\circ \ -3^\circ \ 10^\circ]$  which is roll, pitch and yaw.  $c_{3z}$  is the projection of the  $z_o$ -axis on the  $z_b$ -axis.  $V$  is the total energy of the system.  $c_{1x}$  is the projection of the  $x_o$ -axis on the  $x_b$ -axis.

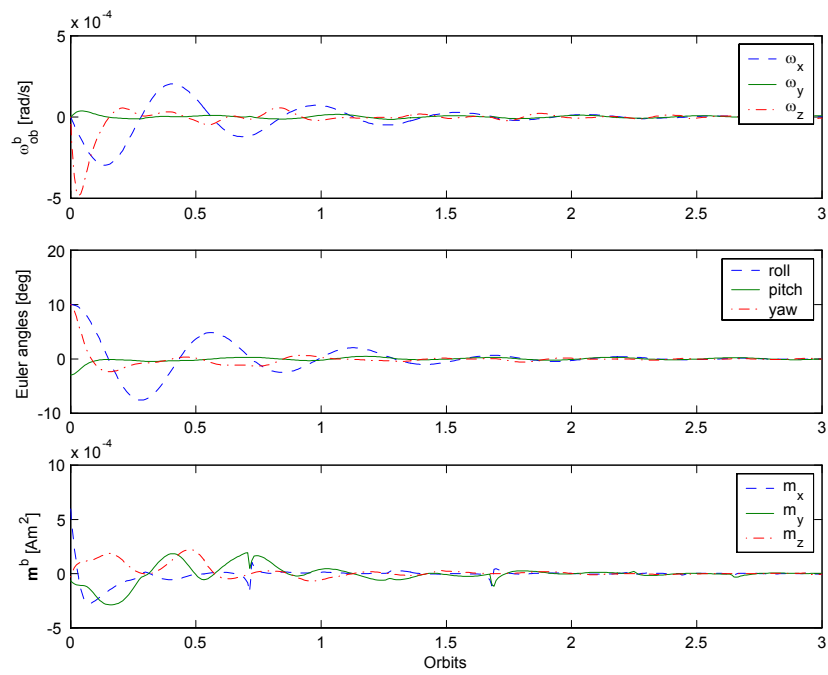


Figure 9.9: The LQ-controller. Topmost plot shows the angular velocities, middle plot shows the euler angles and the lower plot shows the applied torque.

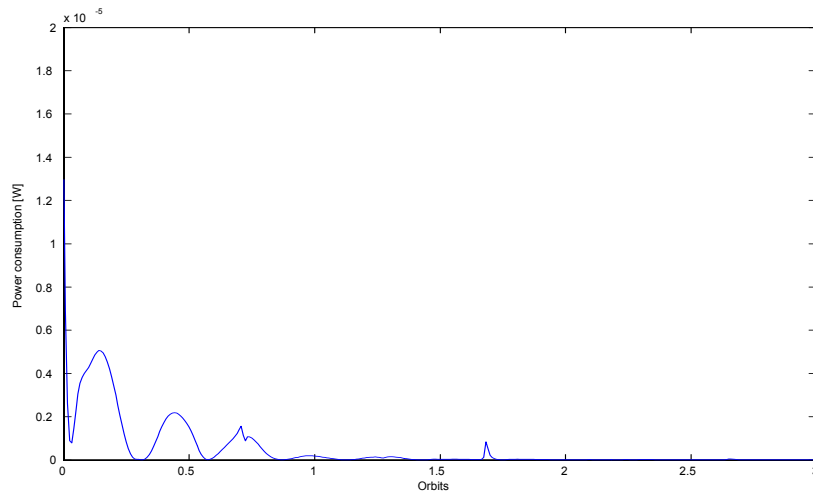


Figure 9.10: The power consumption by the LQ-controller.

**Simulation verification 10.** *Figure 9.10 shows the power consumption of the LQ-controller, and the power consumption is very low. The performance of the controller is very good.*

### 9.3. Comparison

Both the angular velocity controller and the attitude feedback controller may be used in the stabilization mode. But the attitude feedback controller seems to have some questionable stability properties compared to the angular velocity feedback controller. The LQ-controller has good stability properties, and very low power consumption. Though it can only be used in a small are about the equilibrium point.

A good choice is to use the angular velocity controller for stabilization of the satellite and use the LQ-controller close to the equilibrium to keep the satellite stabilized.

**Part III**  
**Conclusion**

## 10. CONCLUDING REMARKS

In this thesis the attitude control and stabilization of the Norwegian student satellite nCube has been studied.

It has been proved that the Wisniewski controller will be stable regardless of the periodicity of the geomagnetic field. This has been done by proving that the Wisniewski controller will be stable for a periodic geomagnetic field by using Krasovskii-LaSalle theorem. In the case of a non periodic geomagnetic field the stabilization is proved by using Matrosov's theorem. The stability is also verified by simulations both for a periodic and a non periodic geomagnetic field model.

Three controllers have been investigated in this thesis. The angular velocity feedback controller (the Wisniewski controller), the attitude controller and the linear quadratic controllers. Based on the results of the simulations it is recommended to use the Wisniewski controller for stabilization and the linear quadratic controller for maintaining the stabilization in a small area around the equilibrium for the satellite.

## BIBLIOGRAPHY

- [1] J. T. Gravdahl and O. Egeland. Modeling and simulation for control.
- [2] P. K. Soglo. 3-aksestyring av gravitasjonsstabilisert satellitt ved bruk av magnetpoler. Master thesis, NTNU 1994
- [3] H.K. Khalil(2000). Nonlinear Systems. (Third Edition)
- [4] M. Vidyasagar(1993). Nonlinear Systems Analysis. (Second Edition)
- [5] Kristiansen. Norwegian micro satellite.Master thesis, NTNU 2000
- [6] F. M. Indergaard. Design and implementation of a gravity boom for the Norwegian nano satellite NCUBE. Master thesis, NTNU 2003
- [7] B. E. Busterud. Orienteringsregulering av mikrosatellitter. Master thesis, NTNU 2003
- [8] J. R. Wertz and W. J. Larson. Space mission analysis and design. Librry of Congress Cataloging-in-Publication Data (1999) third edition
- [9] D. A. Vallado.(2001) Fundamentals of Astrodynamics and Applications(Second Edition)
- [10] R. Wisniewski and M. Blanke (1996) Fully magnetic attitude control for spacecraft subject to gravity gradient
- [11] P. Kearey, M. Brooks and I. Hill(2002). An Introduction to Geophysical Exploration. (Third Edition)
- [12] W. H. Campbell (1997). Introduction to Geomagnetic Fields.
- [13] ESA SP-1279(6) April 2004. Swarm -The Earth's Magnetic Field and Environment Explorers

- [14] [http://www.esa.int/export/esaLP/ESA3QZJE43D\\_swarm\\_0.html](http://www.esa.int/export/esaLP/ESA3QZJE43D_swarm_0.html)
- [15] C.T. Russel IEEE(2000) The Solar Wind Interaction with the Earth's Magnetosphere: A Tutorial
- [16] P. C. Hughes. Spacecraft Attitude Dynamics. (1986)
- [17] V. M. Matrosov. On the stability of motion. PMM Vol.26, No.5 1962, pp. 885-895
- [18] A. Loria, E. Panteley, D. Popovic and A. R. Teel. An extension of Matrosov's theorem with application to stabilization of nonholonomic control systems. (IEEE 2002)
- [19] T. I. Fossen. Marine Control Systems. (2002)
- [20] C. H. Edwards, Jr. and D. E. Penney. Elementary Linear Algebra. (1988)
- [21] K. M. Fauske. NCUBE Attitude Control. Project work, NTNU 2002
- [22] E. Kyrkjebø. Three-axis determination using magnetometers and a star tracker. Master thesis, NTNU 2000
- [23] K. Svartveit. Attitude determination of the NCUBE satellite. Master thesis, NTNU 2003
- [24] <http://www.rockerange\ncube>
- [25] S. Skogestad and I. Postlethwaite. Multivariable feedback control.(1996)
- [26] A. Skullestad. Attitude control of microsatellites. Kongsberg Defence & Aerospace.(2004)

**Part IV**  
**Appendix**

## A. APPENDIX; DETAILED DERIVATIONS

### A.1. Devation of the total energy

The energy can be expressed as:

$$E_{tot} = \frac{1}{2}(\omega_{ob}^b)^T \mathbf{I} \omega_{ob}^b + \frac{3}{2}\omega_o^2((\mathbf{c}_3^b)^T \mathbf{I} \mathbf{c}_3^b - I_z) + \frac{1}{2}\omega_o^2(I_x - (\mathbf{c}_1^b)^T \mathbf{I} \mathbf{c}_1^b) \quad (\text{A.1})$$

expanding the last to terms gives

$$E_{tot} = \frac{1}{2}(\omega_{ob}^b)^T \mathbf{I} \omega_{ob}^b + \frac{3}{2}\omega_o^2(I_x c_{13}^2 + I_y c_{23}^2 + I_z(c_{33}^2 - 1)) + \frac{1}{2}\omega_o^2(I_z c_{31}^2 + I_y c_{21}^2 + I_x(c_{11}^2 - 1)) \quad (\text{A.2})$$

by using

$$\mathbf{c}_i^T \mathbf{I} \mathbf{c}_i = I_x c_{1i}^2 + I_y c_{2i}^2 + I_z c_{3i}^2 \quad (\text{A.3})$$

As stated in chapter 1 the rotation matrix  $\mathbf{R}_o^b$  is orthogonal. Therefore the following must be satisfied  $c_{11}^2 + c_{21}^2 + c_{31}^2 = 1$  and  $c_{13}^2 + c_{23}^2 + c_{33}^2 = 1$  while using this constrains we get

$$E_{tot} = \frac{1}{2}(\omega_{ob}^b)^T \mathbf{I} \omega_{ob}^b + \frac{3}{2}\omega_o^2((I_x - I_z)c_{13}^2 + (I_y - I_z)c_{23}^2) + \frac{1}{2}\omega_o^2((I_x - I_y)c_{21}^2 + (I_x - I_z)c_{31}^2) \quad (\text{A.4})$$

### A.2. Obtaining the linearized satellite model

The satellite model may be expressed as:

$$\mathbf{I} \dot{\boldsymbol{\omega}}_{ib}^b = -\boldsymbol{\omega}_{ib}^b \times (\mathbf{I} \boldsymbol{\omega}_{ib}^b) + \tau_{grav}^b + \mathbf{S}(\mathbf{m}^b) \mathbf{B}^o \quad (\text{A.5})$$

where

$$\boldsymbol{\omega}_{ib}^b = \begin{bmatrix} \omega_x \\ \omega_y \\ \omega_z \end{bmatrix} = \begin{bmatrix} 2\dot{\varepsilon}_1 - 2\omega_o\varepsilon_3 \\ 2\dot{\varepsilon}_2 + \omega_o \\ 2\dot{\varepsilon}_3 + 2\omega_o\varepsilon_1 \end{bmatrix} \quad (\text{A.6})$$

$$\dot{\boldsymbol{\omega}}_{ib}^b = \begin{bmatrix} \dot{\omega}_x \\ \dot{\omega}_y \\ \dot{\omega}_z \end{bmatrix} = \begin{bmatrix} 2\ddot{\varepsilon}_1 - 2\omega_o\dot{\varepsilon}_3 \\ 2\ddot{\varepsilon}_2 \\ 2\ddot{\varepsilon}_3 - 2\omega_o\dot{\varepsilon}_1 \end{bmatrix} \quad (\text{A.7})$$

$$\tau_{grav}^b = 3\omega_o^2 \begin{bmatrix} (I_z - I_y)\varepsilon_1 \\ (I_z - I_x)\varepsilon_2 \\ 0 \end{bmatrix} \quad (\text{A.8})$$

$$\tau_m^b = \mathbf{S}(\mathbf{m}^b)\mathbf{B}^o = \begin{bmatrix} B_z^o m_y - B_y^o m_z \\ B_x^o m_z - B_z^o m_x \\ B_y^o m_x - B_x^o m_y \end{bmatrix} \quad (\text{A.9})$$

using that

$$\mathbf{R}_o^b = 2 \begin{bmatrix} \frac{1}{2} & \varepsilon_3 & -\varepsilon_2 \\ -\varepsilon_3 & \frac{1}{2} & \varepsilon_1 \\ \varepsilon_2 & -\varepsilon_1 & \frac{1}{2} \end{bmatrix} \quad (\text{A.10})$$

inserted in the satellite model results in

$$I_x(2\ddot{\varepsilon}_1 - 2\omega_o\dot{\varepsilon}_3) = (I_y - I_z)(2\omega_o\dot{\varepsilon}_3 + 8\omega_o^2\varepsilon_1) + (B_z^o m_y - B_y^o m_z) \quad (\text{A.11})$$

$$I_y(2\ddot{\varepsilon}_2) = -6(I_x - I_z)\omega_o^2\varepsilon_2 + (B_x^o m_z - B_z^o m_x) \quad (\text{A.12})$$

$$I_z(2\ddot{\varepsilon}_3 - 2\omega_o\dot{\varepsilon}_1) = (I_y - I_x)(2\omega_o\dot{\varepsilon}_3 + 2\omega_o^2\varepsilon_1) + (B_y^o m_x - B_x^o m_y) \quad (\text{A.13})$$

then using that

$$\begin{aligned} k_x &= \frac{I_y - I_z}{I_x} \\ k_y &= \frac{I_x - I_z}{I_y} \\ k_z &= \frac{I_y - I_x}{I_z} \end{aligned} \quad (\text{A.14})$$

results in

$$\ddot{\varepsilon}_1 = (1 - k_x)\omega_o\dot{\varepsilon}_3 - 4k_x\omega_o^2\varepsilon_1 + \frac{1}{2I_x}(B_z^o m_y - B_y^o m_z) \quad (\text{A.15})$$

$$\ddot{\varepsilon}_2 = -3k_y\omega_o^2\varepsilon_2 + \frac{1}{2I_y}(B_x^o m_z - B_z^o m_x) \quad (\text{A.16})$$

$$\ddot{\varepsilon}_3 = -(1 - k_z)\omega_o\dot{\varepsilon}_1 - k_z\omega_o^2\varepsilon_3 + \frac{1}{2I_x}(B_y^o m_x - B_x^o m_y) \quad (\text{A.17})$$

## B. APPENDIX; VECTORS AND SKEW-SYMMETRIC MATRICES

This chapter presents some basic operations and definitions used in vector and matrix algebra used in this thesis. They are from [1], [19] and [20].

$$\mathbf{x} \times \mathbf{x} = \mathbf{0} \quad (\text{B.1})$$

$$\mathbf{x} \times \mathbf{y} = -\mathbf{y} \times \mathbf{x} \quad (\text{B.2})$$

$$\mathbf{x} \times (\mathbf{y} + \mathbf{z}) = \mathbf{x} \times \mathbf{y} + \mathbf{x} \times \mathbf{z} \quad (\text{B.3})$$

$$\mathbf{x} \times (\mathbf{y} \times \mathbf{z}) = (\mathbf{x}^T \mathbf{z})\mathbf{y} - (\mathbf{x}^T \mathbf{y})\mathbf{z} \quad (\text{B.4})$$

$$\mathbf{x}^T (\mathbf{y} \times \mathbf{z}) = \mathbf{y}^T (\mathbf{z} \times \mathbf{x}) = \mathbf{z}^T (\mathbf{x} \times \mathbf{y}) \quad (\text{B.5})$$

$$\mathbf{S}(\mathbf{x}) = \begin{bmatrix} 0 & -x_3 & x_2 \\ x_3 & 0 & -x_1 \\ -x_2 & x_1 & 0 \end{bmatrix} \quad (\text{B.6})$$

$$\mathbf{S}(\cdot) = -\mathbf{S}^T(\cdot) \quad (\text{B.7})$$

$$\mathbf{y} \times \mathbf{x} = \mathbf{S}(\mathbf{y})\mathbf{x} \quad (\text{B.8})$$

$$-\mathbf{x} \times \mathbf{y} = -\mathbf{S}(\mathbf{x})\mathbf{y} \quad (\text{B.9})$$

$$\mathbf{S}(\mathbf{x})\mathbf{x} = \mathbf{S}^T(\mathbf{x})\mathbf{x} = \mathbf{0} \quad (\text{B.10})$$

$$\mathbf{S}(\mathbf{x})\mathbf{S}(\mathbf{y})\mathbf{z} = \mathbf{y}\mathbf{x}^T\mathbf{z} - \mathbf{x}^T\mathbf{y}\mathbf{z} = (\mathbf{y}\mathbf{x}^T - \mathbf{x}^T\mathbf{y}\mathbf{I}_{3 \times 3})\mathbf{z} \quad (\text{B.11})$$

$$\mathbf{S}(\mathbf{x})\mathbf{S}(\mathbf{y}) = \mathbf{y}\mathbf{x}^T - \mathbf{x}^T\mathbf{y}\mathbf{I}_{3 \times 3} \quad (\text{B.12})$$

$$\mathbf{S}(\mathbf{x})\mathbf{S}(\mathbf{x}) = \mathbf{x}\mathbf{x}^T - \mathbf{x}^T\mathbf{x}\mathbf{I}_{3 \times 3} \quad (\text{B.13})$$

## C. APPENDIX; STEC 2004

April 14th-16th in 2004 a small group from the nCube project got the opportunity to go to the Space Technology Education Conference at EPFL, Lausanne in Switzerland. The participants from nCube was Egil Eide, Ola-Gunnar E. Julesrud and Eli J. Øverby. We represented the project nCube project and I wrote a poster for the conference. The poster is in shown in Appendix.

The motivation for the conference is stated as: "The Space Technology Education Conference would like to serve as a discussion platform for this question by bringing together students and personalities from universities, industry and ESA working in the field of low cost satellite design, construction and launch." The major part of the conference was presentations of different European satellite projects. There was also an exhibition where it was possible to ask questions to different project groups. It was very motivating and interesting to attend the conference.



Figure C.1: The STEC 2004 poster.

Figure C.2: The exhibition

## D. APPENDIX; nCUBE POSTER



norwegian student satellite

www.rocketrange.no/ncube



---

### ADCS, Attitude determination and control system

Department of Engineering Cybernetics, Norwegian University of Science and Technology  
E. J. Øverby, S. S. Ose, J. T. Gravdahl and K. M. Fauske

**Satellite model:**

$$J\dot{\omega}_b^b + \omega_b^b \times (J\omega_b^b) = \tau^b$$

$J$ : inertia matrix  
 $\omega_b^b$ : angular velocity (body - inertial frame)  
 $\tau^b$ : torques

**Actuators:**

$$\tau^b = \tau_m^b + \tau_g^b$$

- Magnetic torquers; magnetic coils
$$\tau_m^b = B \times I N A$$

$B$ : Earth's magnetic field  
 $I$ : coil current  
 $N$ : coil number  
 $A$ : coil area- Gravity gradient; gravity boom for passive stabilization
$$\tau_g^b = 3\omega_e^e \mu_e \times I u_e$$

$\omega_e^e$ : Earth's angular velocity  
 $\mu_e$ : Earth's magnetic moment  
 $I$ : inertia matrix

**Control modes:**

- Rate detumbling
- Angular detumbling
- Stabilization
- Spin
- Inverted boom recovery

**Controllers:**

- Detumbling controller
$$\dot{m}^b = -k\dot{B} - m_e$$
- Angular velocity feedback controller
$$\dot{m}^b = h\omega_b^b \times B$$

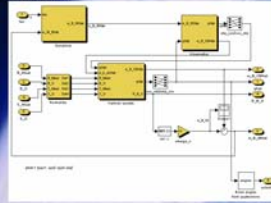
$B$ : Earth's magnetic field  
 $h$ : angular velocity feedback gain- Linear Optimal (LQ) controller
$$\dot{x}(t) = Ax(t) + B(u(t))$$

$$J(u) = \frac{1}{2} \min \int_0^T \dot{x}^T Q \dot{x} + u^T P u dt$$

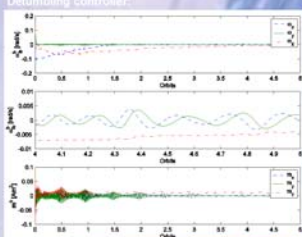
**Sensors:**

- Three axis smart digital magnetometer HMR 2300

**Kalman filter:**



**Detumbling controller:**



**Participants**





**Supporting partners**






Figure D.1:

## E. APPENDIX; MATLAB AND SIMULINK

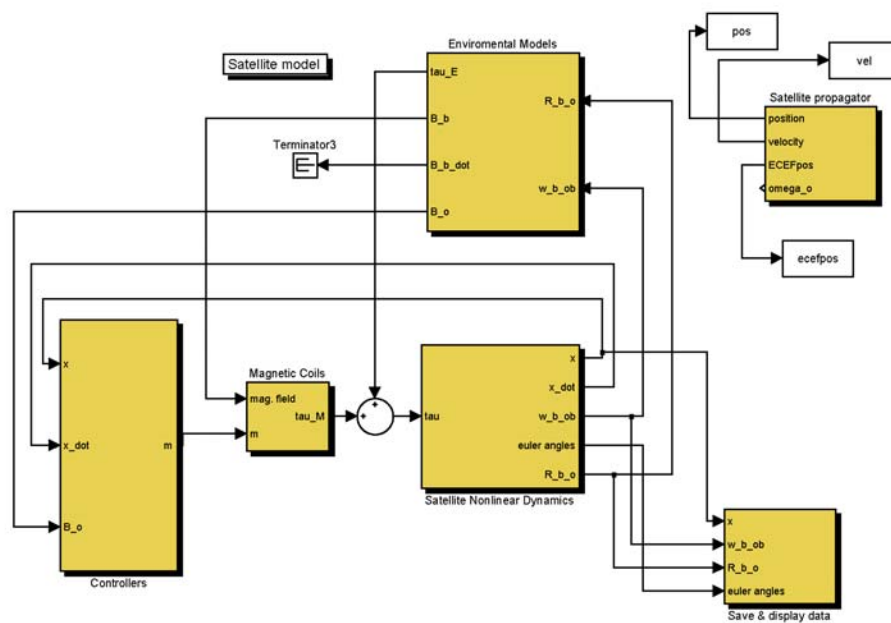
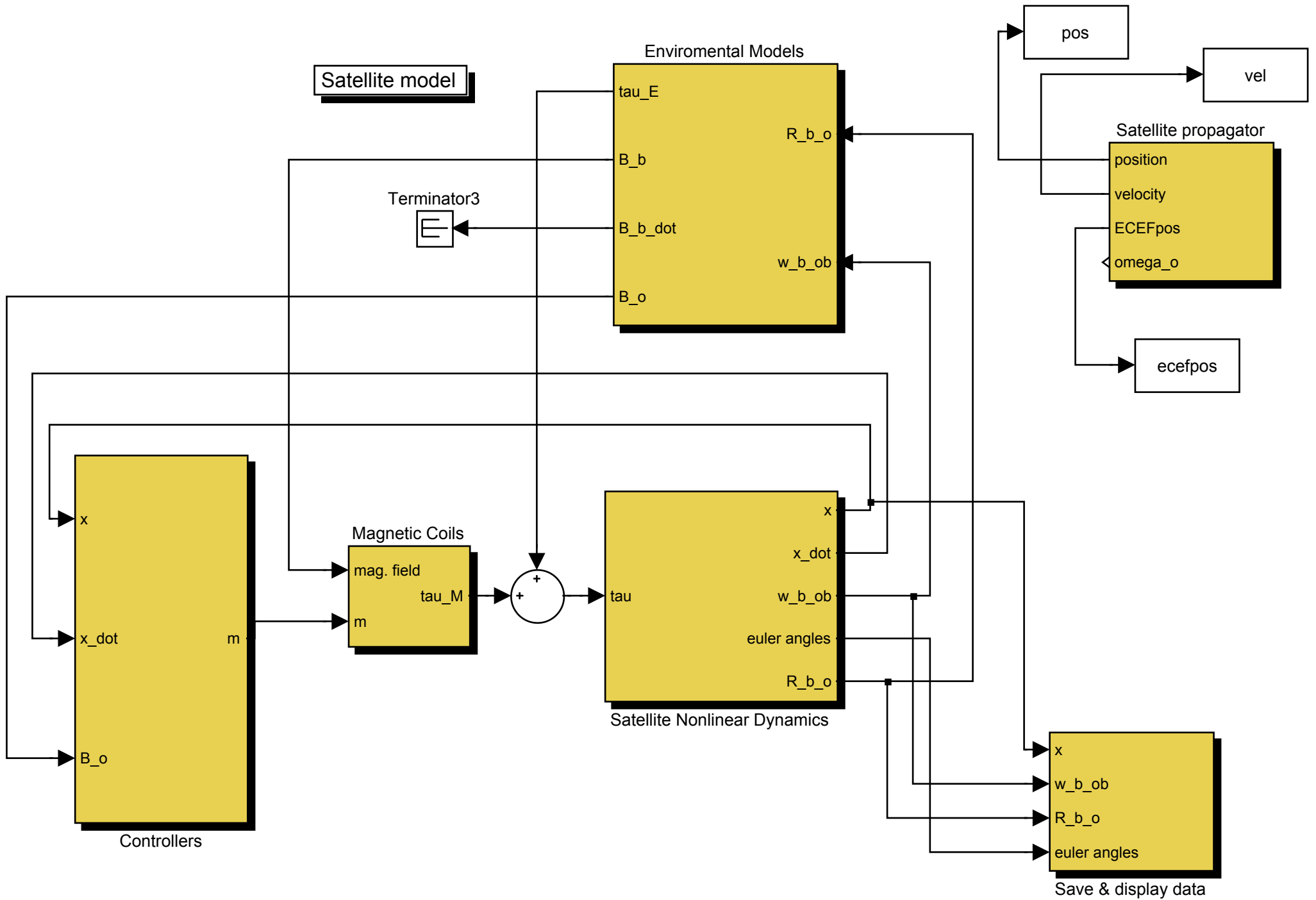
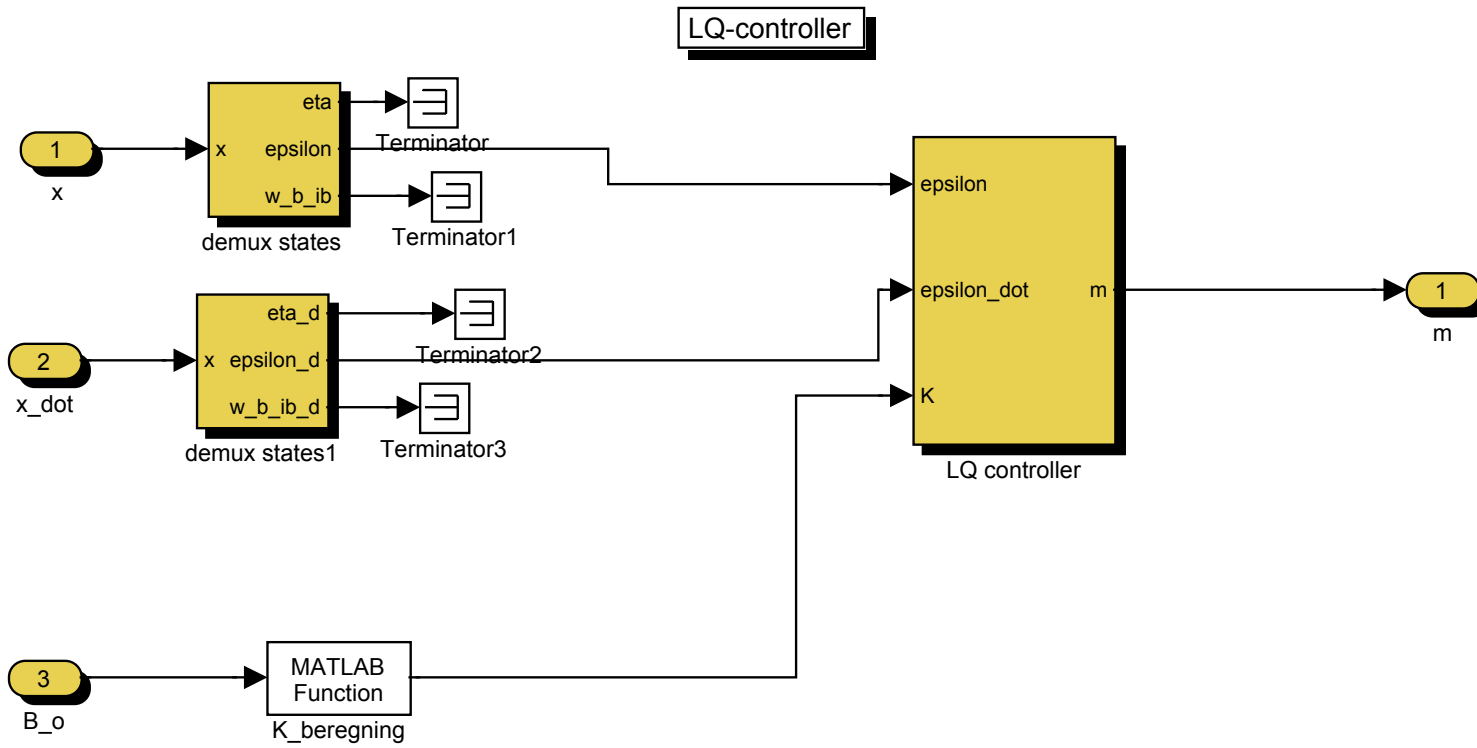
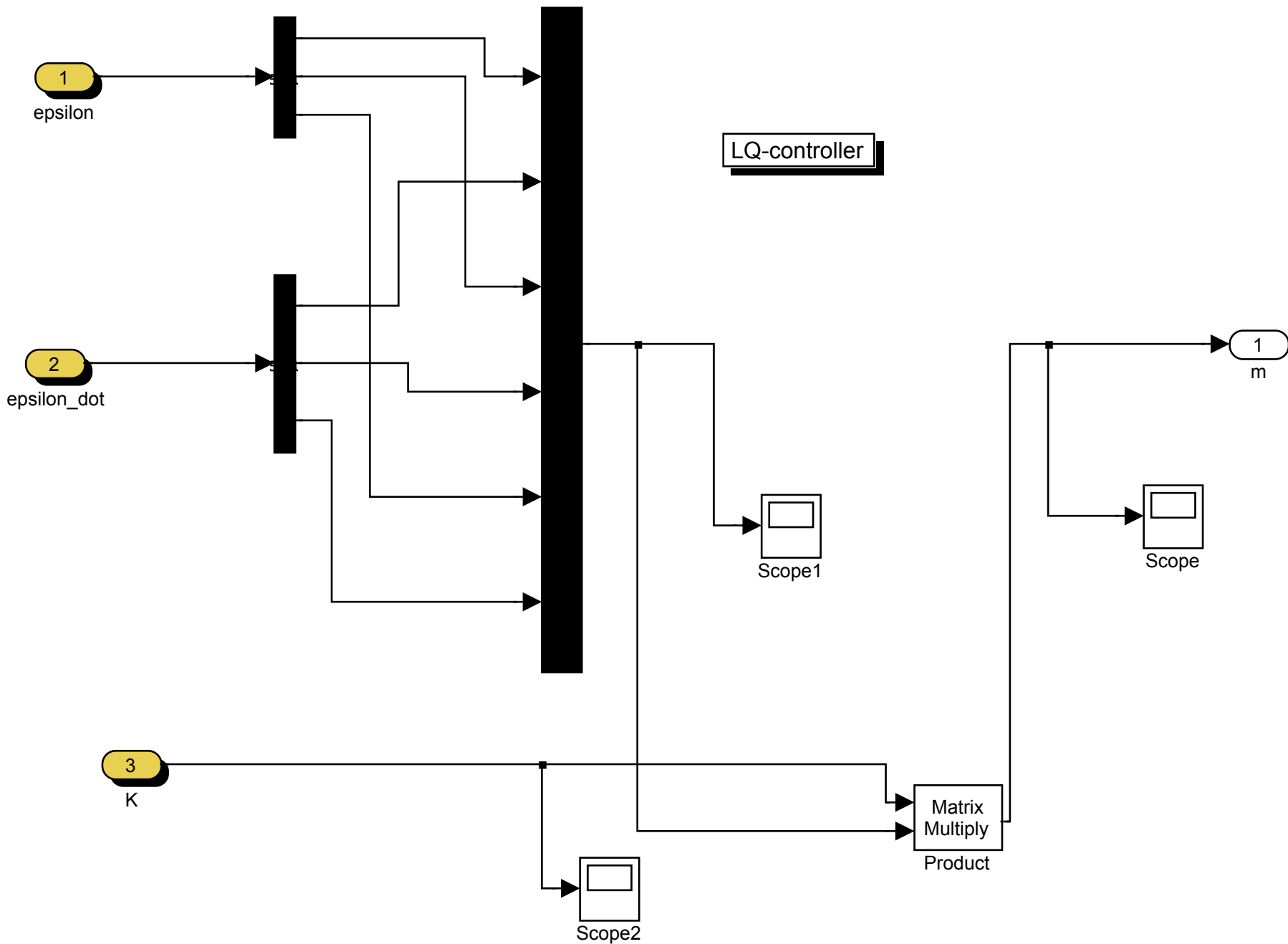
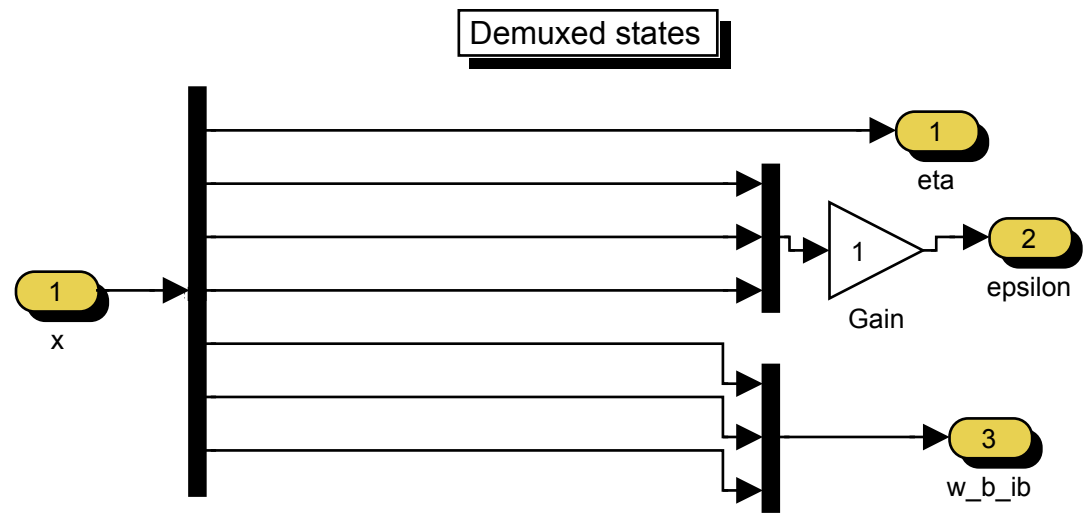


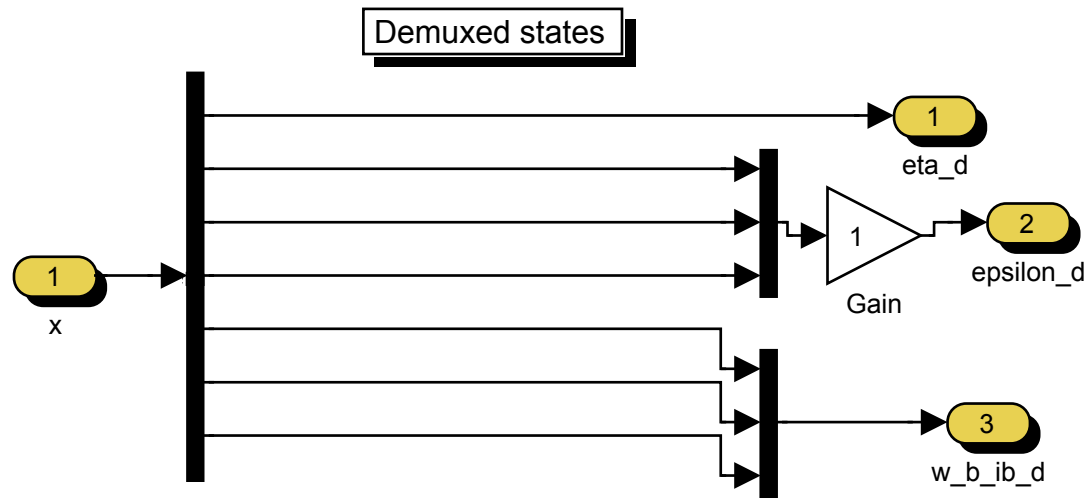
Figure E.1: The satellite model top level, when LQ-controller.



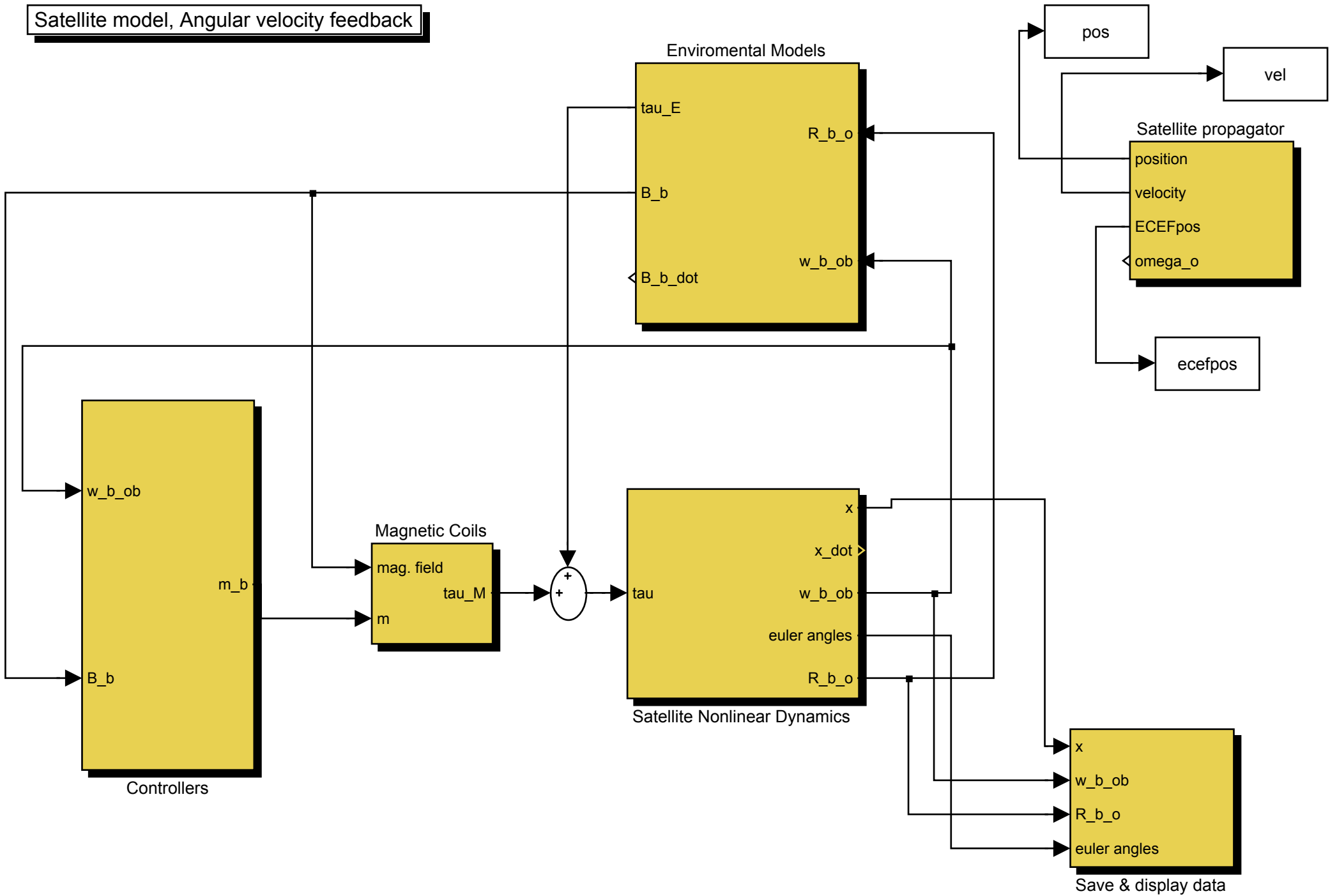




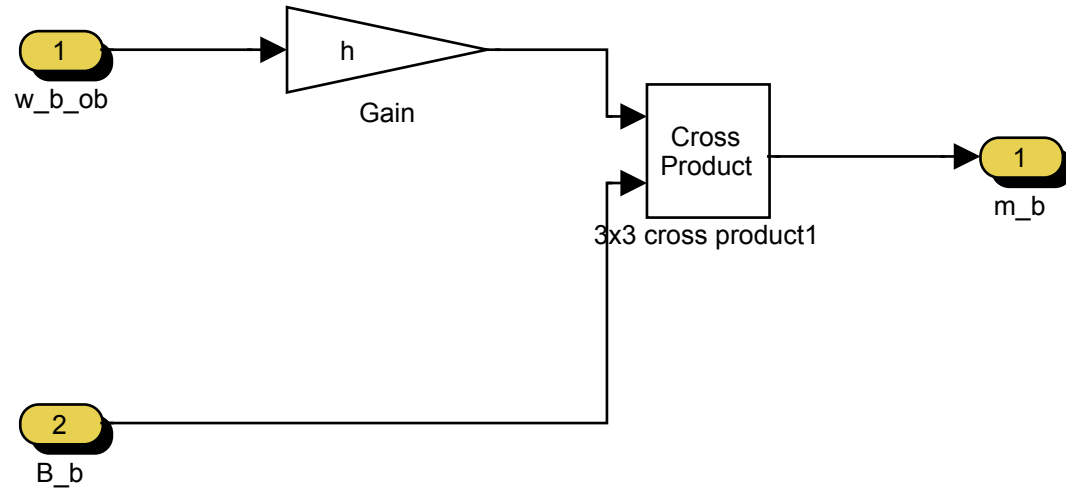




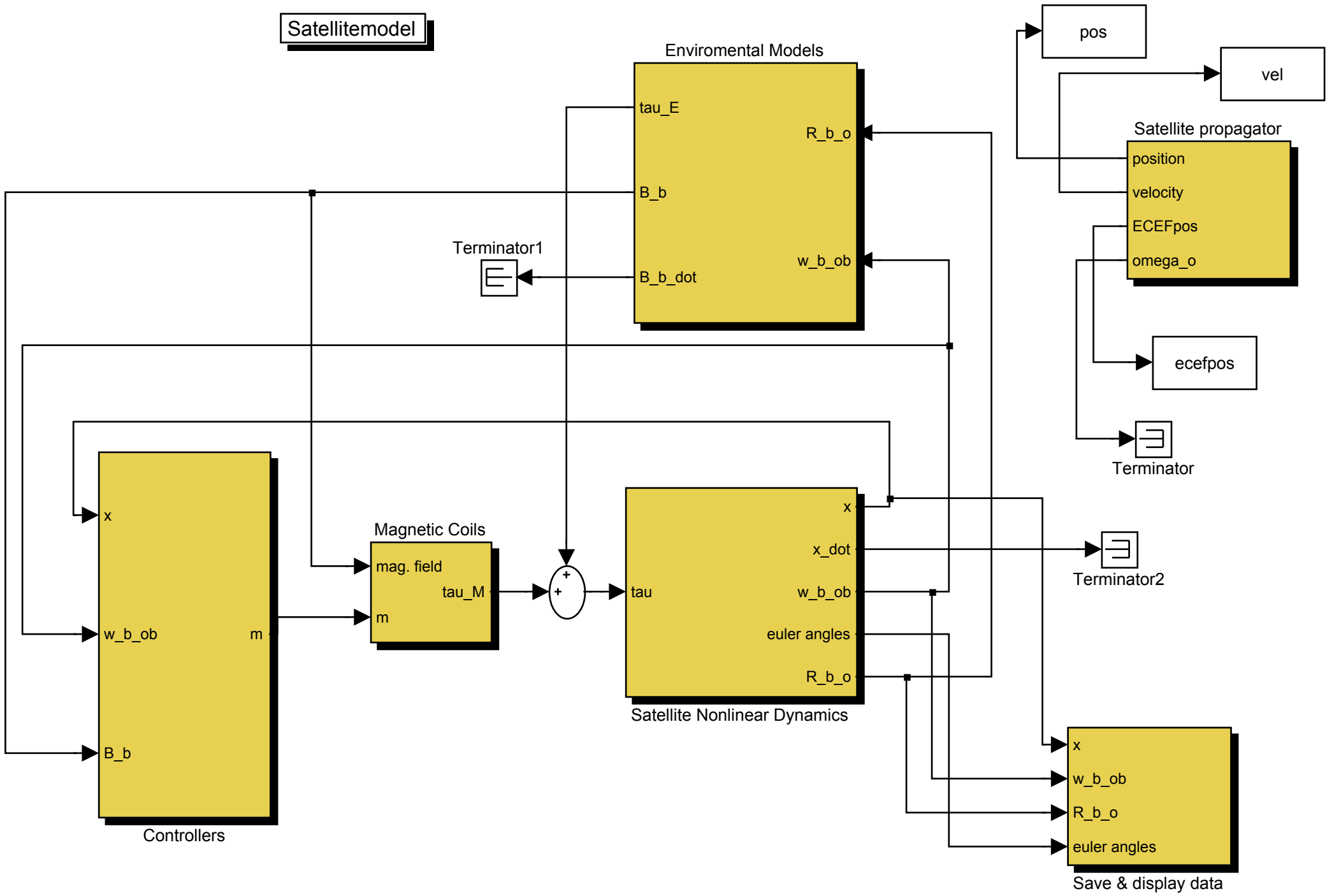
# Satellite model, Angular velocity feedback



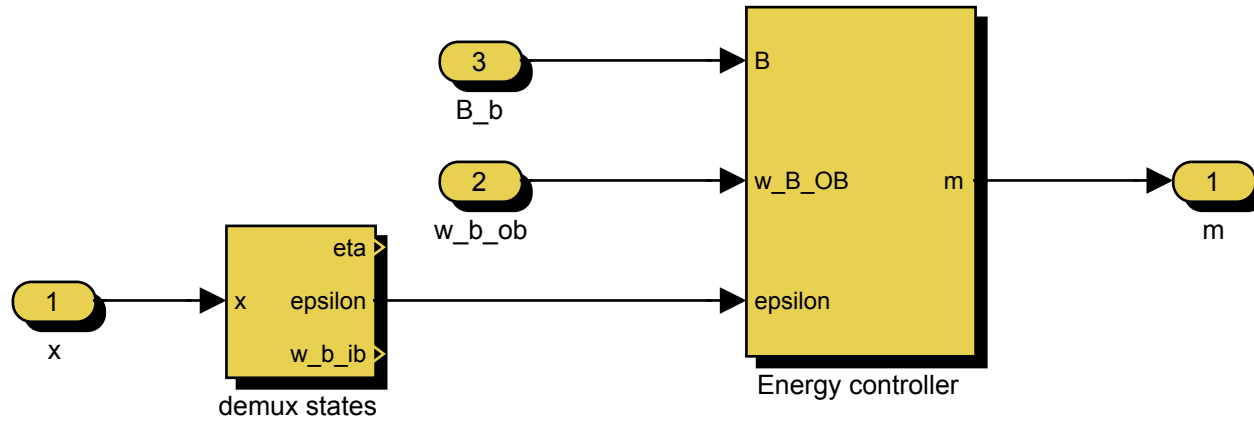
# Angular velocity feedback controller

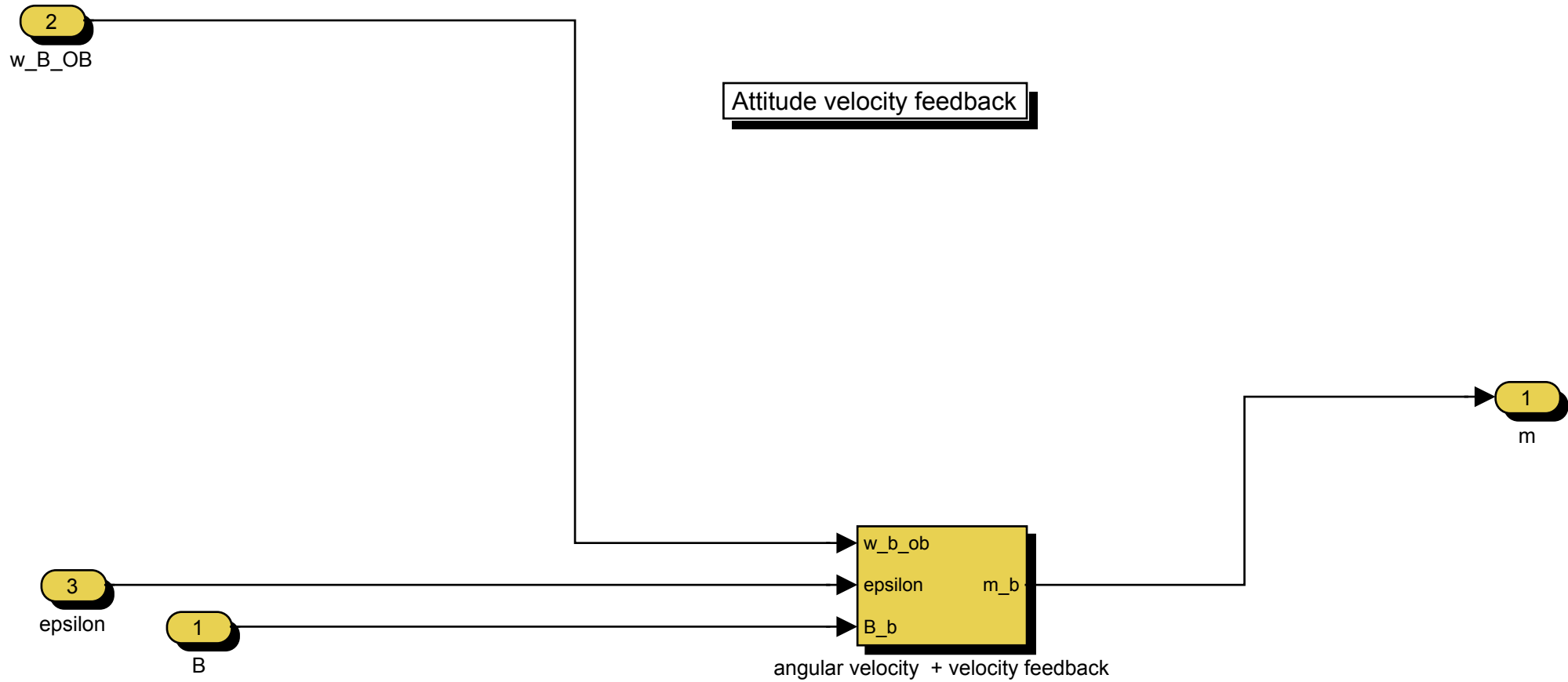


# Satellitemodel

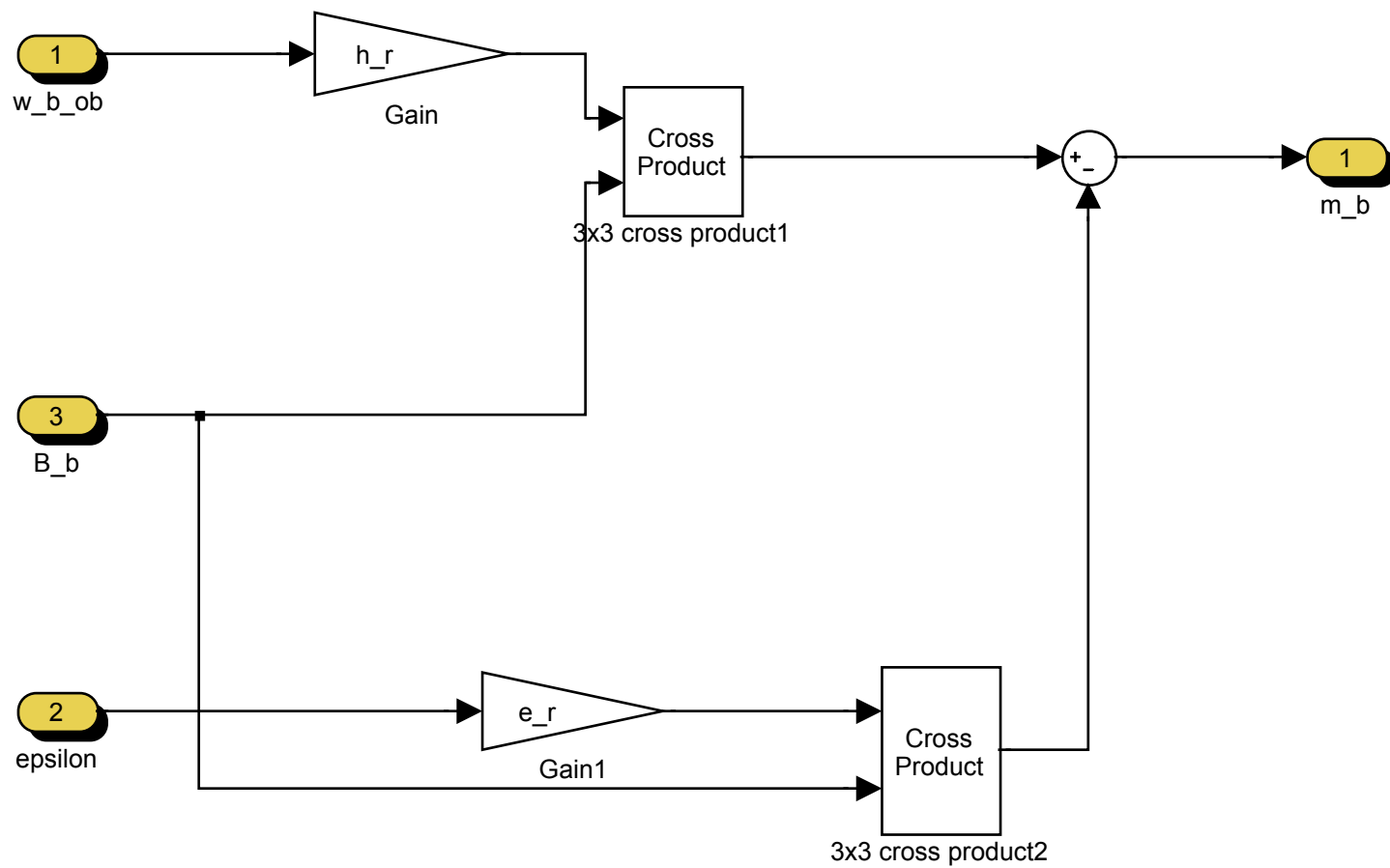


# Energy controller

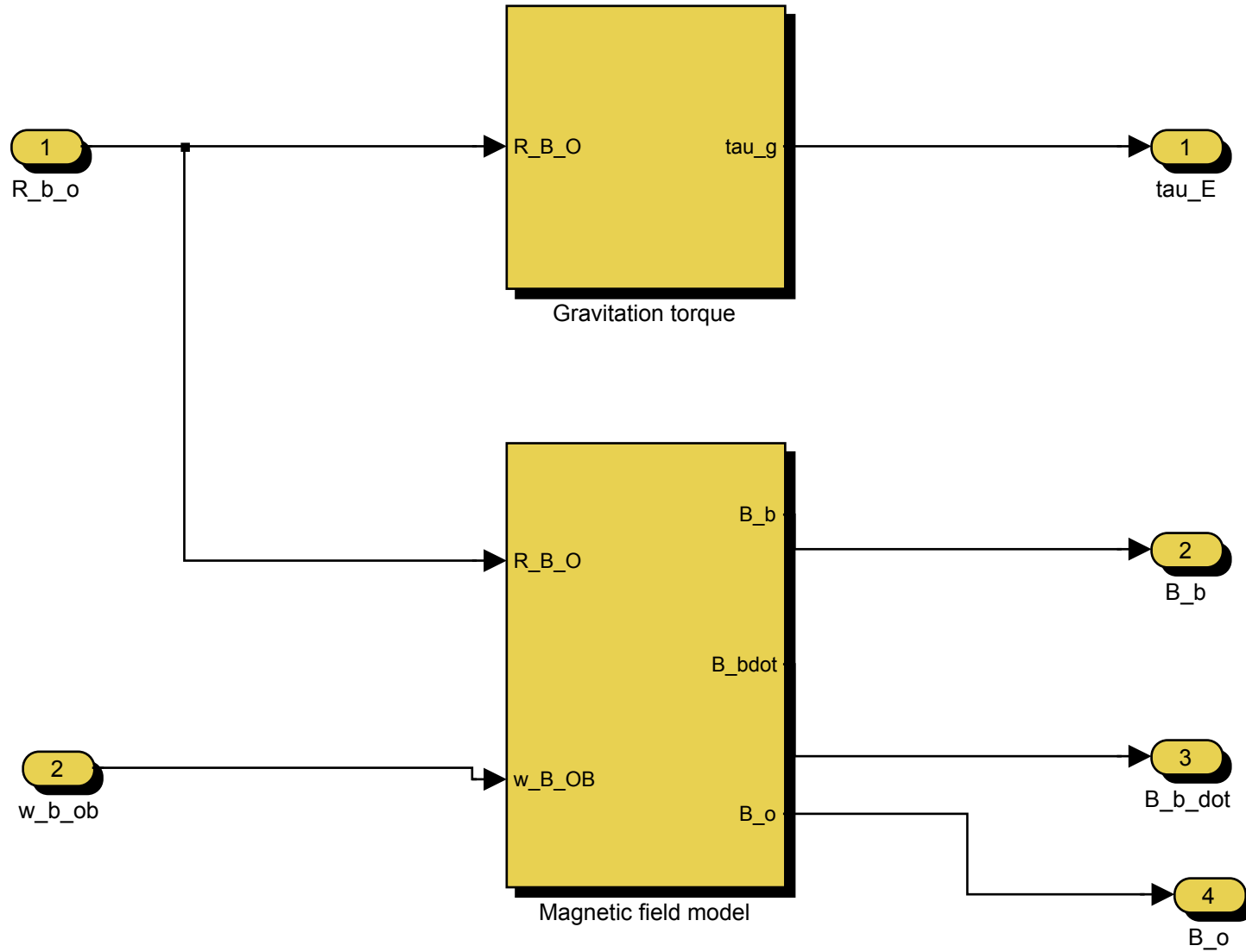




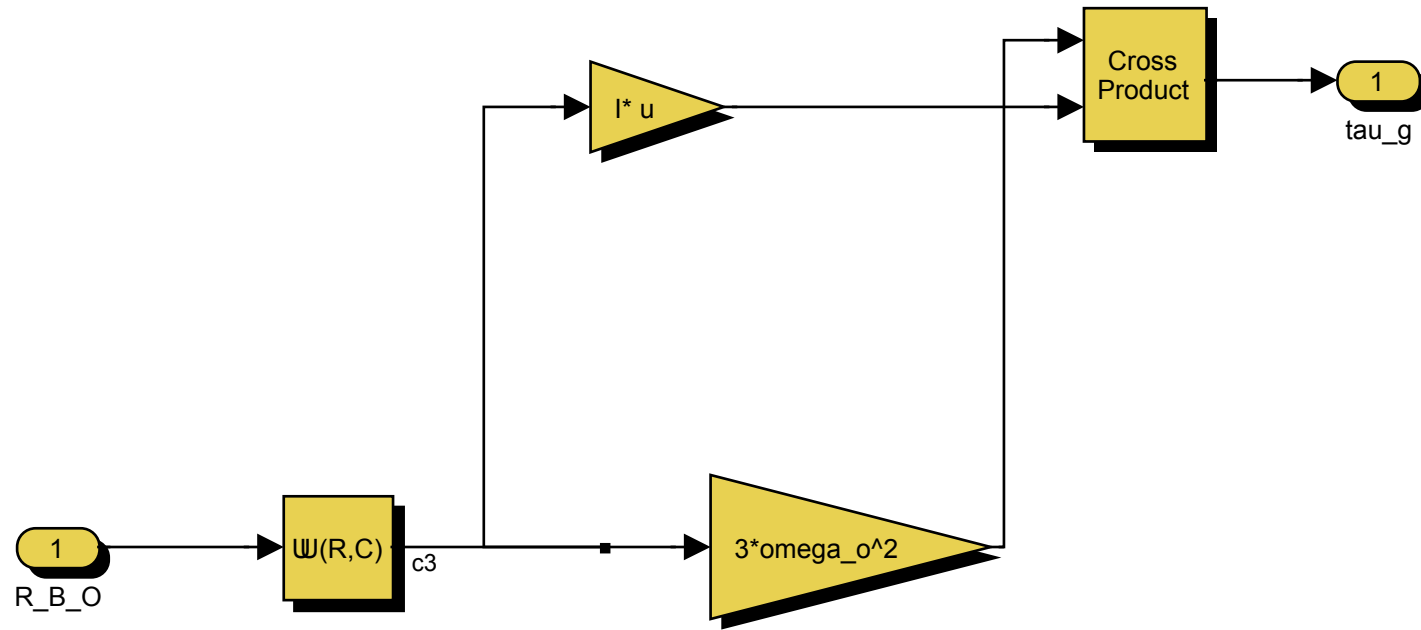
Attitude feedback



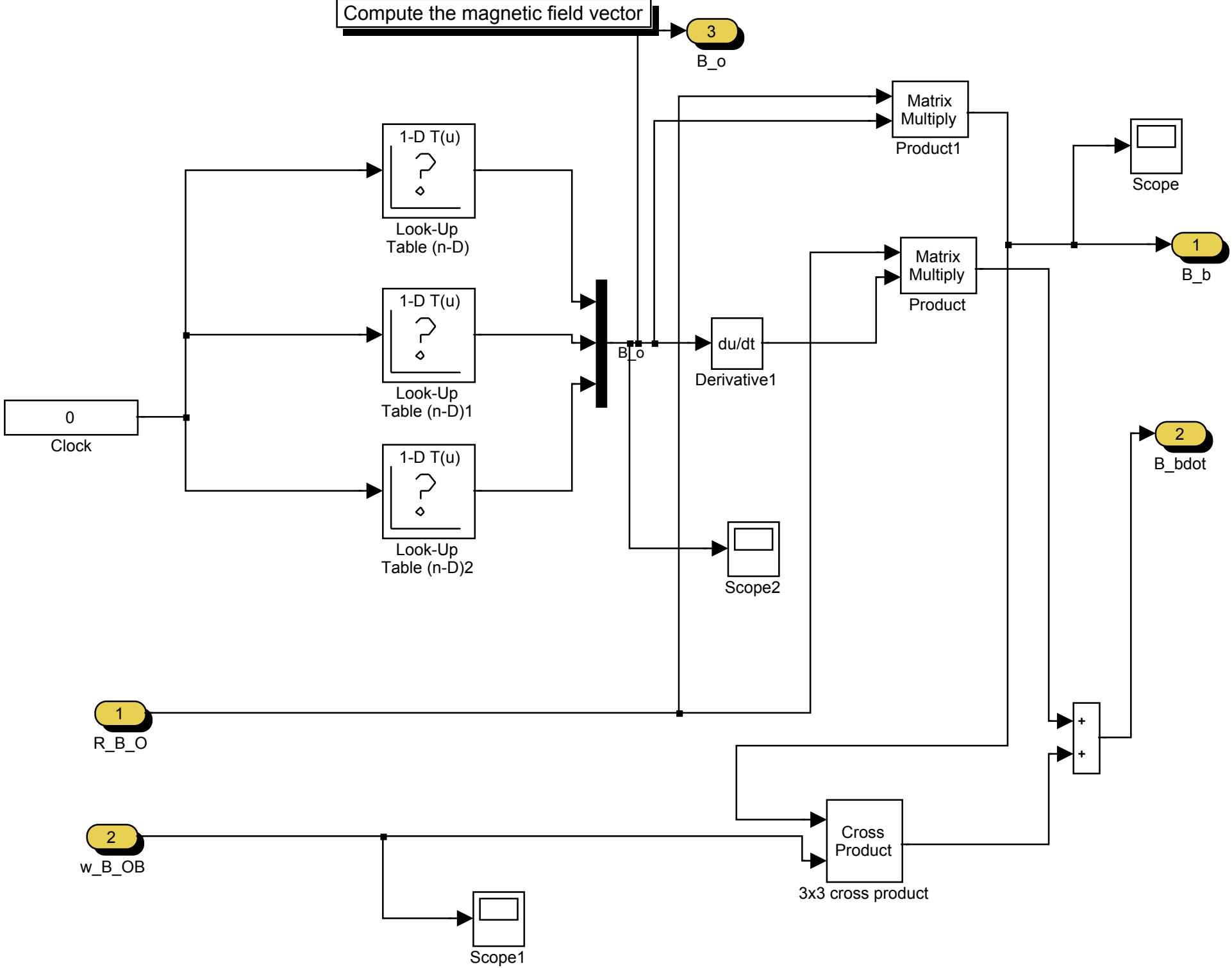
# Environment Models



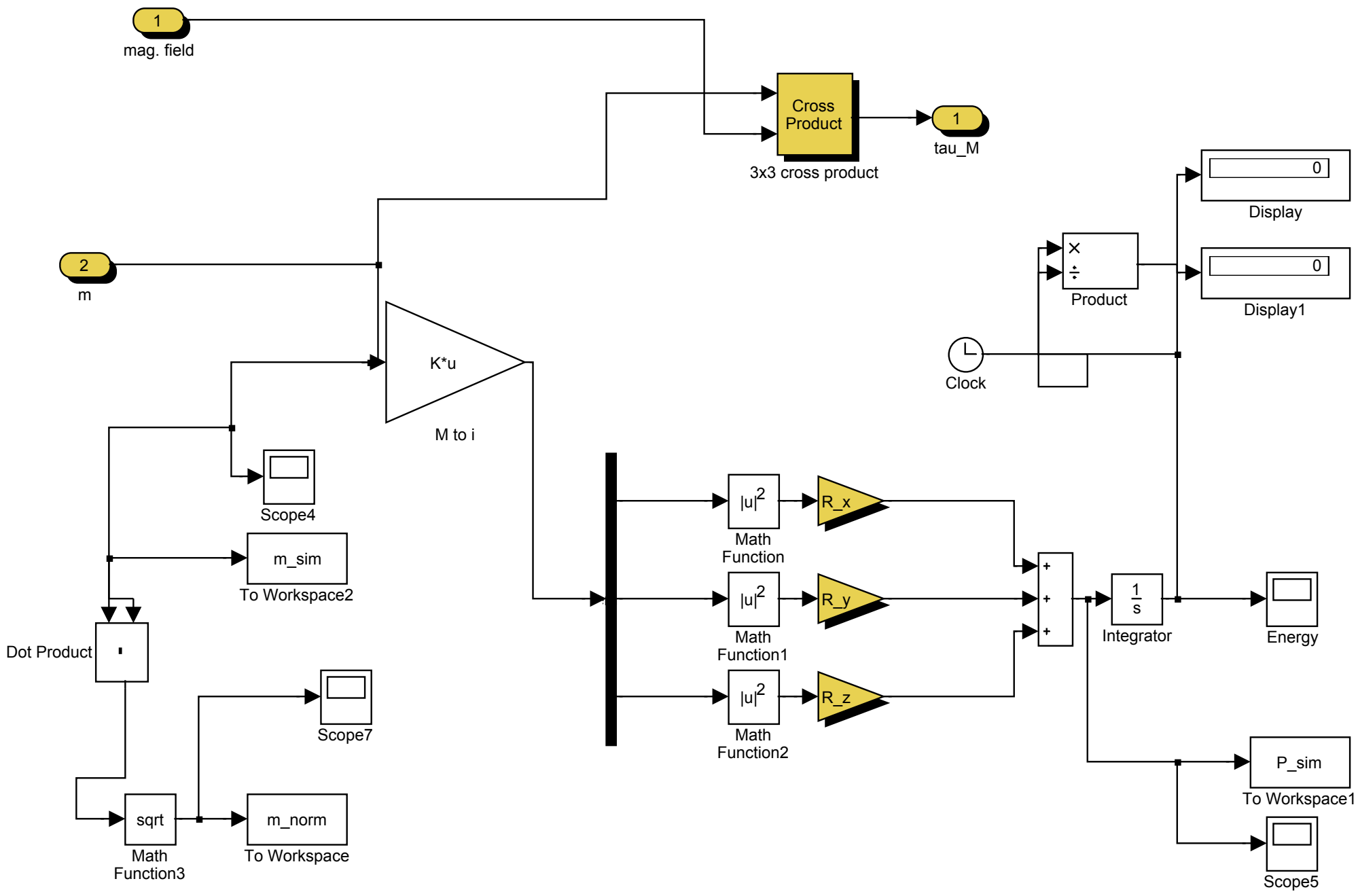
# Gravitation torque



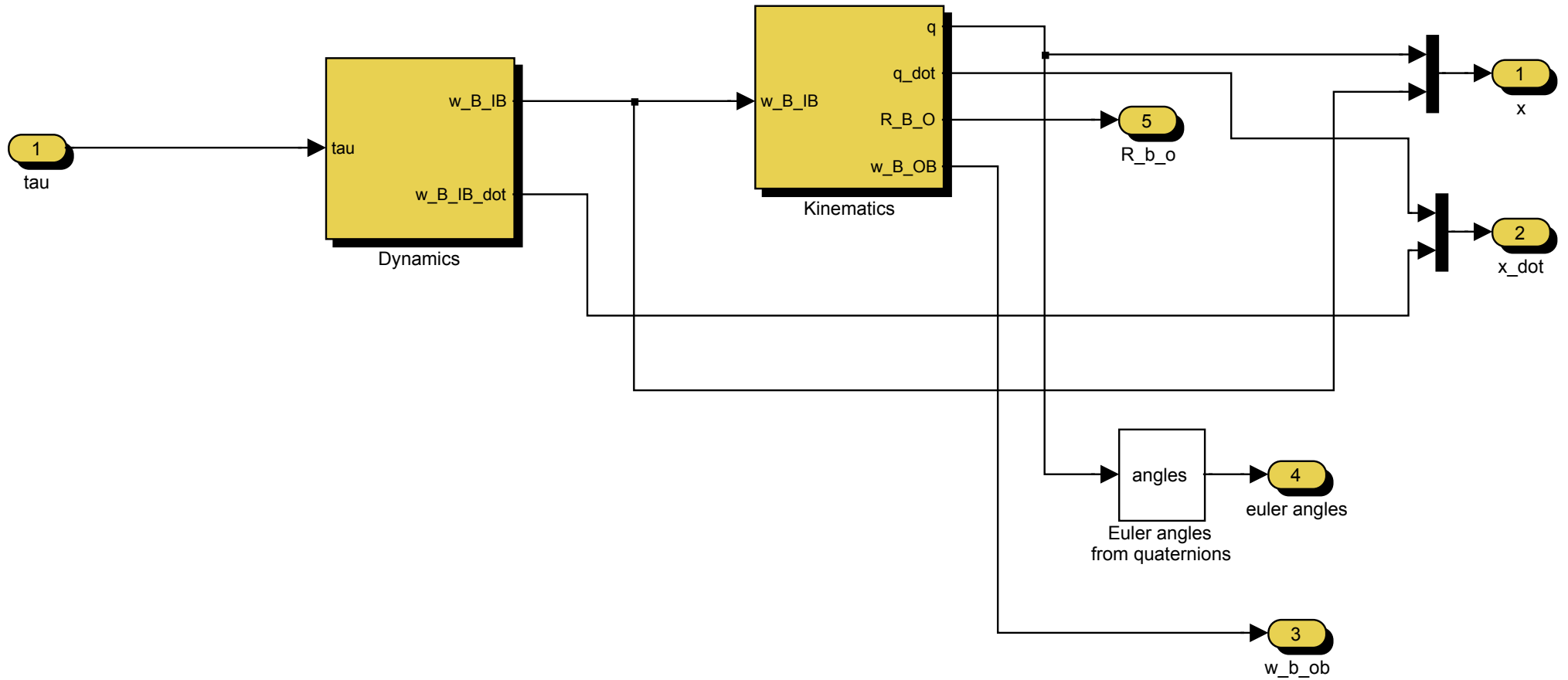
# Compute the magnetic field vector

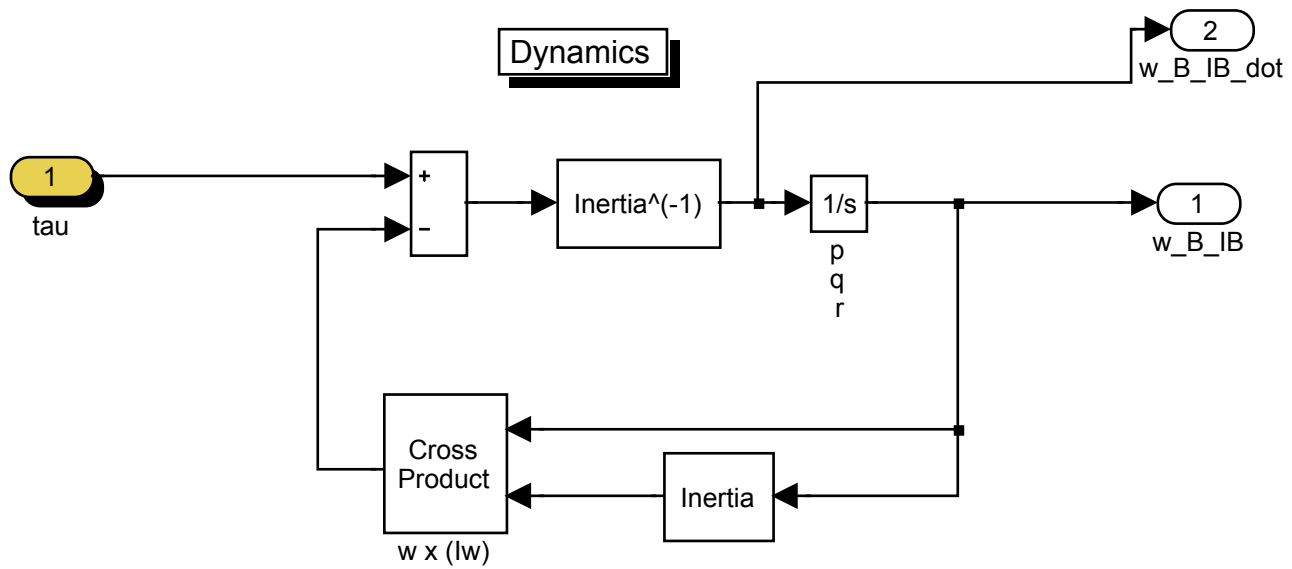


# Magnetic coils model

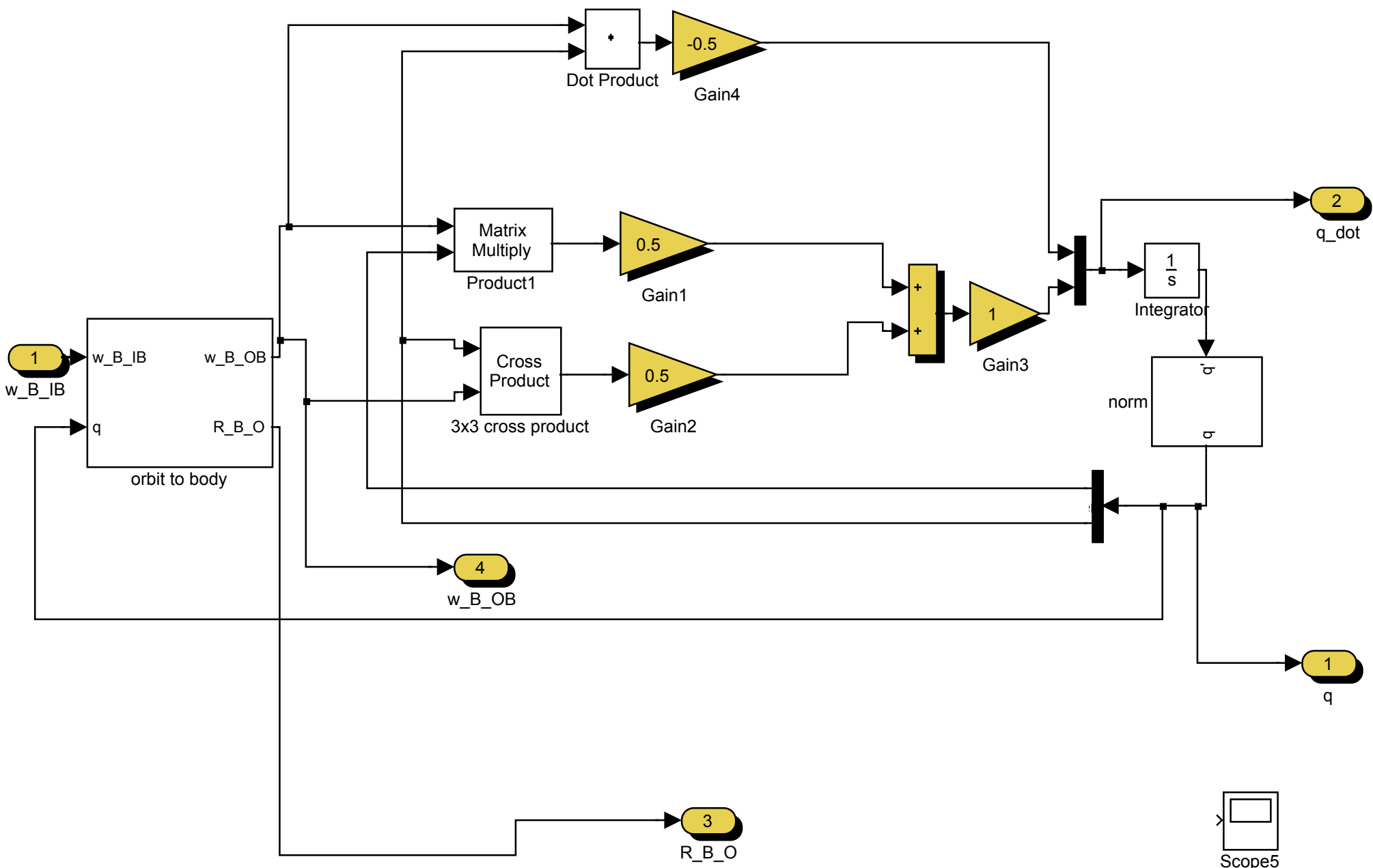


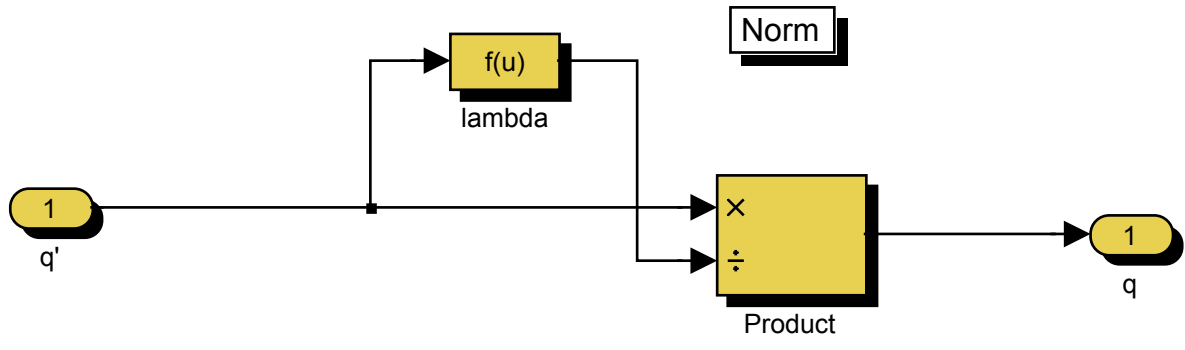
# Satellite Nonlinear Dynamics



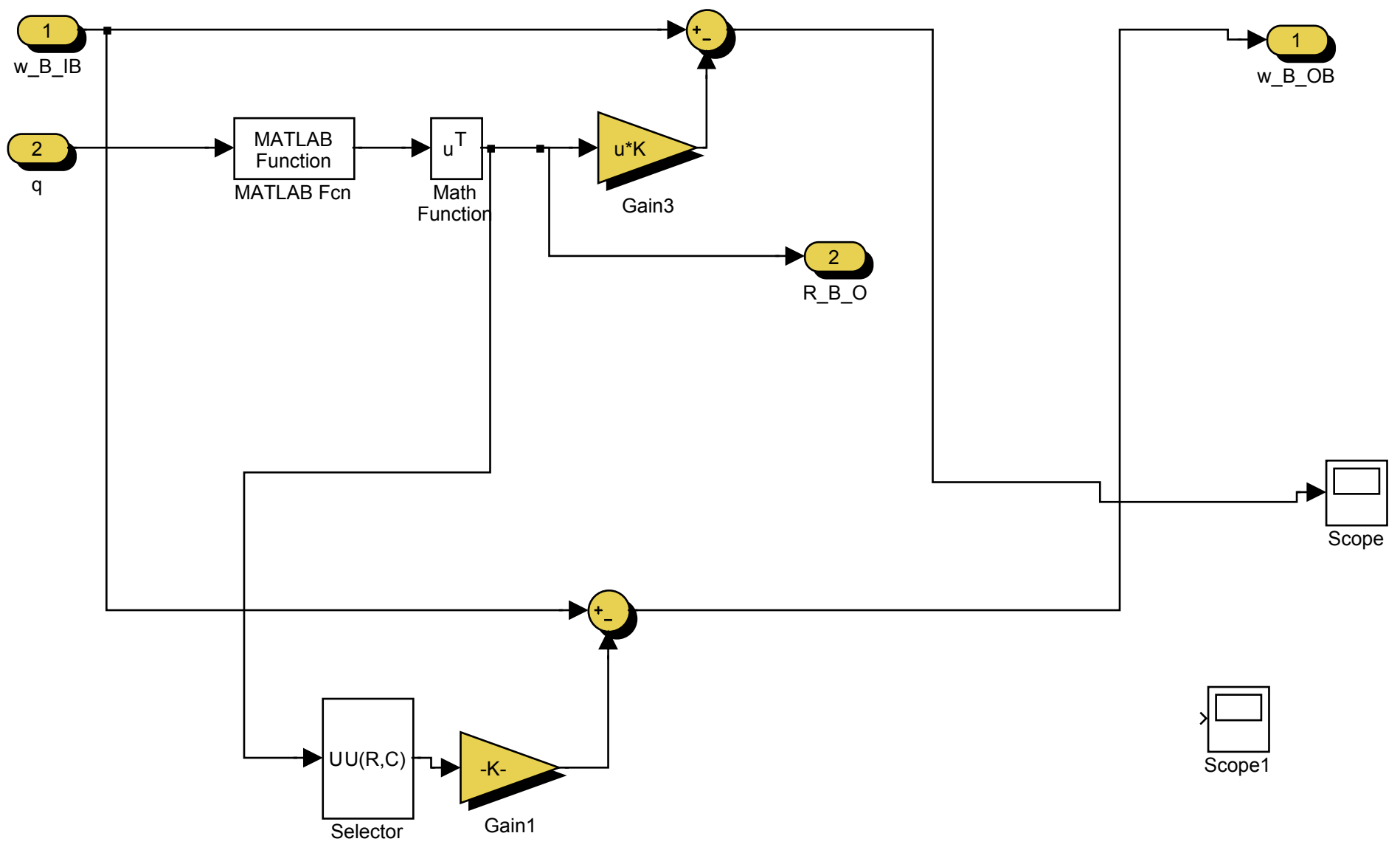


# Kinematics

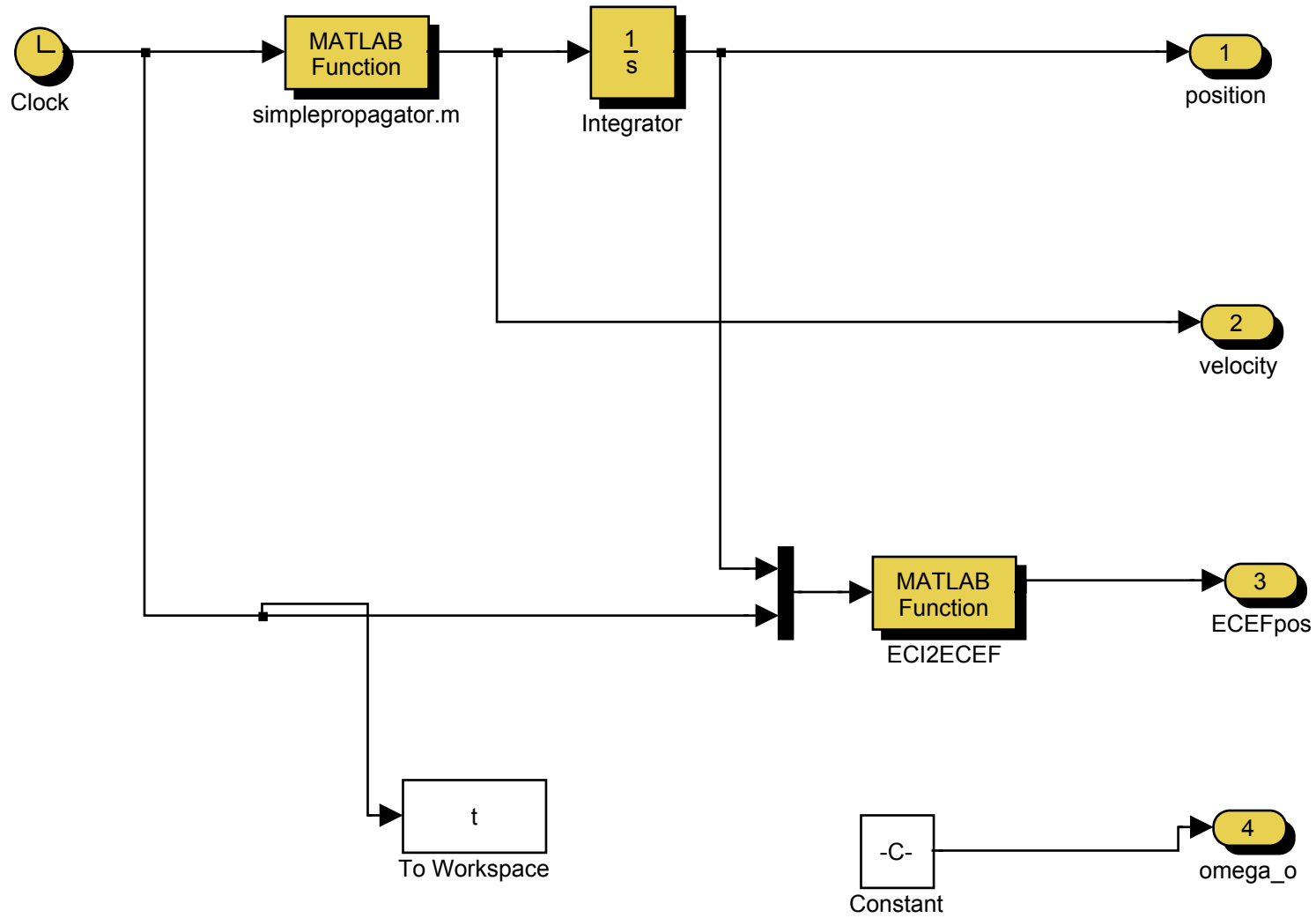


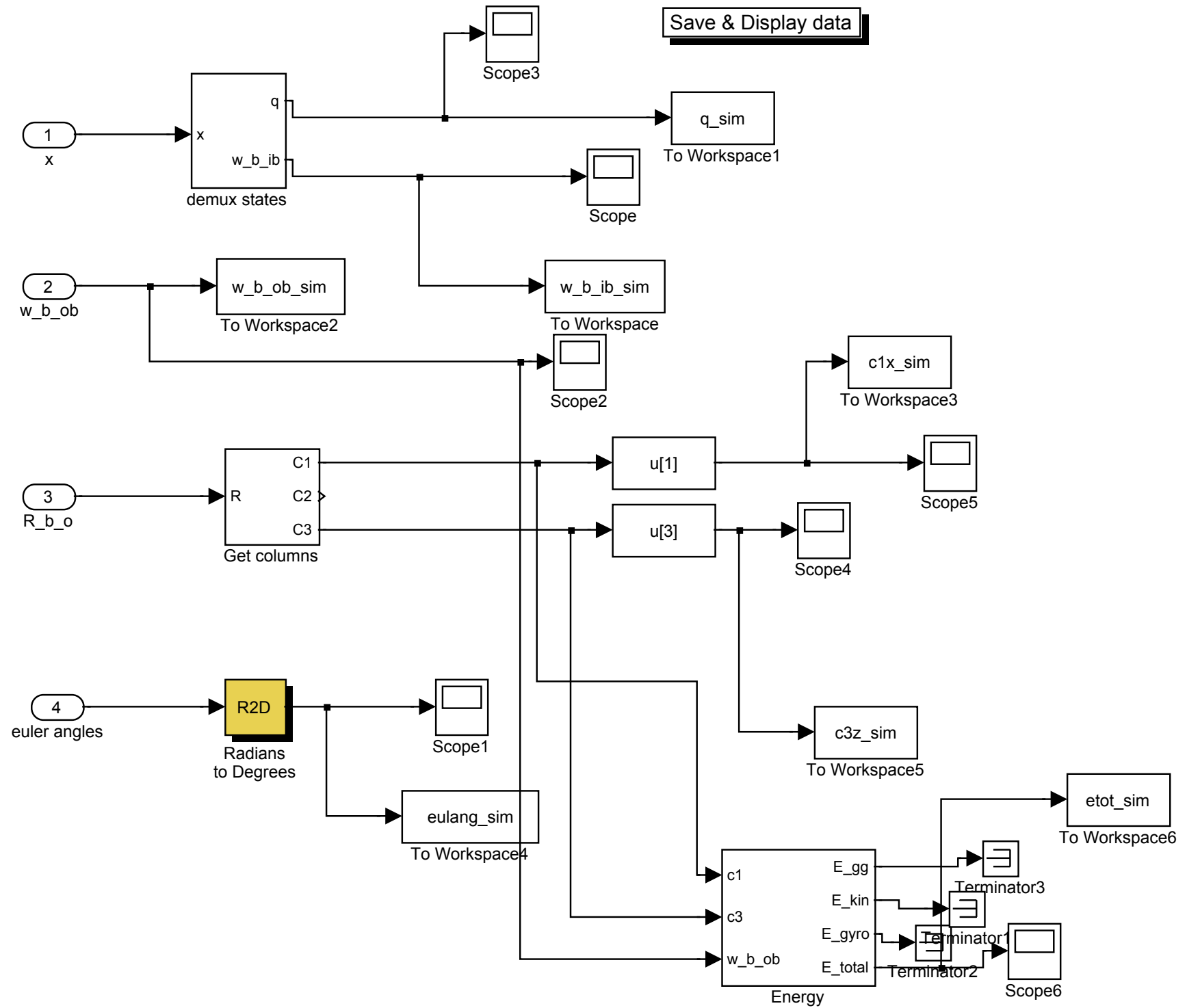


# Orbit to body

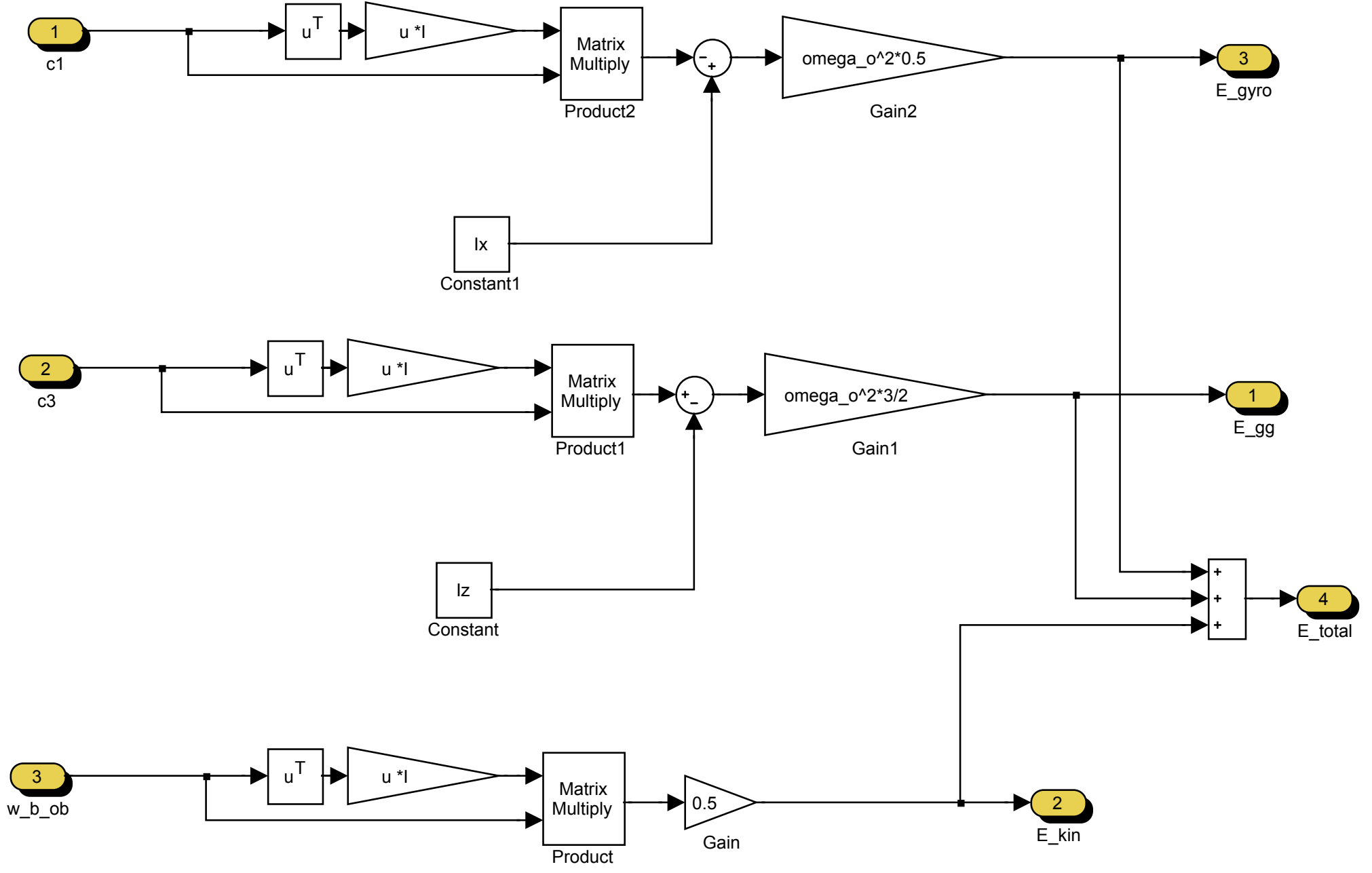


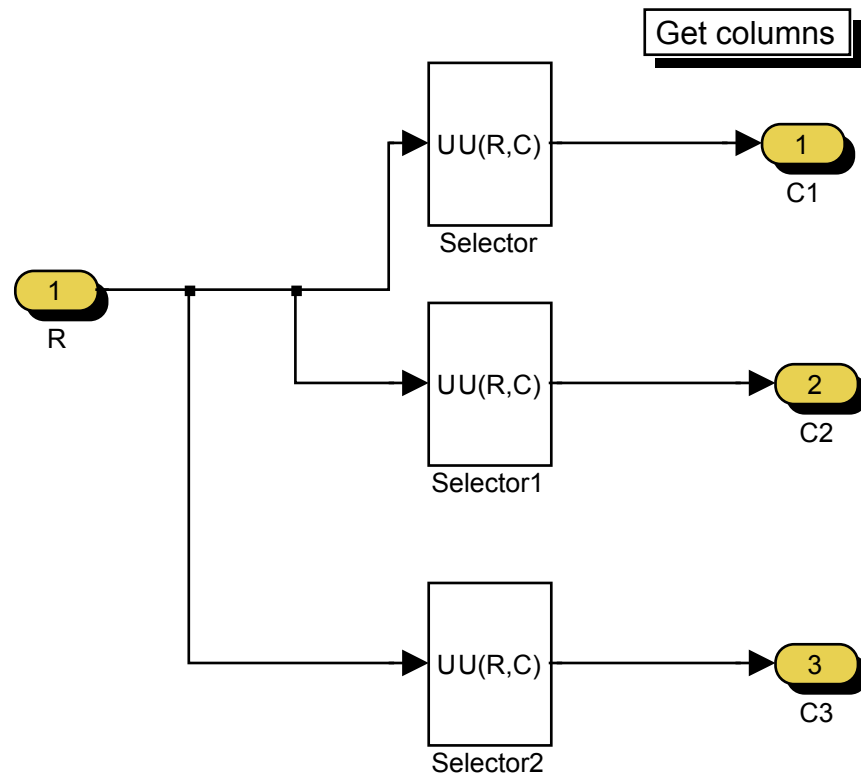
# Simulation of the satellite position and velocity in the ECI frame



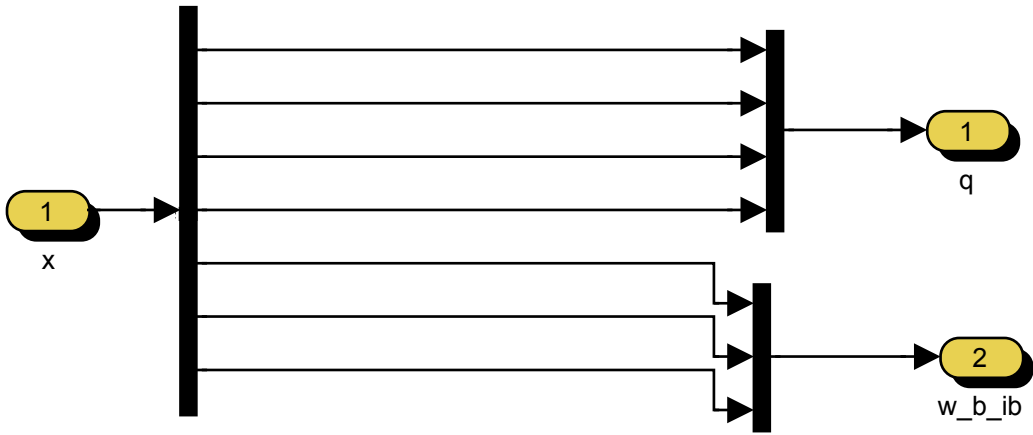


# Energy





Demuxed states



```
*****
% Initialization file for the nCube satellite model, LQ-controller.
%
% Written by Kjell Magne Fauske, modified by Eli J. Øverby May 2004.
%
*****

%*****
% Inertia matrix
%*****

boom = 1;
satellite = 'ncube'
mode = 'lq'

m_const = [0 0 -0.01]';
k = 0.1*10e4;
if boom

    Ix = 0.1043;
    Iy = 0.1020;
    Iz = 0.0031;

else
    Iy = 0.0018056;
    Ix = 0.0032097;
    Iz = 0.0031197;
end

InertialMatrix=[Ix 0 0; 0 Iy 0; 0 0 Iz];
I=InertialMatrix;

%*****
% Initial values
%*****

global r_p;
M_earth = 5.9742e24; % Mass of Earth
omega_o=1.083*10^-3;

h=6.378e6+600.00e3;
r_p=[h 0 0]'; % initial satellite position

w_O_IO = [0 -omega_o 0]';
w_b_rb = [0 0 0]';

k = 0.1*10e4; % [Am^2s/T]
m_const = [0 0 -0.01]'; % [Am^2]
% m_const = [0 0 0]'; % [Am^2]
q_0=euler2q(pi/180*[10 -3 10]); % attitude
R_O_B=Rquat(q_0);
R_B_O=R_O_B';

c1=R_B_O(:,1);
w_B_OB=[0 0 0]'; %endret her

w_B_IB_0 = w_B_OB+omega_o*c1;
%w_B_IB_0 = [0.0001 0.0001 0.0001]'+omega_o*c1;
w_b_rb = [0 0 0]';
```

```
%*****  
%   Magnetic field  
%*****  
  
global G;  
global H;  
[G,H] = IGRF2000;  
  
%*****  
%   Coil parameters  
%   -----  
%   N_x, N_y, N_z - Number of coil windings  
%   A_x, A_y, A_z - Coil area [m^2]  
%   R_x, R_y, R_z - Coil resistanse [ohm]  
%   i_max          - Max allowed current [Amp.]  
%*****  
  
% Number of coil windings  
N_x = 100;  
N_y = 100;  
N_z = 100;  
% Coil area [m^2]  
A_x = 0.0075;  
A_y = 0.0075;  
A_z = 0.0075;  
R_x = 20;  
R_y = 20;  
R_z = 20;  
m_max = 0.1 % [Am^2]
```

```
function K = K_beregning(B)

%*****
%
% LQ Initialization
%
%*****

% Initial values
Ix = 0.1043;
Iy = 0.1020;
Iz = 0.0031;
omega_o=1.083*10^-3;
w_O = omega_o;

kx = (Iy - Iz)/Ix;
ky = (Ix - Iz)/Iy;
kz = (Iy - Ix)/Iz;

% The geomagnetic field
Bx_0 = B(1);
By_0 = B(2);
Bz_0 = B(3);

% The linearized system matrix
A = [0 1 0 0 0 0 ;
     -4*kx*w_O^2 0 0 0 0 (1 - kx)*w_O;
     0 0 0 1 0 0;
     0 0 -3*ky*w_O^2 0 0 0;
     0 0 0 0 0 1;
     0 -(1 - kz)*w_O 0 0 -kz*w_O^2 0
     ];

% The input matrix for the linearized system
B = [0 0 0;
     0 Bz_0/(2*Ix) -By_0/(2*Ix);
     0 0 0;
     -Bz_0/(2*Iy) 0 Bx_0/(2*Iy);
     0 0 0;
     By_0/(2*Iz) -Bx_0/(2*Iz) 0 ];

% LQ-weighting matrices when using a gravity boom
Q = diag([1 0 1 0 1 0])*inv(10*pi/180)^2;
P = diag([1 1 1])*inv(0.001)^2;

K = -lqr(A,B,Q,P);
```

```
*****
% Initialization file for the nCube satellite model,
% Angular velocity feedback-controller.
%
% Written by Kjell Magne Fauske, modified by Eli J. Øverby May 2004.
%
*****

%*****
% Inertia matrix
%*****

boom = 1;
satellite = 'ncube'
mode = 'stabilization'

m_const = [0 0 -0.01]';
k = 0.1*10e4;
if boom

    Ix = 0.1043;
    Iy = 0.1020;
    Iz = 0.0031;

else
    Iy = 0.0018056;
    Ix = 0.0032097;
    Iz = 0.0031197;
end

InertialMatrix=[Ix 0 0; 0 Iy 0; 0 0 Iz];
I=InertialMatrix;

%*****
% Initial values
%*****

global r_p;
M_earth = 5.9742e24; % Mass of Earth
omega_o=1.083*10^-3;

h=6.378e6+600.00e3;
r_p=[h 0 0]'; % initial satellite position

w_O_IO = [0 -omega_o 0]';
w_b_rb = [0 0 0]';

k = 0.1*10e4; % [Am^2s/T]
m_const = [0 0 -0.01]'; % [Am^2]

%controller data
h = 2.25*10^5;
q_0=euler2q(pi/180*[60 40 20]); % attitude
w_B_OB=[0.0005 0.0003 -0.003]';
R_O_B=Rquat(q_0);
R_B_O=R_O_B';
c2=R_B_O(:,2);
c1=R_B_O(:,1);

w_B_IB_0 = w_B_OB+omega_o*c1;
```

---

---

```
w_b_rb = [0 0 0]';
```

```
%*****  
%   Magnetic field  
%*****
```

```
global G;  
global H;  
[G,H] = IGRF2000;
```

```
%*****  
%   Coil parameters  
%   -----  
%   N_x, N_y, N_z - Number of coil windings  
%   A_x, A_y, A_z - Coil area [m^2]  
%   R_x, R_y, R_z - Coil resistanse [ohm]  
%   i_max          - Max allowed current [Amp.]  
%*****
```

```
% Number of coil windings  
N_x = 100;  
N_y = 100;  
N_z = 100;  
% Coil area [m^2]  
A_x = 0.0075;  
A_y = 0.0075;  
A_z = 0.0075;  
R_x = 20;  
R_y = 20;  
R_z = 20;  
m_max = 0.1 % [Am^2]
```